Searches with Negative Muons

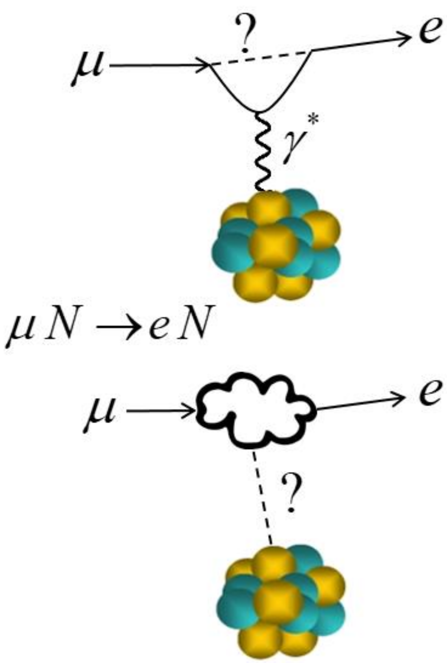

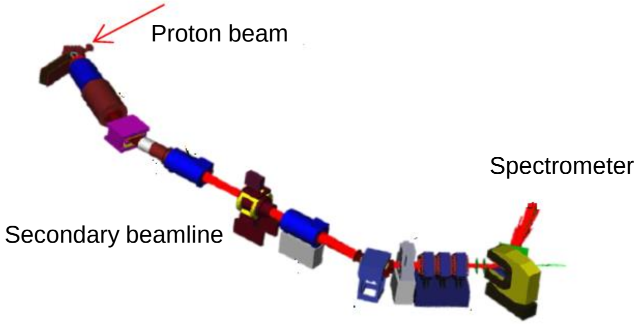

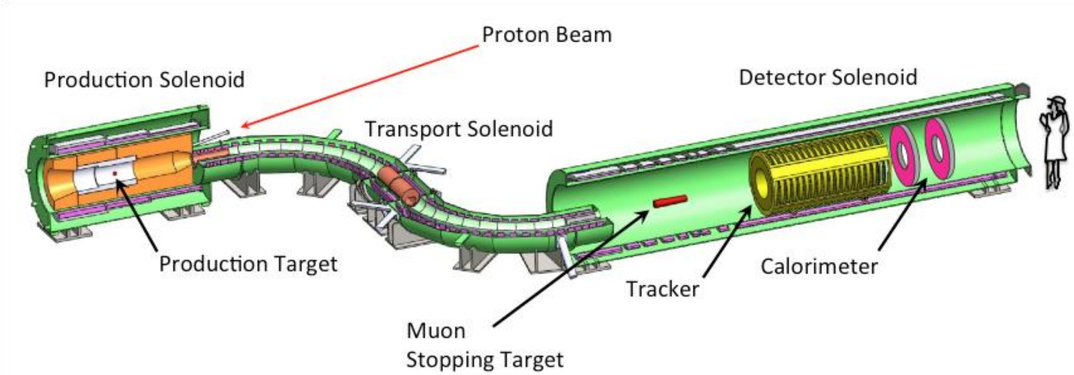

David Hitlin
Beijing CLFV School
June 3-7, 2019
Lecture 2

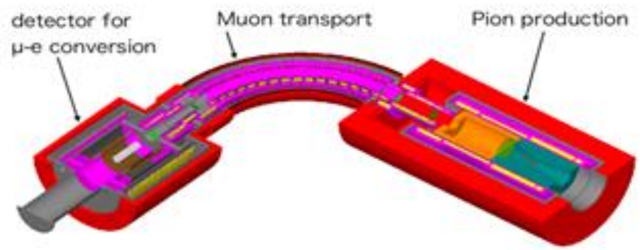

Solenoids

Comet Capture Solenoid

- Superconducting solenoid magnets with Al-stabilized conductor
- High field 5T to capture π^-
- Large bore 1300mm
- High radiation environment
- Decreasing field to focus trapped pions
- Thick radiation shielding 450mm
- Proton beam injection tilted at 10°
- Simple mandrel

	CS0	CS1	MS1	MS2
Length (mm)	175	1350	1800	380
Diameter (mm)	662	662	662	662
Layer	9	9	5	8
Thickness (mm)	144	144	80	128
Current density (A/mm²)	35	35	35	35
Maximum field (T)		5.7	4.0	3.9
Hoop stress (MPa)		59	51	30

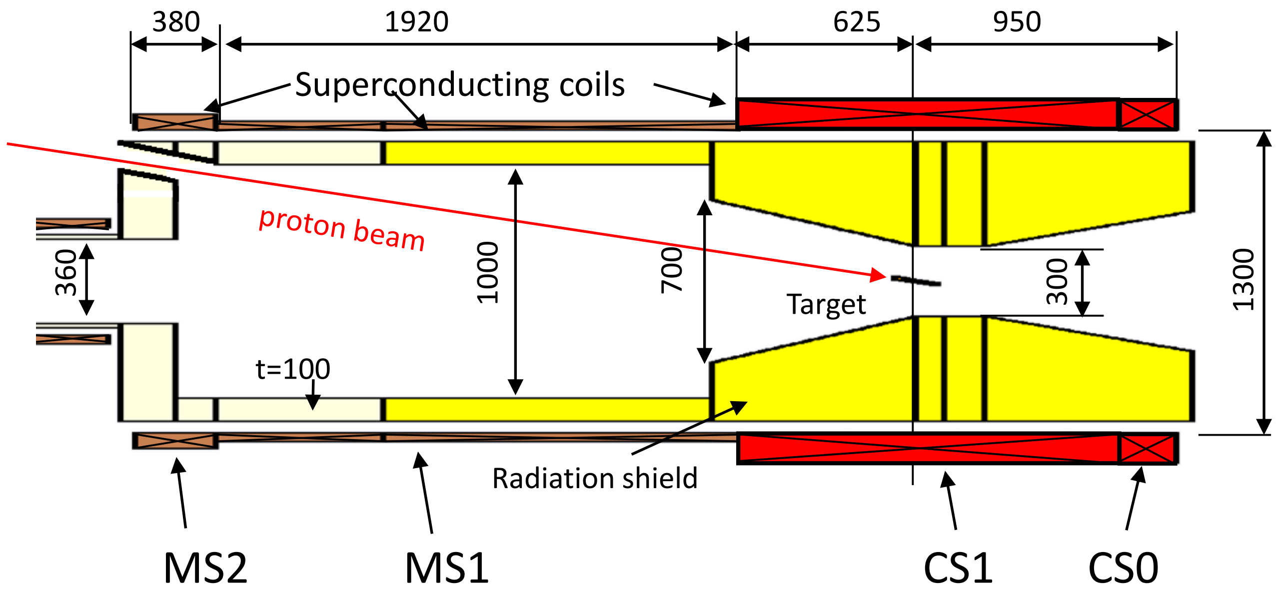

- Axially graded (~5T → 2.5T) solenoid captures low energy backward and *reflected* pions, directing to the Transport Solenoid

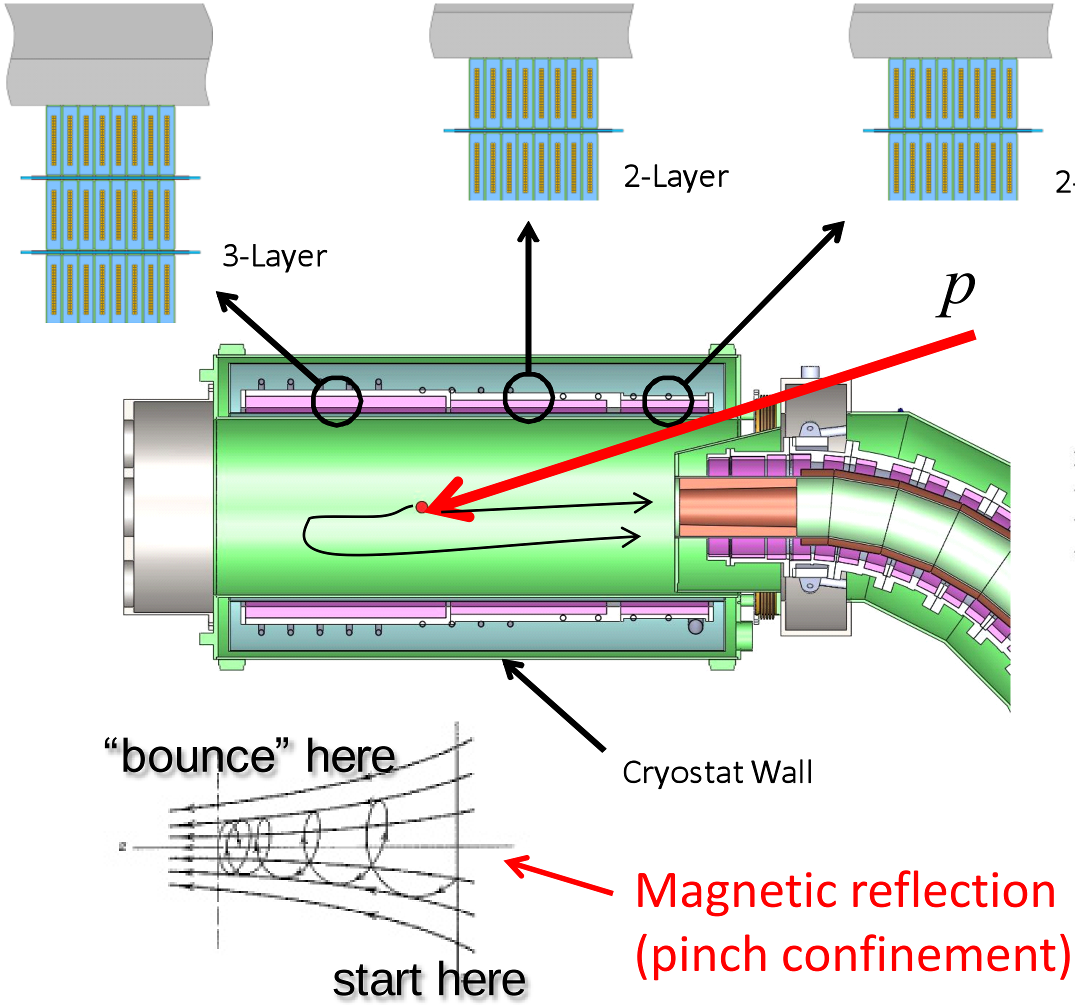

Magnetic Gradient

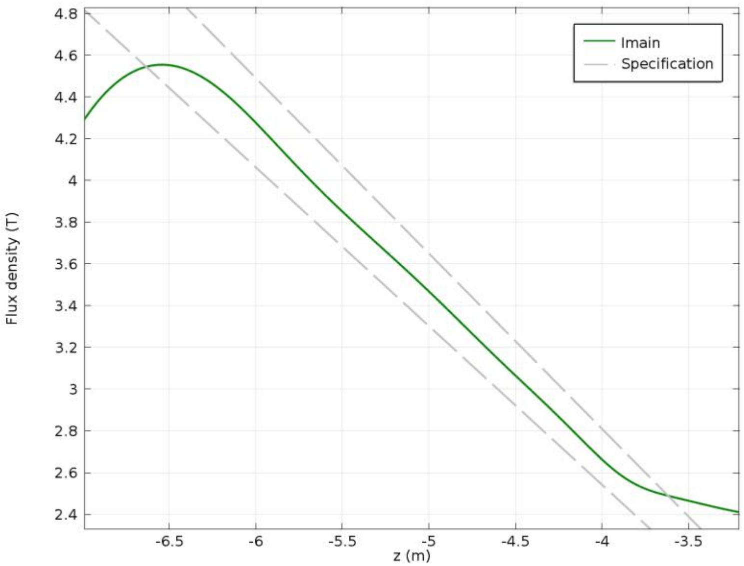

Mu2e Solenoid Scope

- Production Solenoid (PS)
- Transport Solenoid (TSu,TSd)
- Detector Solenoid (DS)
- Cryogenic Distribution

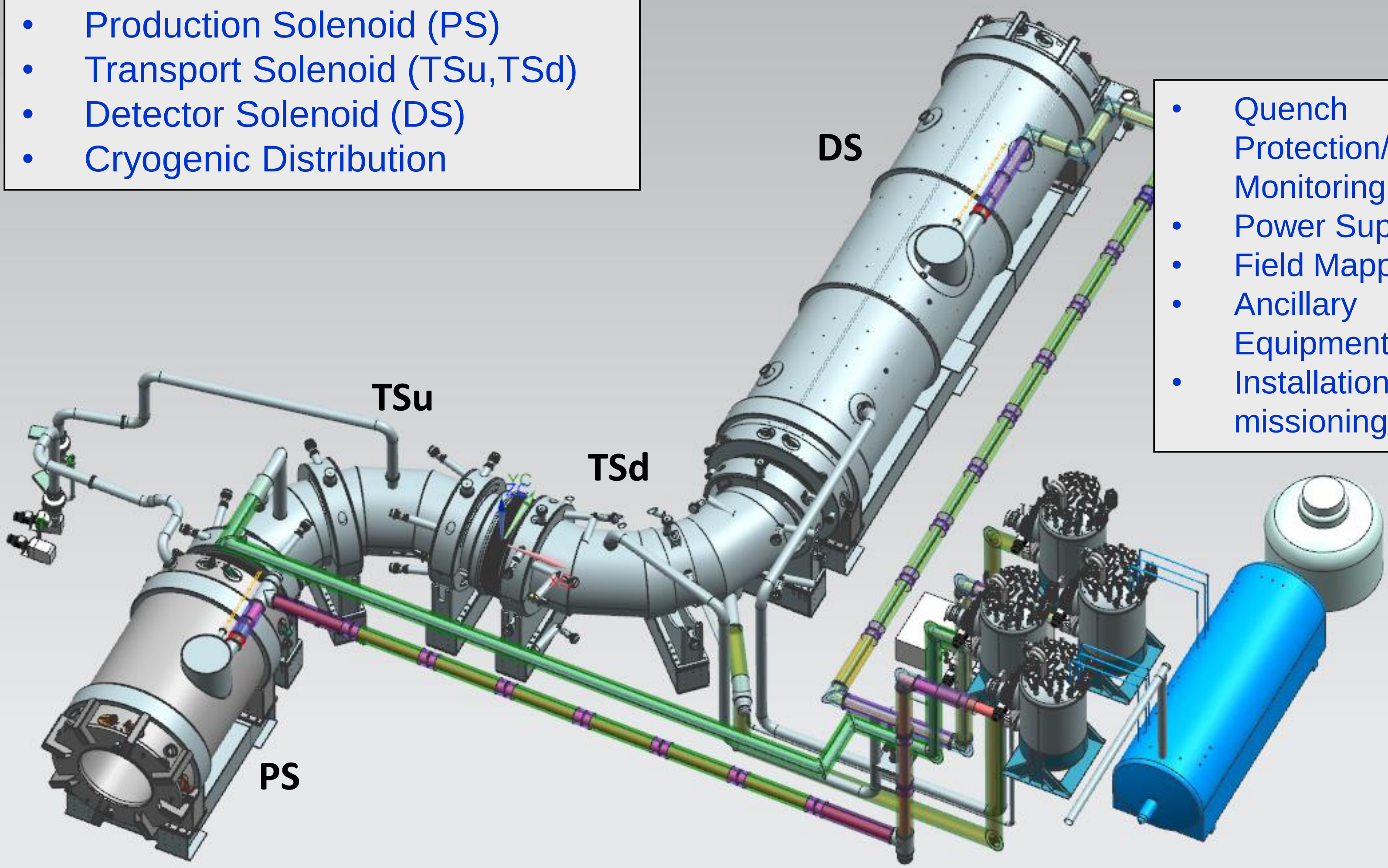

- Quench Protection/Slow Monitoring
- Power Supplies
- Field Mapping
- Ancillary Equipment
- Installation/Commissioning

Magnetic Field Gradient

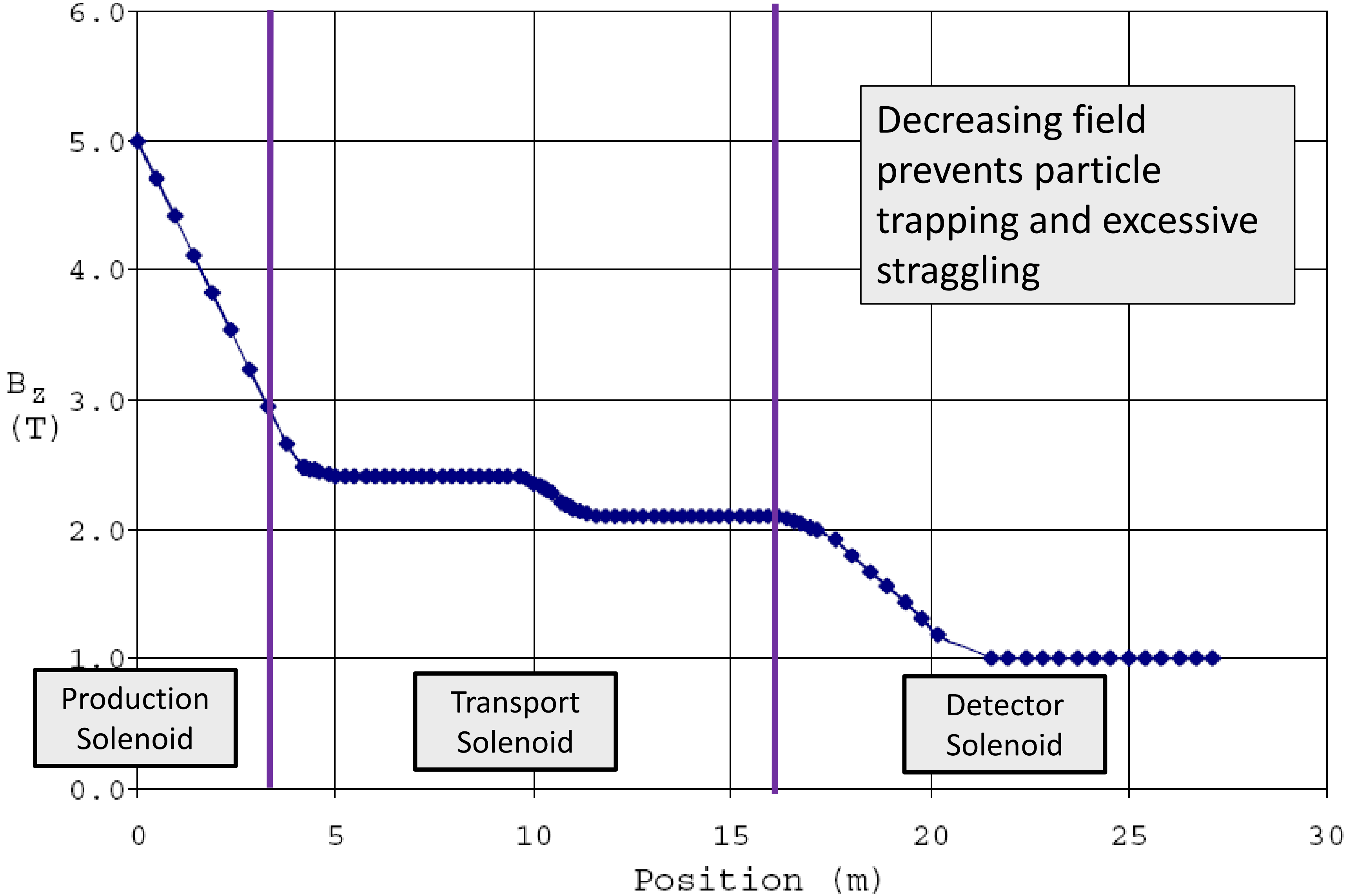

Production Solenoid (PS)

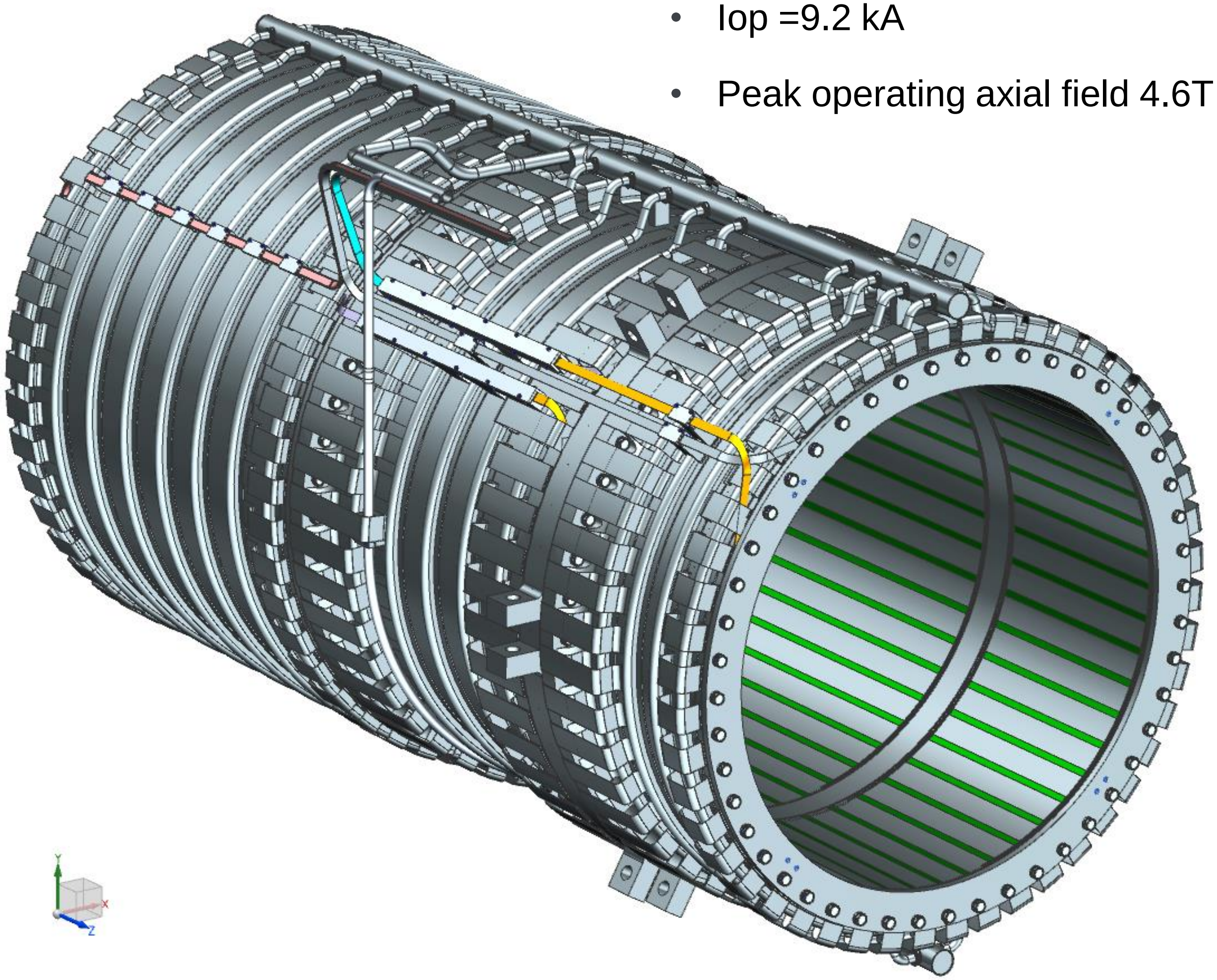

- 1.6 m aperture
- Iop =9.2 kA
- Peak operating axial field 4.6T

- PS consists of three coil modules with 3-2-2 layers of the same Al-stabilized cable wound the "hard way"
- Each module has an outer support structure made of Al 5083-O to manage the forces
- The shells are bolted together to form a single cold mass assembly
- The coil modules are installed inside of a cryostat with axial and transverse supports

Mu2e Transport Solenoid

- TS1,TS3,TS5: Straight sections with an axial gradient
- TS2/TS4: approximate toroidal field
- 52 solenoid coils with different amp-turns
- Two cryostats: TSu,
- TS3: ➔ TS3u, TS3d.

  Wider coils to compensate for gaps

  Coil fabrication similar to MRI coils

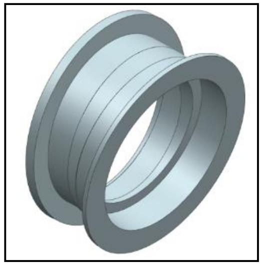

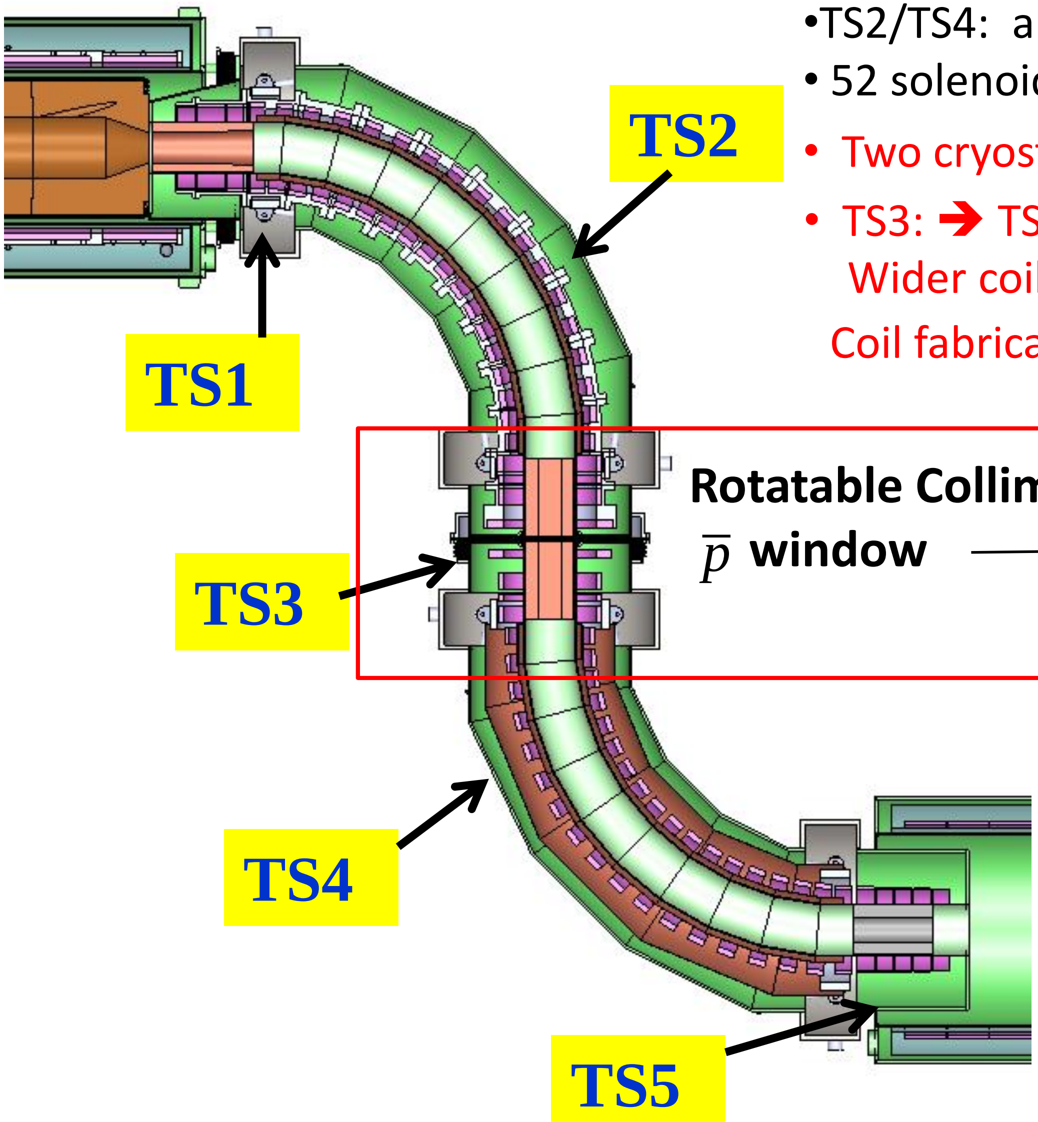

Rotatable Collimator

$\bar{p}$ window →

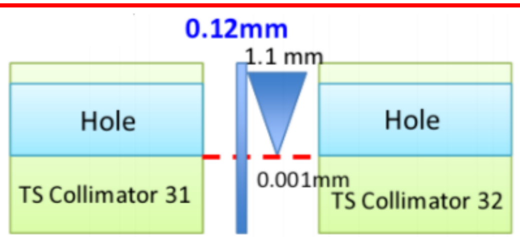

- 'S' shape blocks line-of-sight
- Bend induces momentum and charge-dependent vertical shift
- An symmetric collimator rejects positive and high-momentum particles
  - Could be rotated to select positive particles

Detector and Detector Solenoid

- The field around the stopping target has a gradient to increase acceptance via magnetic reflection
- Magnetic field is uniform in the tracking volume
- Electromagnetic calorimeter identifies electrons

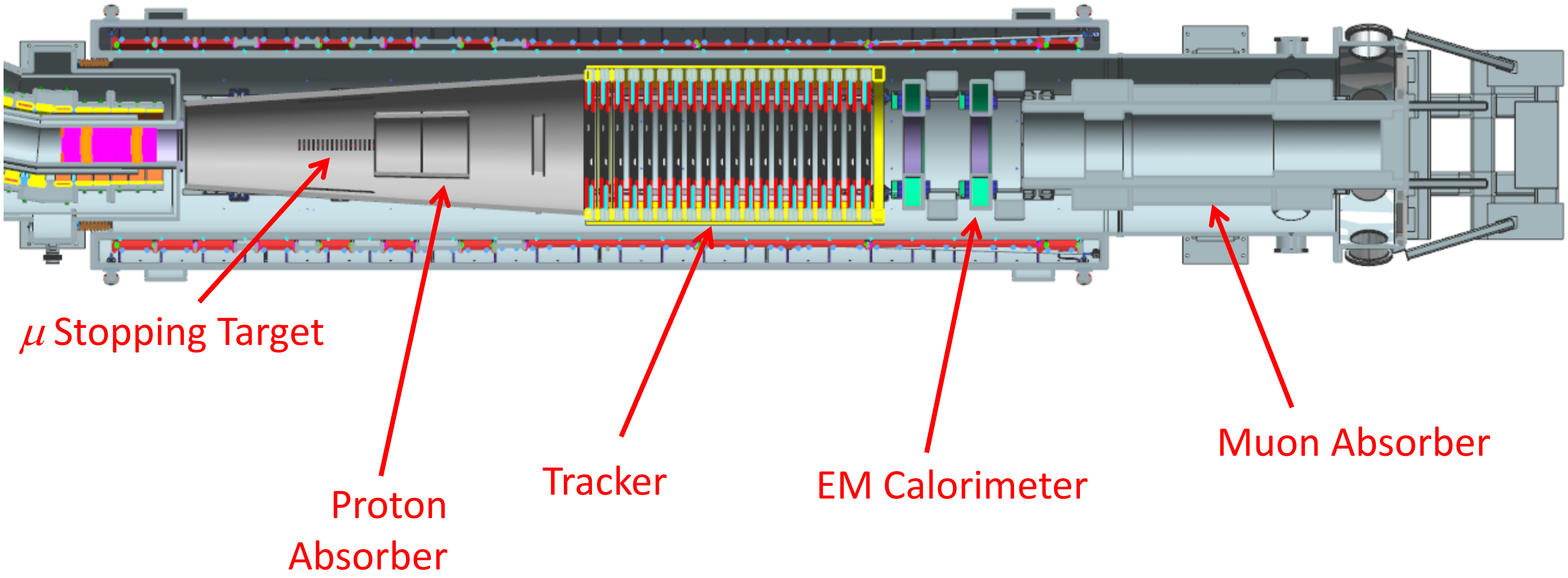

Detector Solenoid (DS)

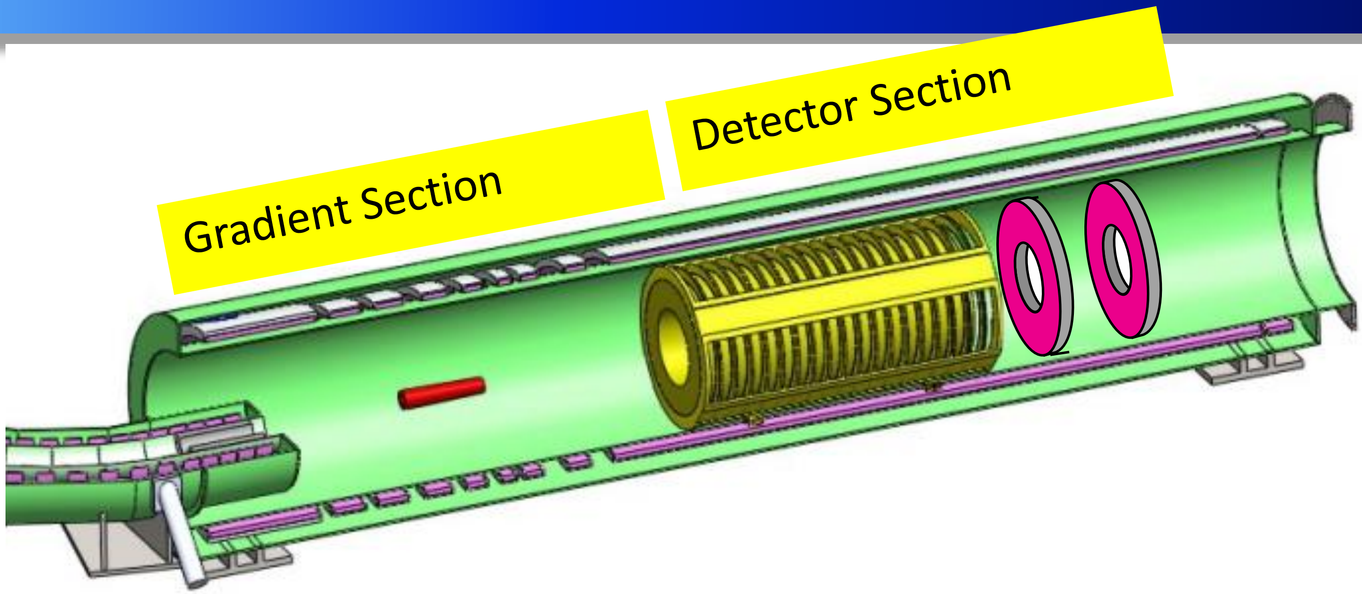

- 1.8 m Aperture   Operating Current ~6kA
- Gradient section 2T➔ I T field
- Spectrometer section 1 T field with small axial gradient superimposed to reduce backgrounds
- 11 Coils in total
  - Axial spacers in Gradient Section
  - Spectrometer section made in 3 sections to simplify fabrication and reduce cost
- **Fabrication technology similar to PS**

Detector Solenoid (DS)

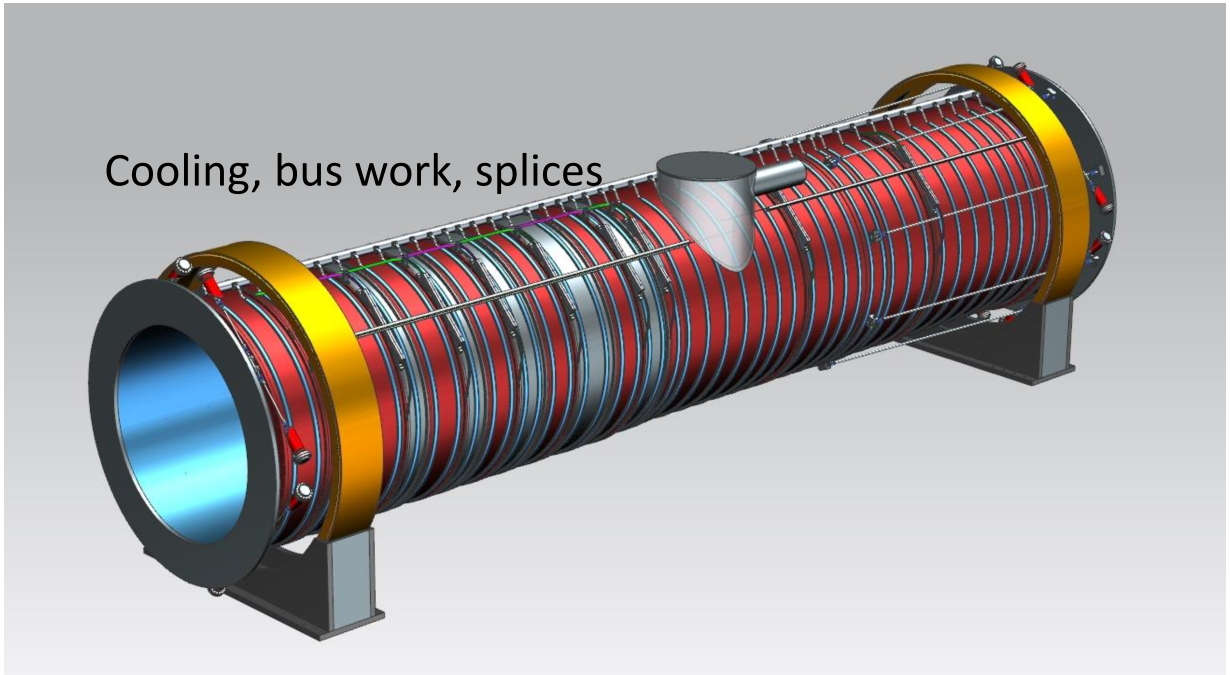

TS cold mass – first test unit

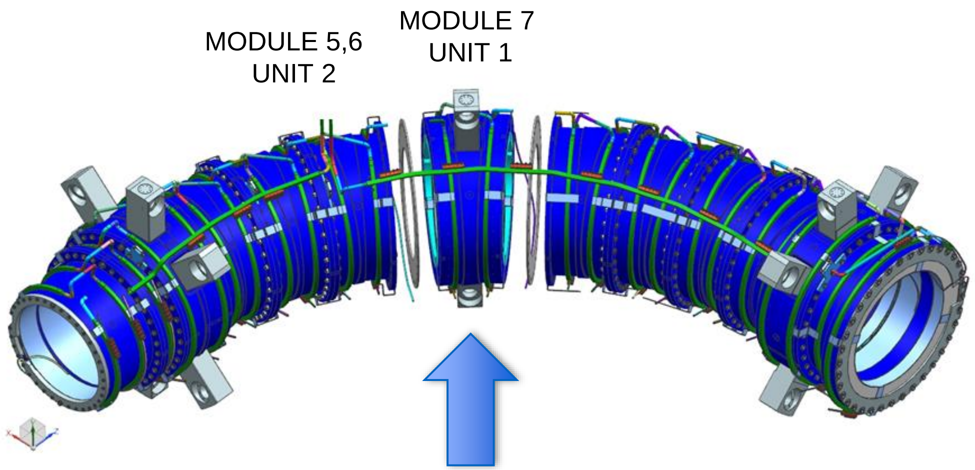

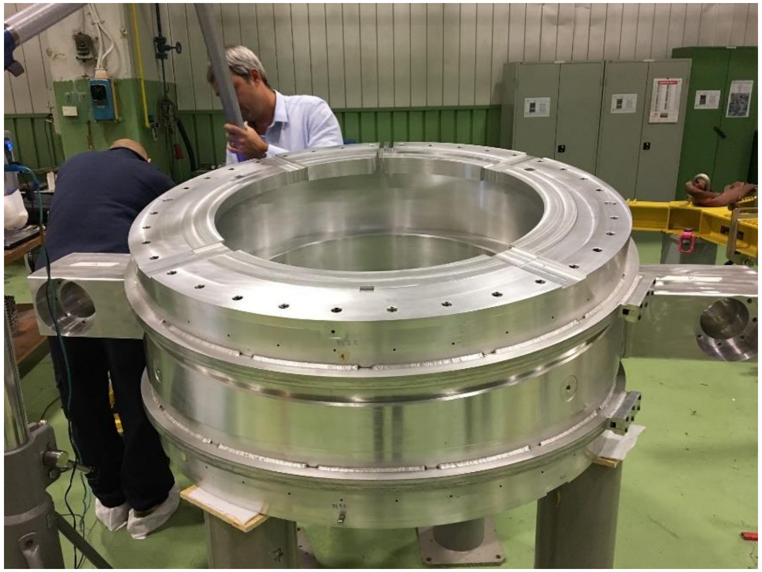

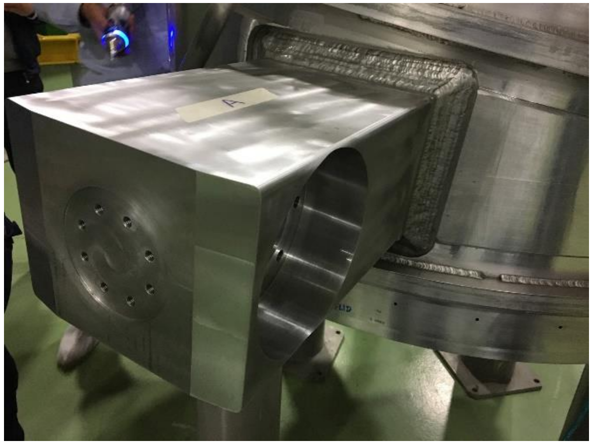

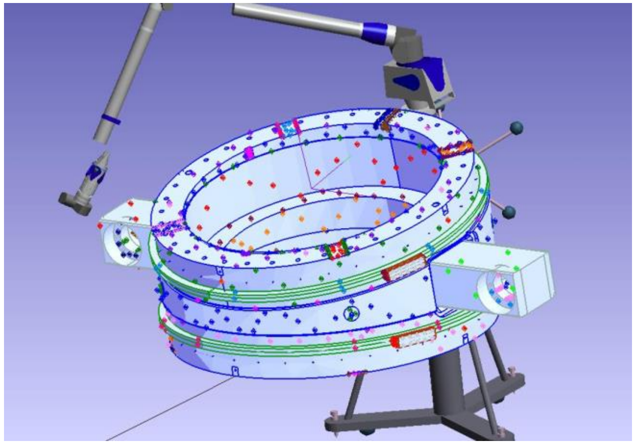

Production Solenoid
20 turn winding demonstration

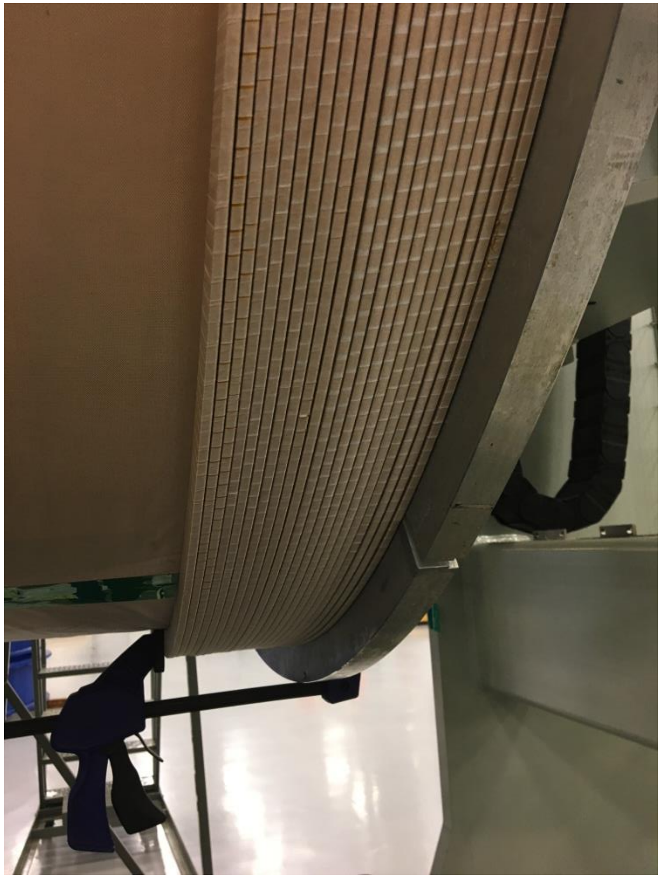

Transport Solenoid Production

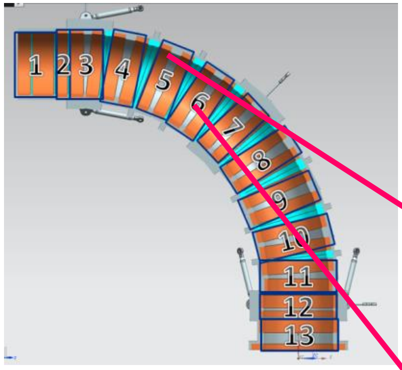

Cryogenic Distribution Boxes

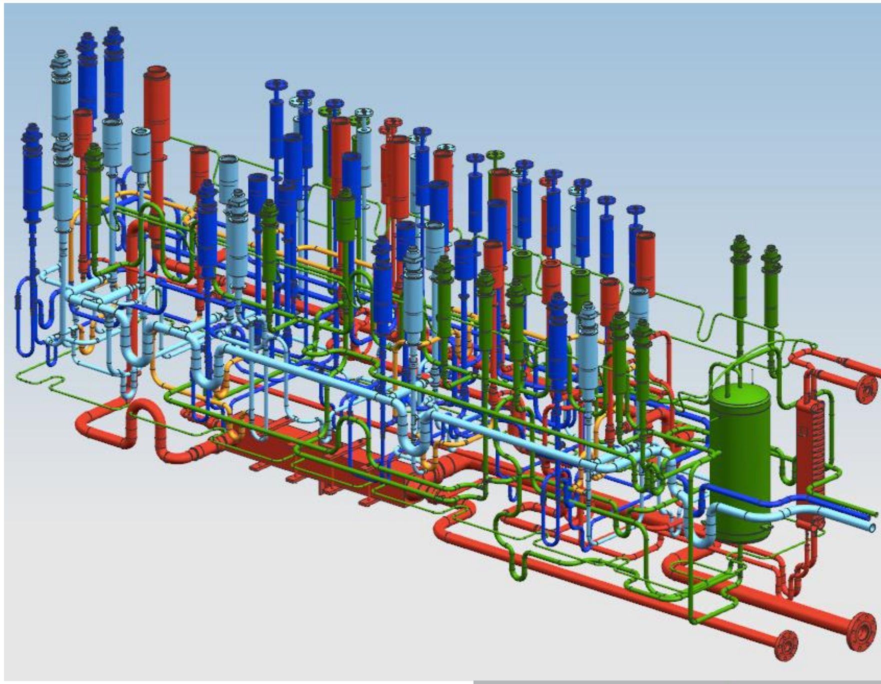

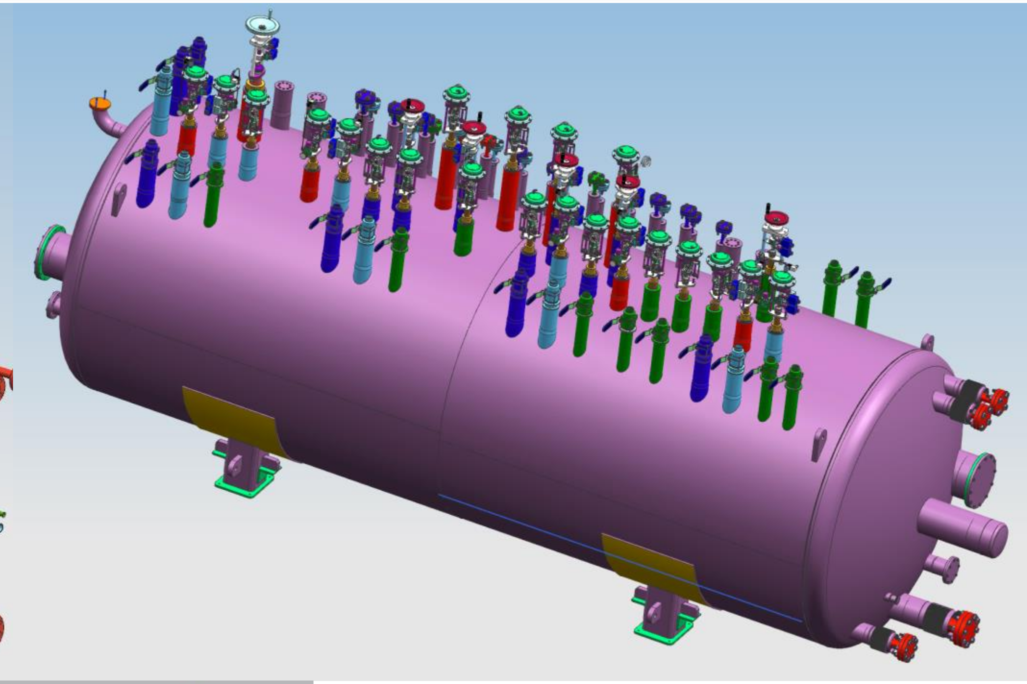

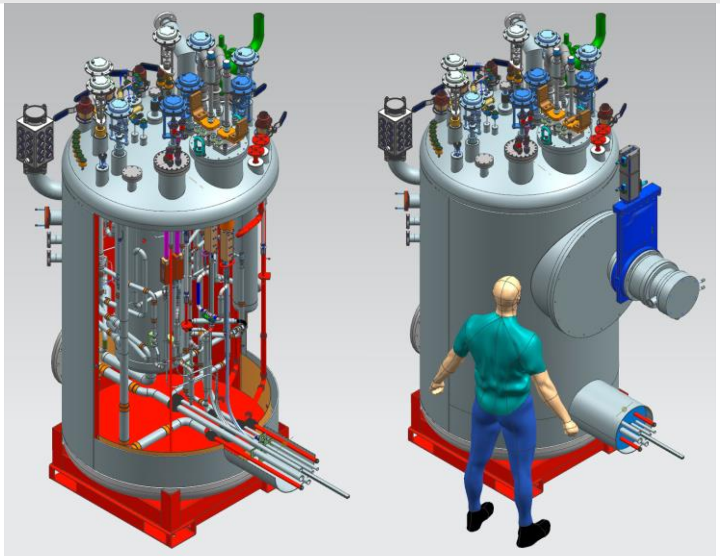

Solenoid cold mass position monitoring system

Mu2e needs to know the position of the Detector Solenoid Cold Mass with a precision better than 1 mm. The system will need to work remotely, as the cryostat is inaccessible. It has to seal against vacuum better than 10^{-7} torr and withstand overpressure of 15 psi, and survive a dose of 1 kGray/year. The system has to work for the ~3 year lifetime of the experiment in a magnetic field.

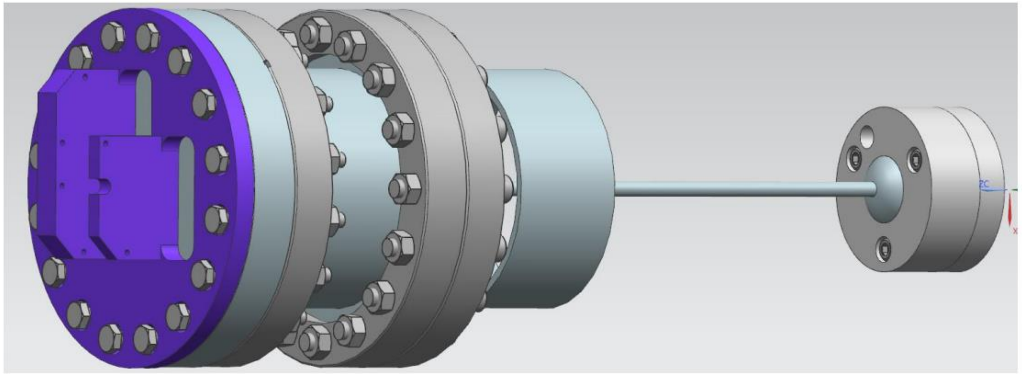

The Cold Mass Position Monitoring device

The Components

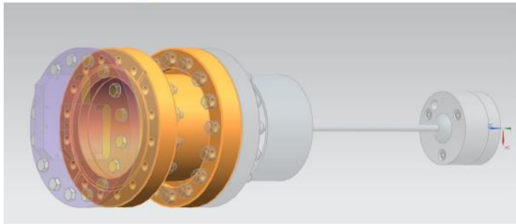

Port Tube

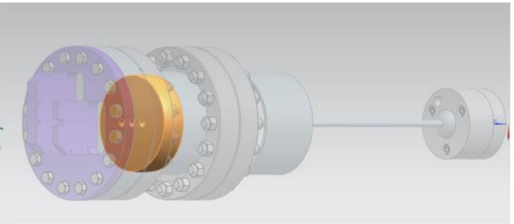

Circular planar disk

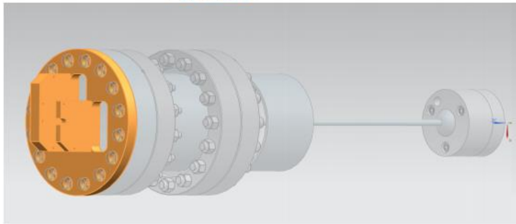

Laser Sensor Mounting plate

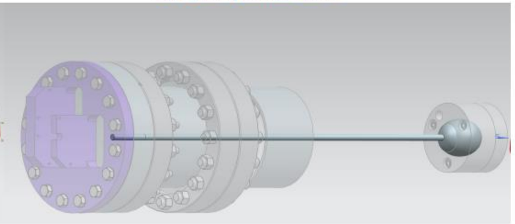

Sphere and Rod connecting to Cold Mass

The solenoid is a rigid body and we survey 4 locations to measure its movements. At each survey point, a spherical mount is affixed to the Cold Mass. A second circular planar disk moving freely in a port tube is connected to the cold mass via a fixed length rod. Three Keyence IL-065 laser sensors, with 45 mm range and 2 micrometer accuracy, are mounted on a plate fitted to a Quartz vacuum window. We measure distances between the mounting plate and disk along calibrated laser paths. The angle of the port tube axis w.r.t. the sensor plate is surveyed, and thus we translate the disk movement into the displacement of the sphere affixed to the Cold Mass.

Keyence IL-065 laser sensor

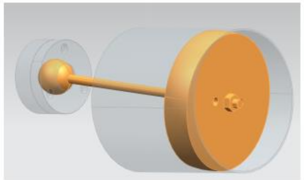

Visualization of the disk tilt when the sphere moves

The expected resolution

We will calibrate the path of the Keyence IL-065 laser sensors after affixing them to the mounting plate. This results in a readback error of less than 2 microns for the IL-065 (plus 2 microns syst.). Assuming a 10 cm lever rod the geometrical displacement of the sphere thus has a position error of 20 microns. The port tube and sensor plate will be aligned via CMM to 25 microns, the length of the rod is known better than 25 microns too. In total we expect the error on the cold mass reading to be less than 100 microns in three dimensions.

Stray magnetic field at beam height

Lower Level solenoid height (y = 0), i.e. 2.3 m above floor

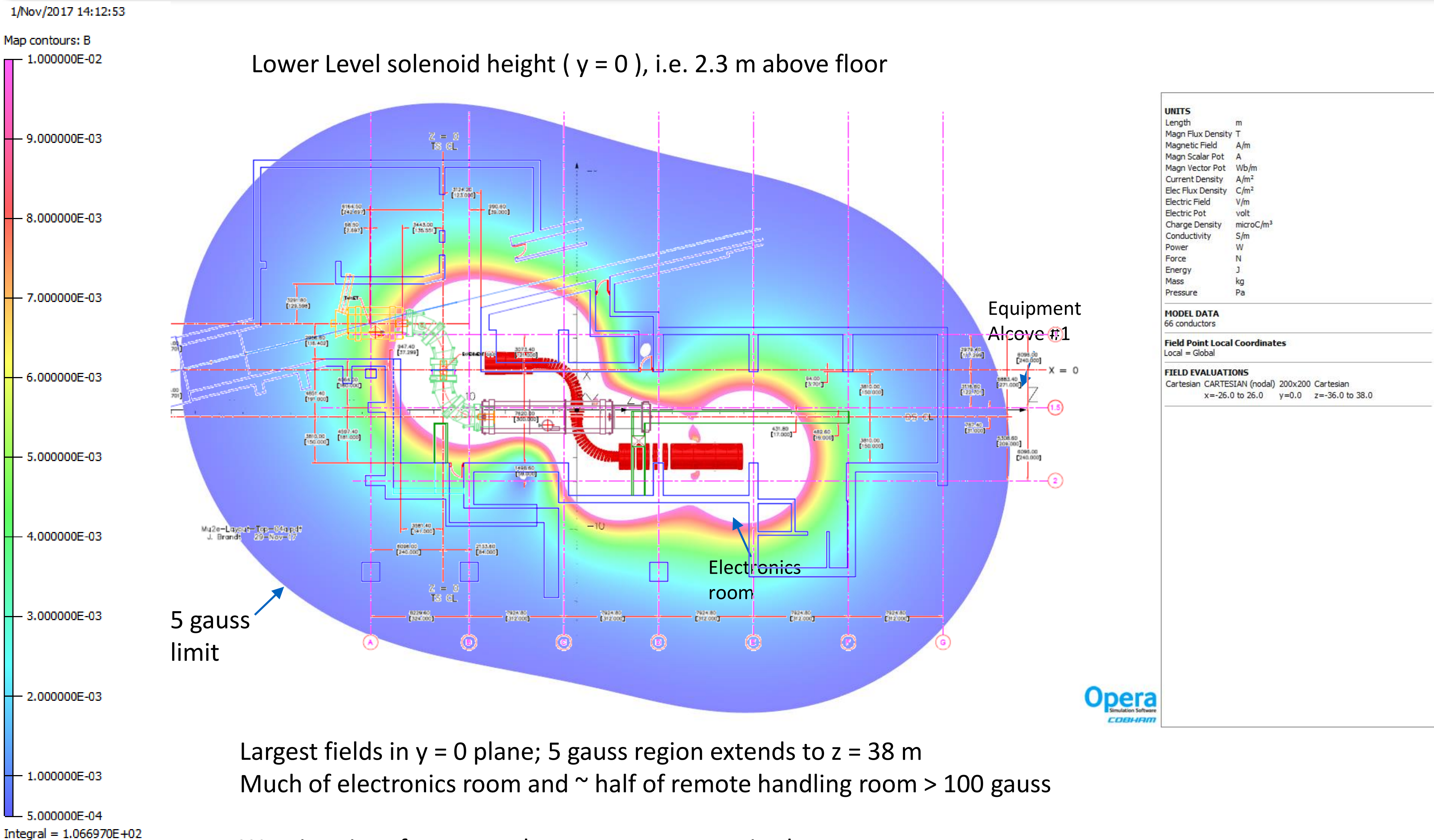

Largest fields in y = 0 plane; 5 gauss region extends to z = 38 m

Much of electronics room and ~ half of remote handling room > 100 gauss

Warning signs for pacemaker wearers are required

COMET Phase I Superconducting Solenoids

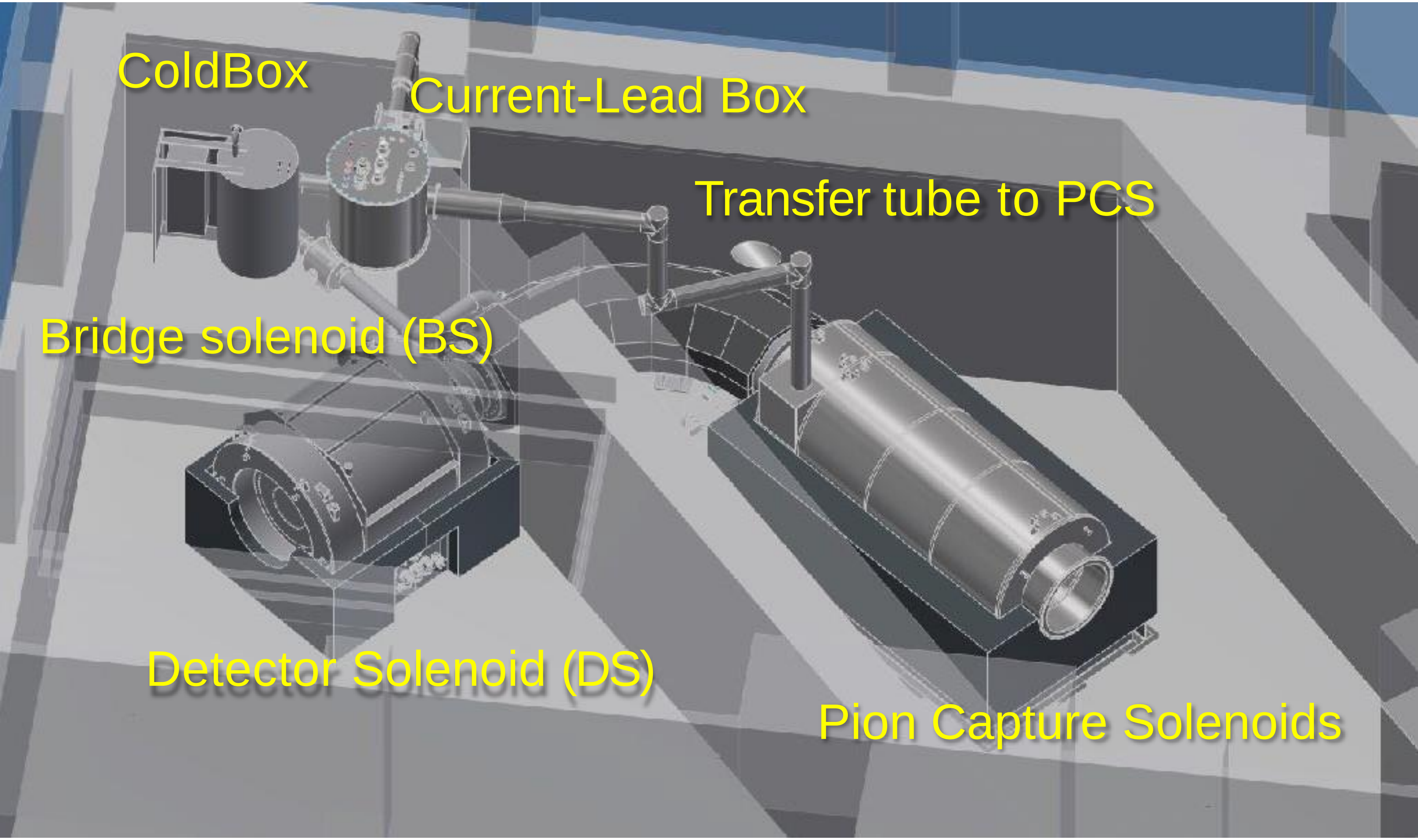

Pion Capture Solenoid

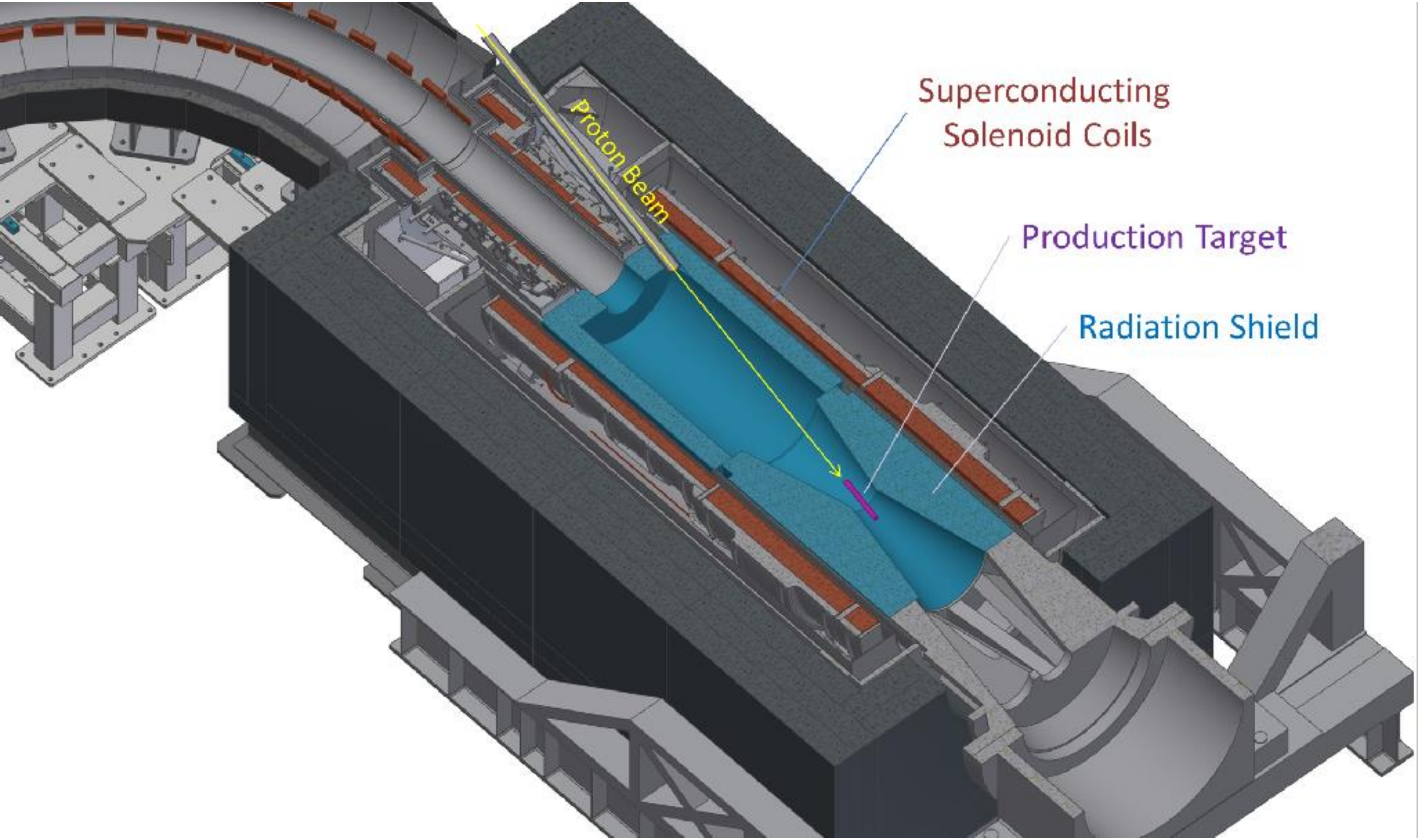

Production of Pion Capture Solenoid

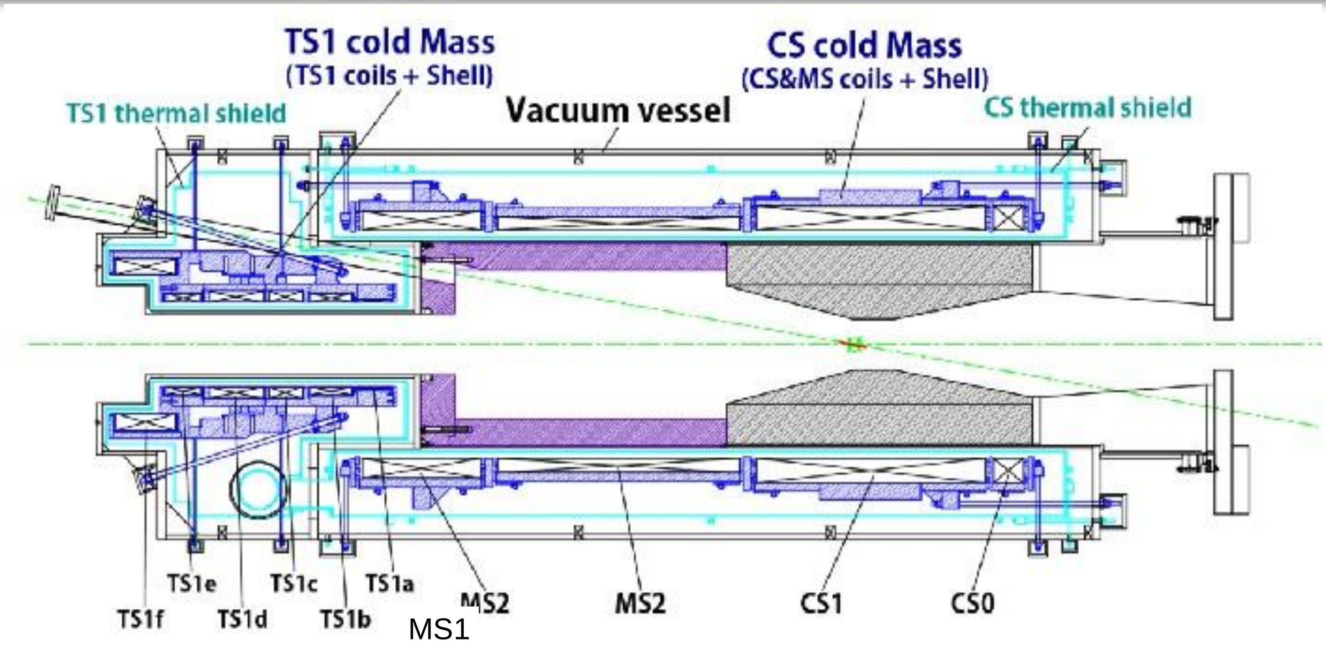

- Coil winding of TS1a – TS1f and CS0 completed.
- MS2 coil winding started in 2018.
- MS1 coil winding by March 2019.
- Prototype cryostat for 3000 A HTS current leads under preparation
- Transfer-line to Muon Transport Solenoid underway

- In 2019 and following years:
  - winding of the CS1 coil
  - Installation of TS1 coils in support shell
  - Installation of CS0-MS2 coils in support shell
  - Cryostats

Secondary pion yields

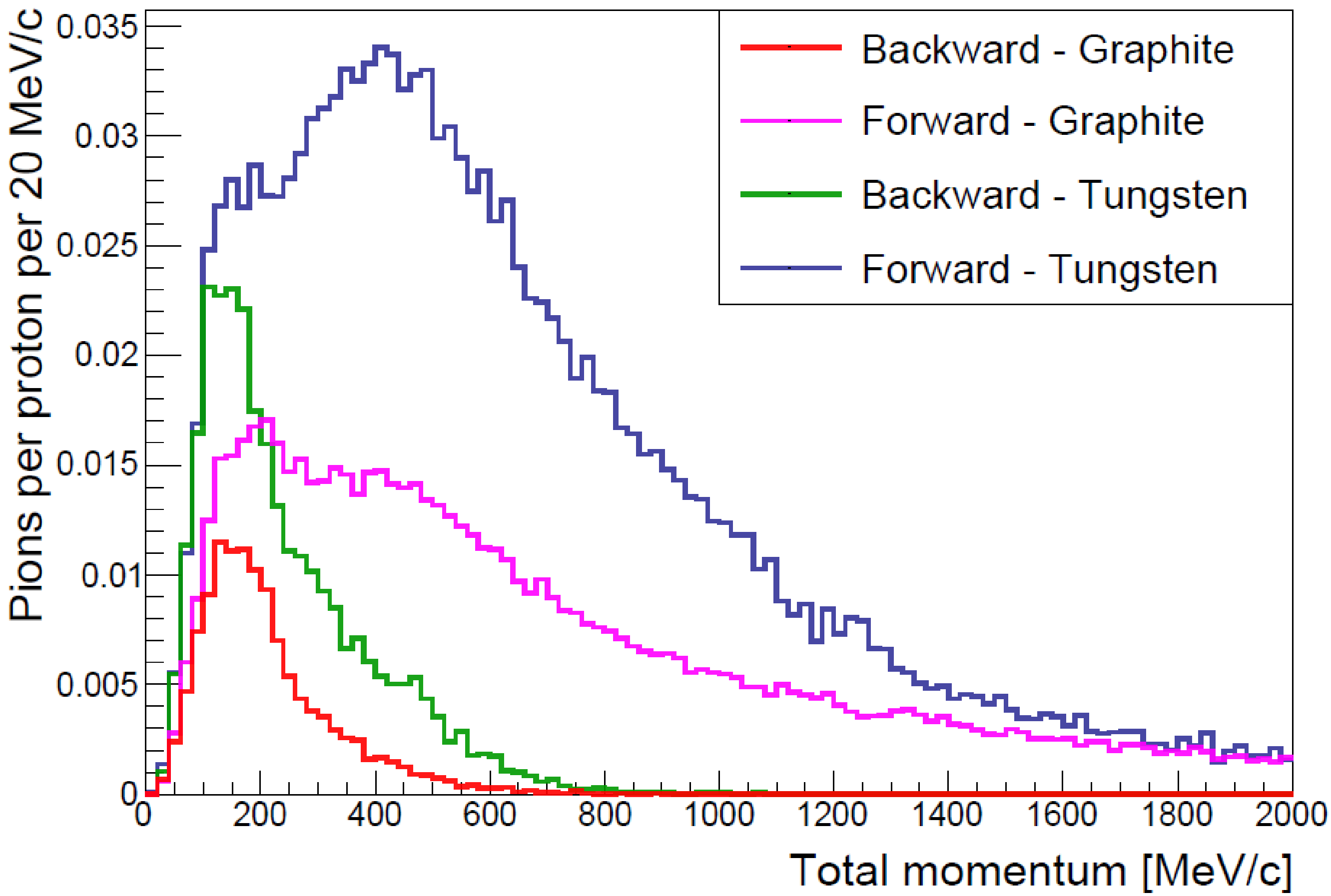

Momentum distribution of beam particles at the exit of the first 90° curved solenoid (graphite target)

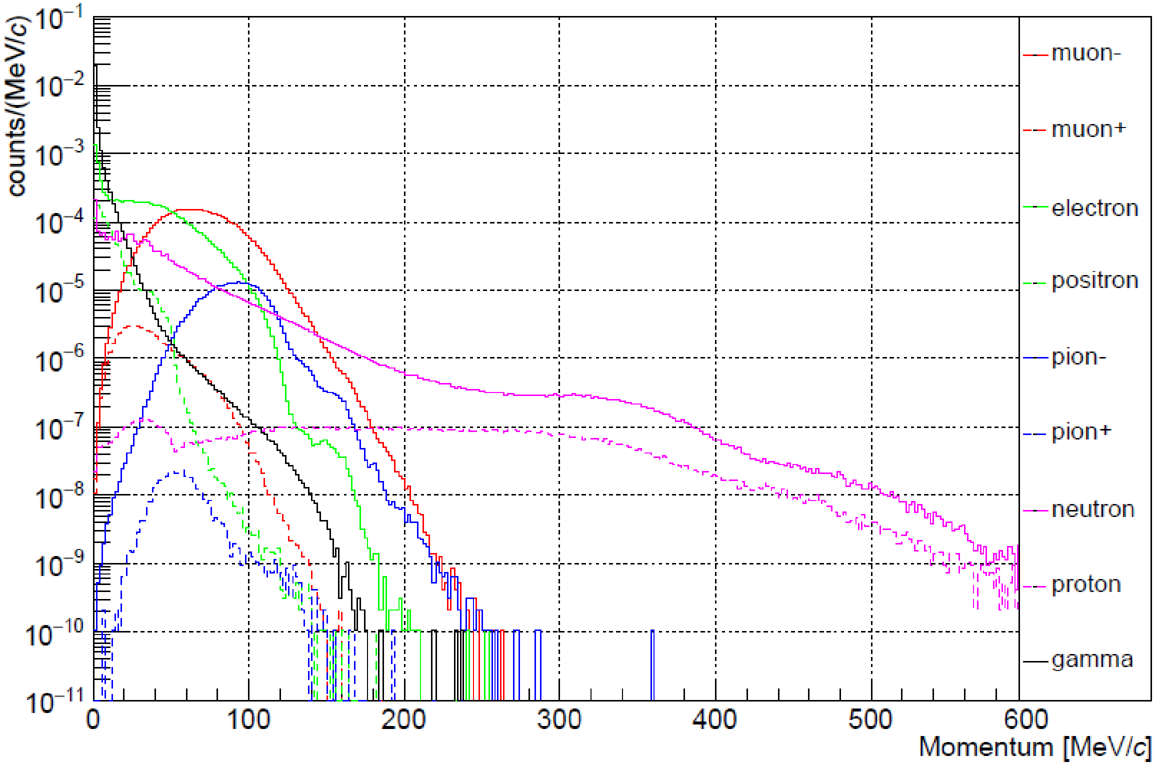

Production target

Target and Heat Shield

Target, inside the PS, produces pions, which decay into muons

Target

- 8 kW beam power
- 700 W power absorption in target
- Radiatively cooled – 2000K
- Bicycle wheel design
  Target rod: Pencil-sized tungsten cylinder
  3.15 mm radius 160 mm length
- Conical hubs at support ends
  ~ 25 mm at 42º
  1mm tungsten spokes
- Ball and socket at hub
  Sprung attachment to wheel
  150 MW/m^3 power density

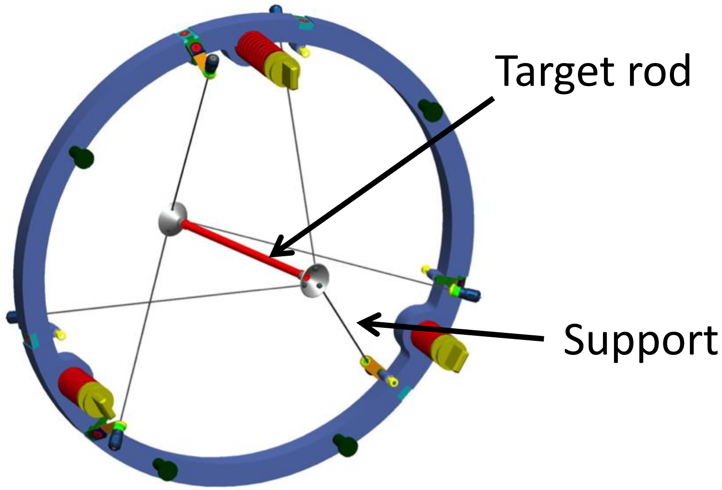

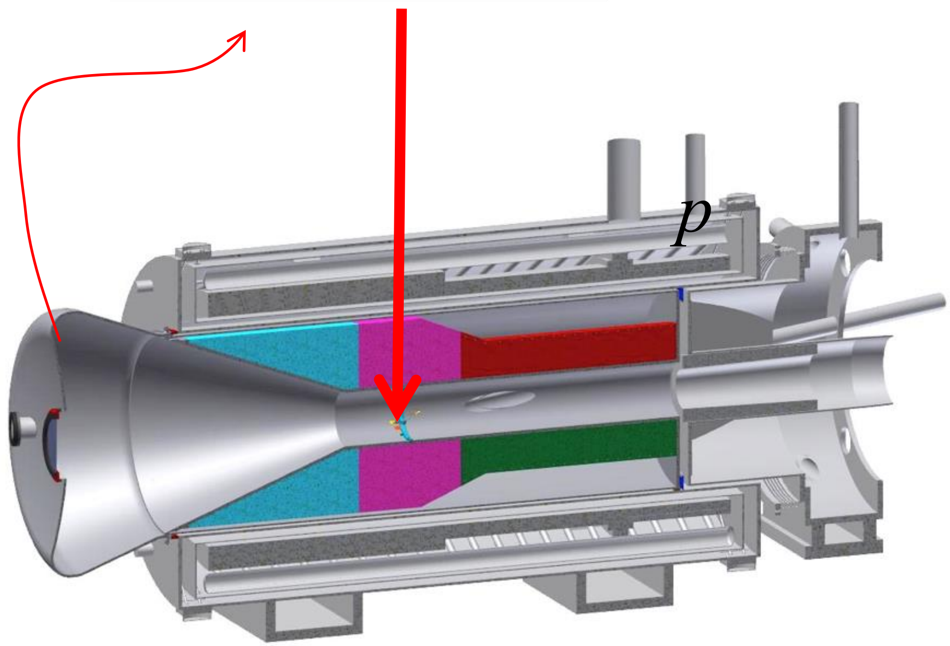

- A heat shield, a massive bronze insert is needed to protect the PS superconductor from the 3.3 kW heat load

Target is optimized for muon yield

Vary

- Target radius
- Target length
- Target position
- Target angle
- Beam profile

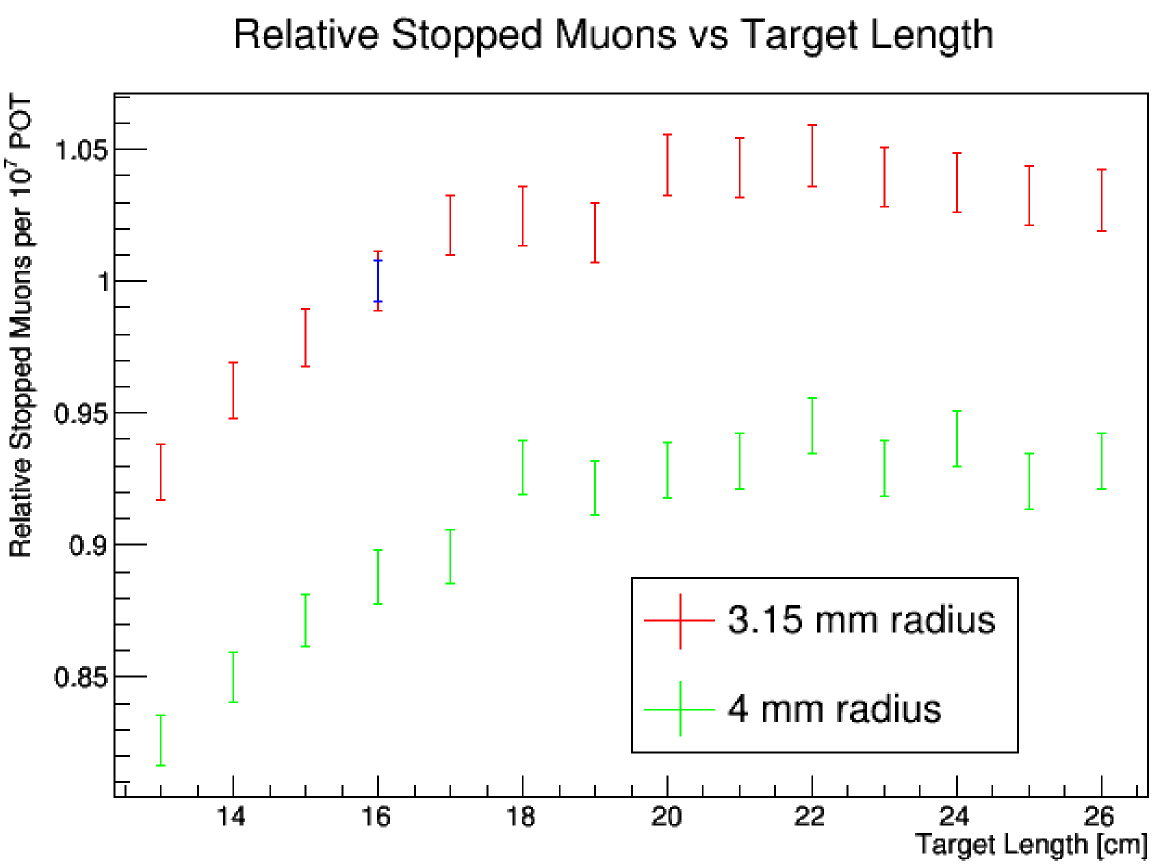

Target environment is hostile

The target is mounted in a vacuum inside the bore of the PS

- This engenders severe heat and radiation load constraints
  - radiative cooling is inefficient
  - there is a non-negligible O_2 partial pressure, leading to chemical erosion
  - high power- density beam produces radiation damage
  - power cycling on many time scales causes fatigue and recrystallization
  - high peak temperature results in erosion and creep

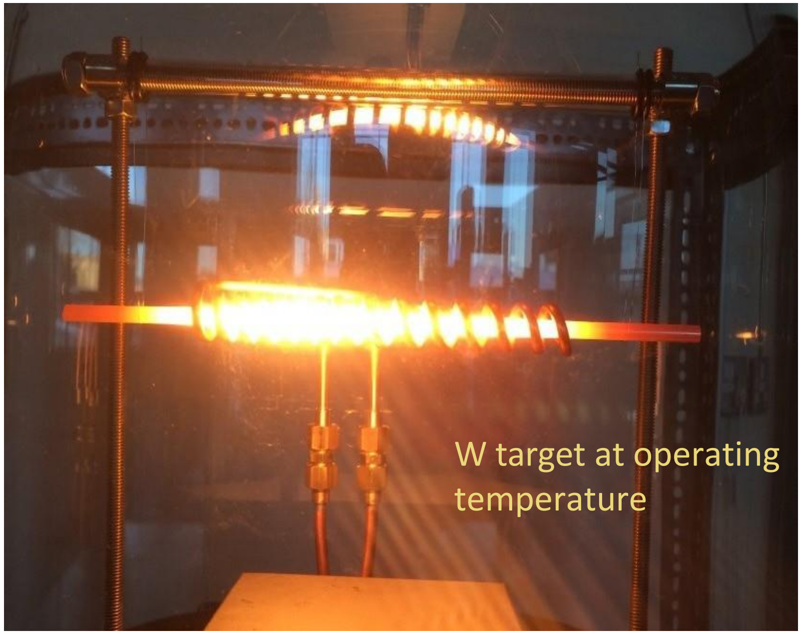

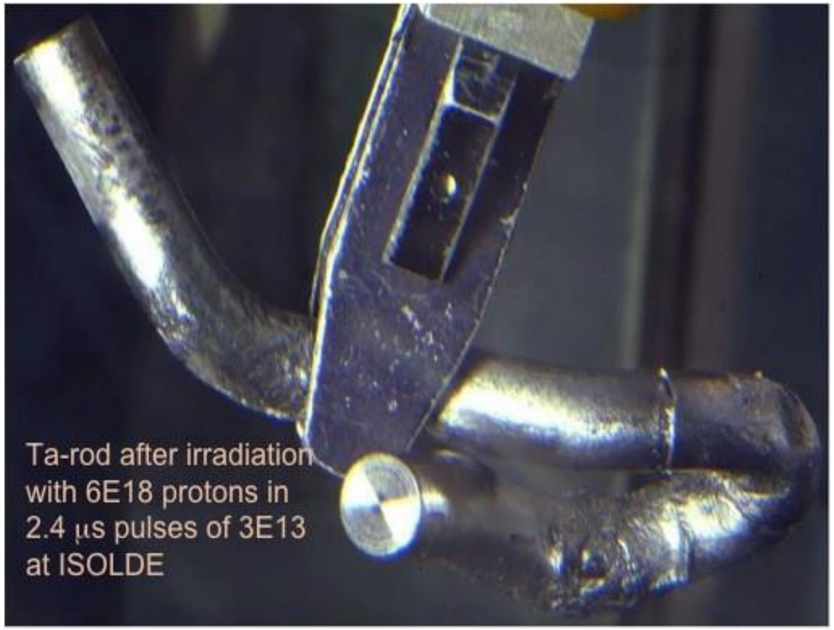

Oxidative Erosion

While tungsten has a low vapor pressure and is thus robust at high temperatures, tungsten oxides are highly volatile, leading to chemical erosion

Tungsten erosion rates

Total Pressure *(Torr)*	Recession Rate *(mm/year)*
1×10^{-6}	Few Microns
1×10^{-5}	0.12
1×10^{-4}	1.8

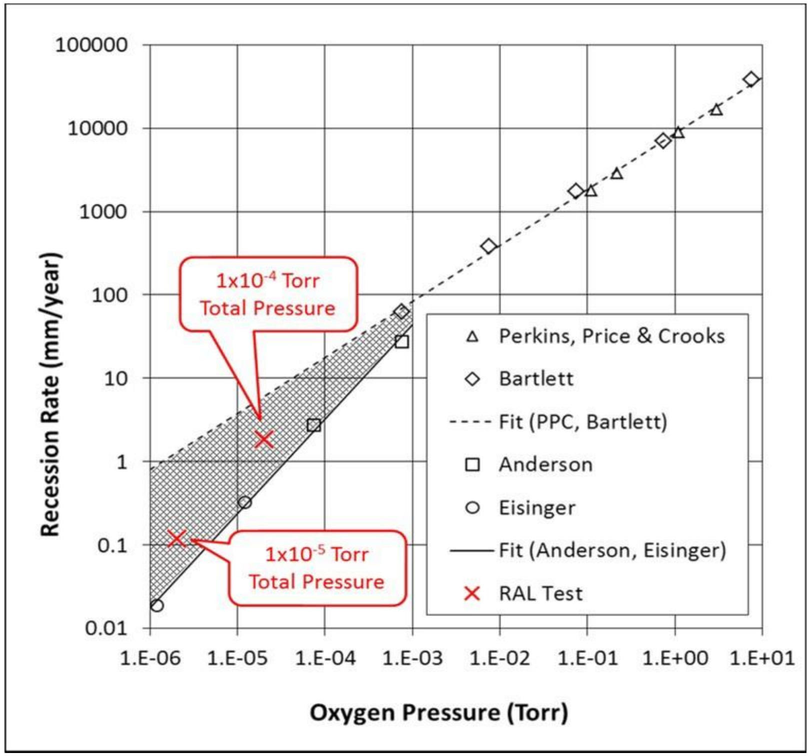

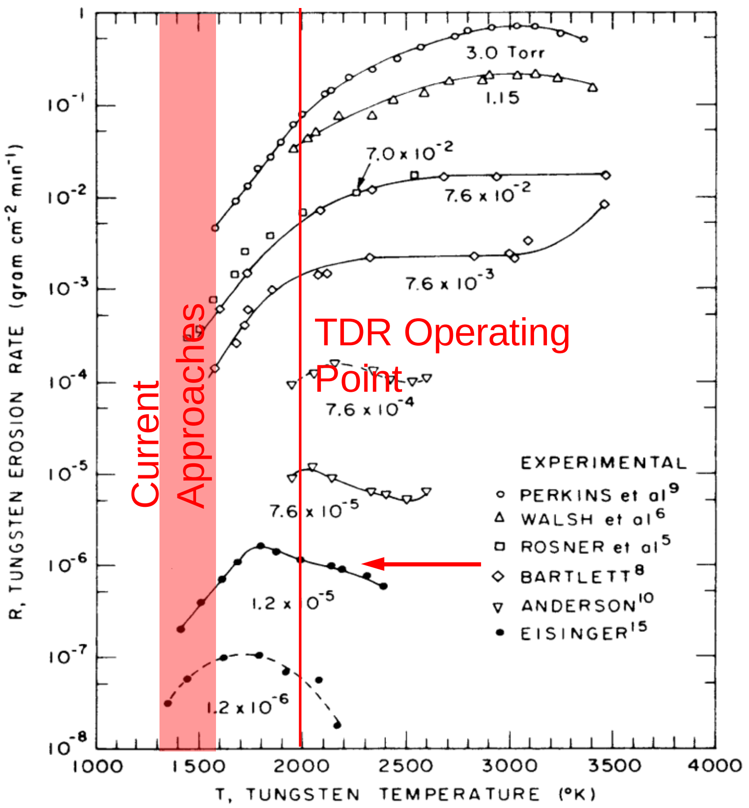

Mu2e tightened PS vacuum requirements to mitigate erosion

Creep at elevated temperature

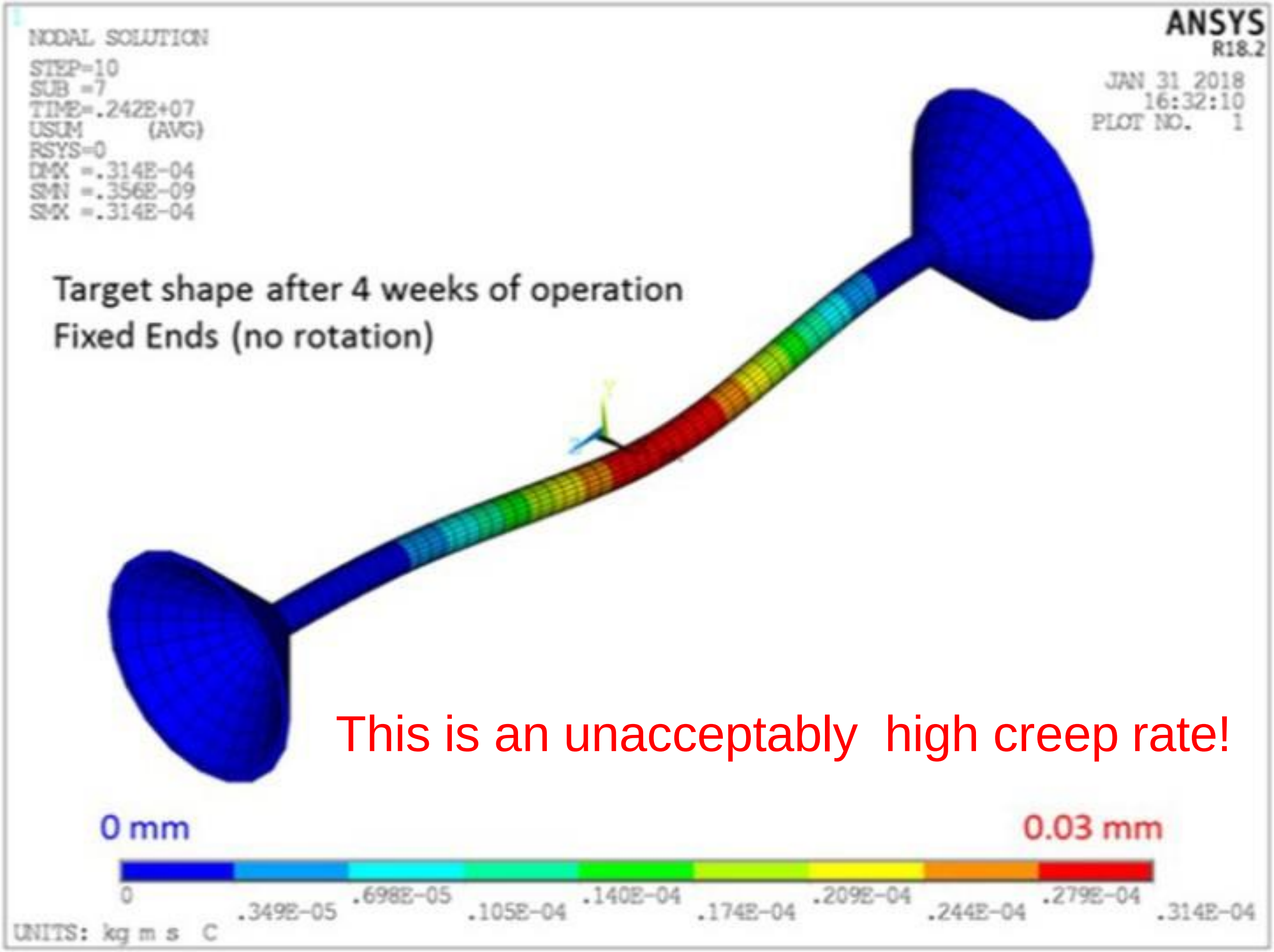

New target designs

Strawman 1

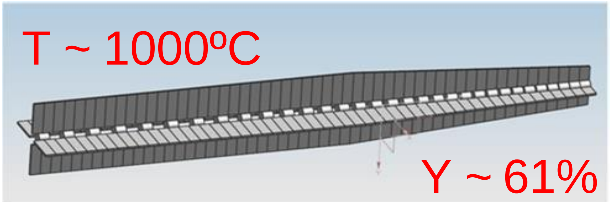

Strawman 3

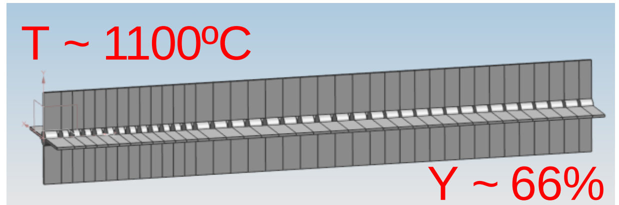

Hangman

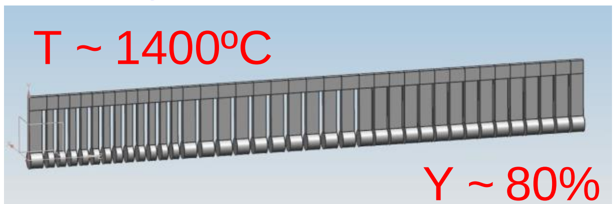

Hayman

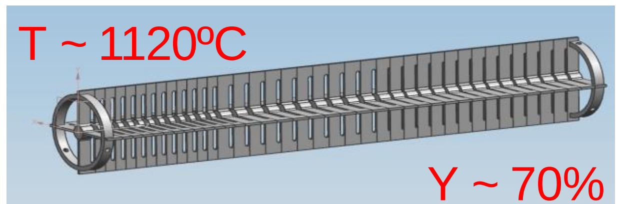

- Segmenting the target reduces mechanical stress
  Fins improve radiative cooling
- However, the additional material reduces muon yield

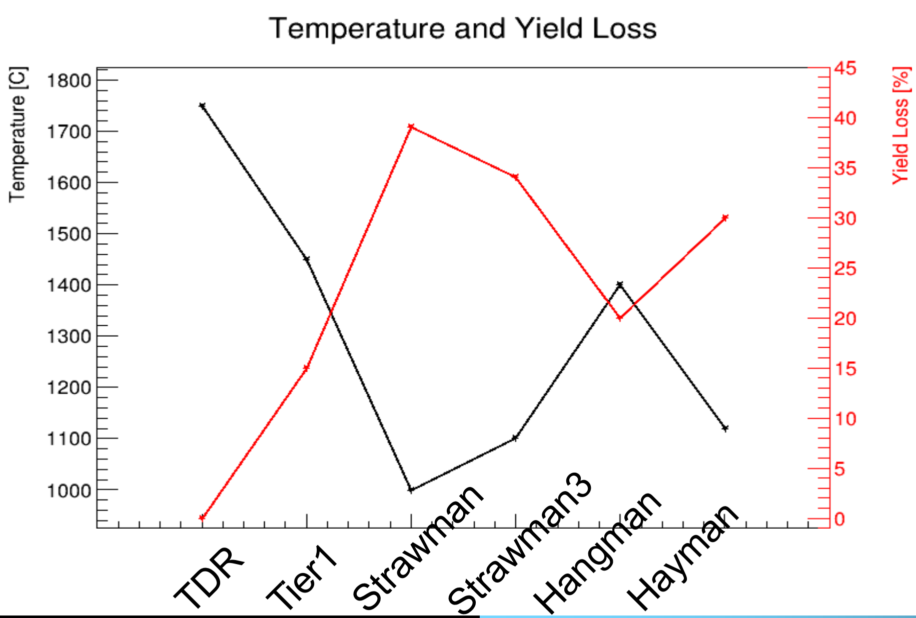

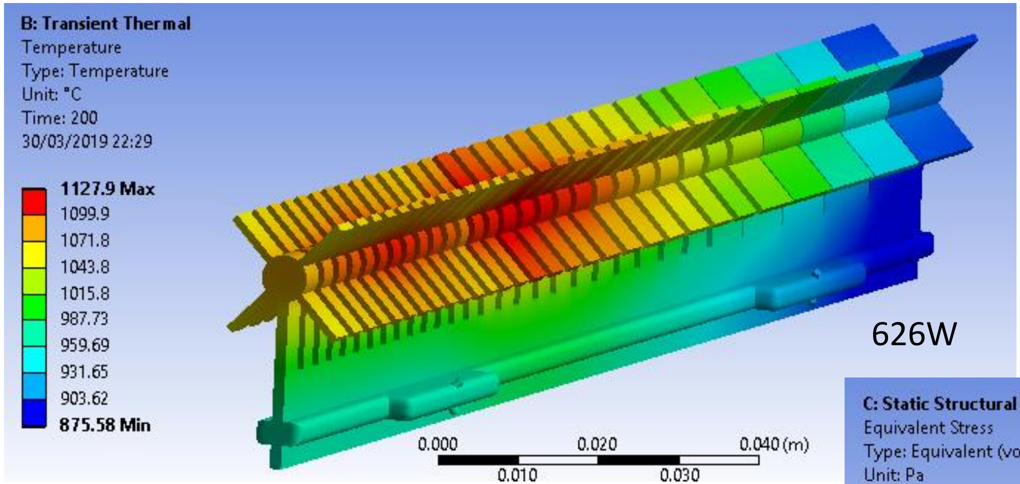

626W

Thermal

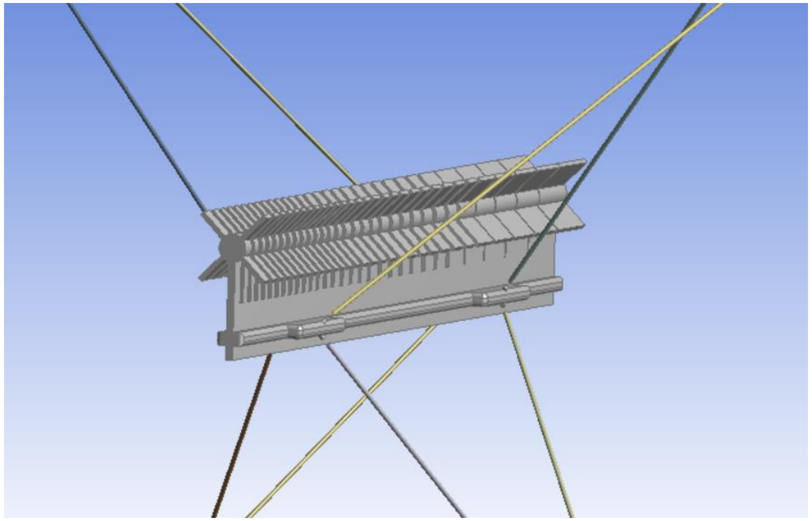

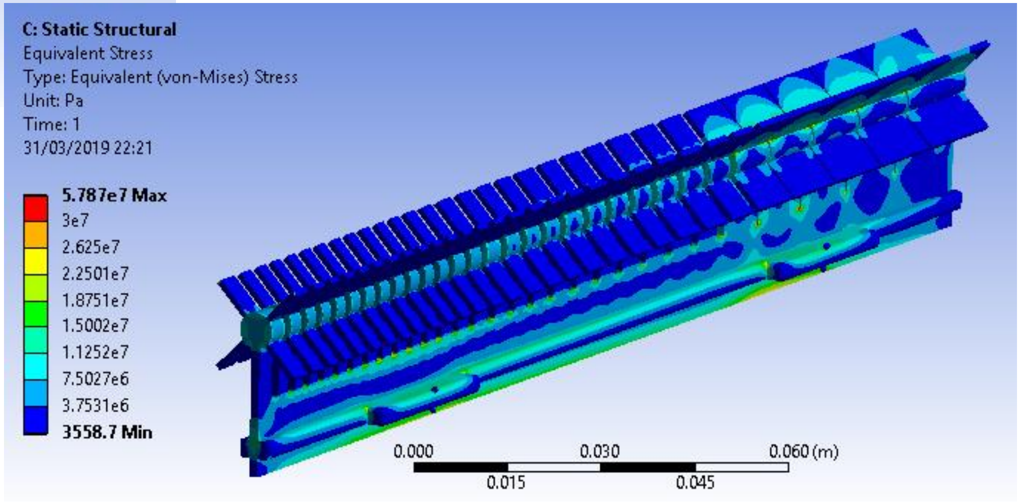

Stress

- **Proton target**
  - Graphite(or SiC)/Tungsten target for Phase-I/Phase-II Geometry
  - optimized to increase the stopping muon yields, **R=13mm, L=700mm**

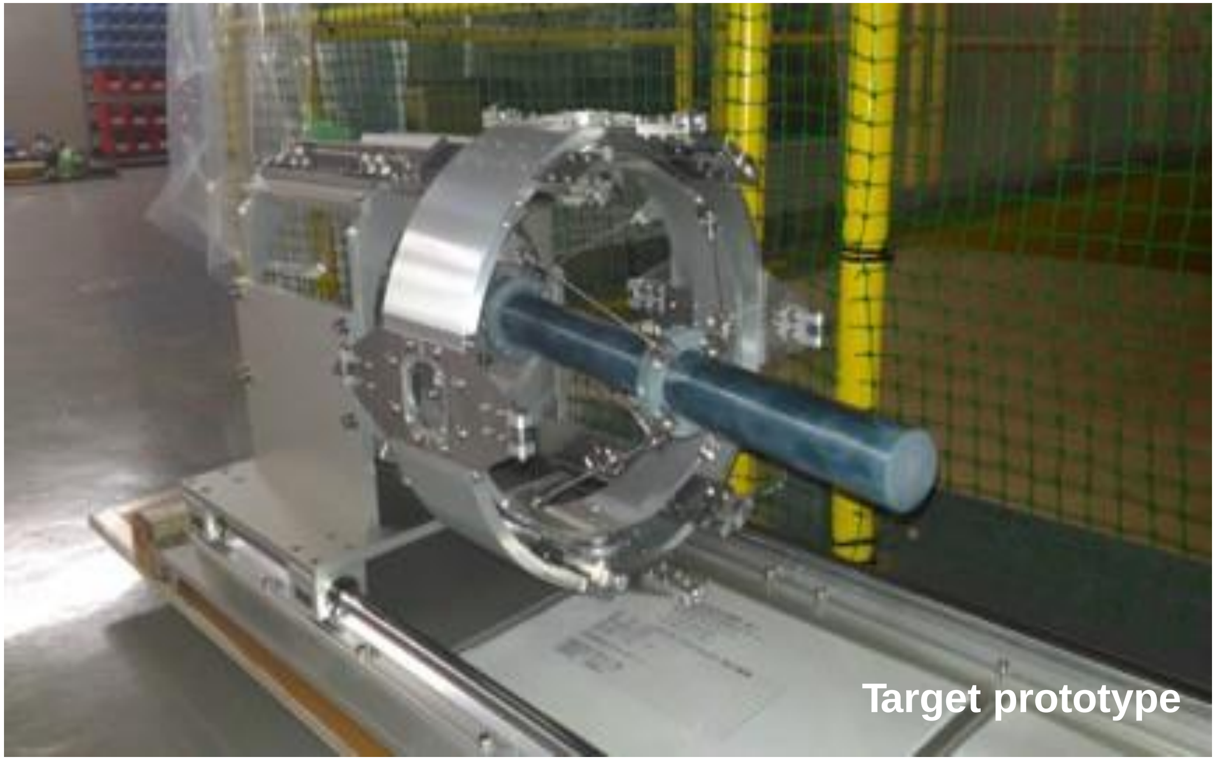

Stopping target

Mu2e Stopping Target

- The Al target has multiple thin layers to allow decay or conversion electrons to exit with minimal scattering
  Baseline: 162 g
  - 37 Aluminum foils with a hole at center
  - 75 mm radius ~100 μm thick

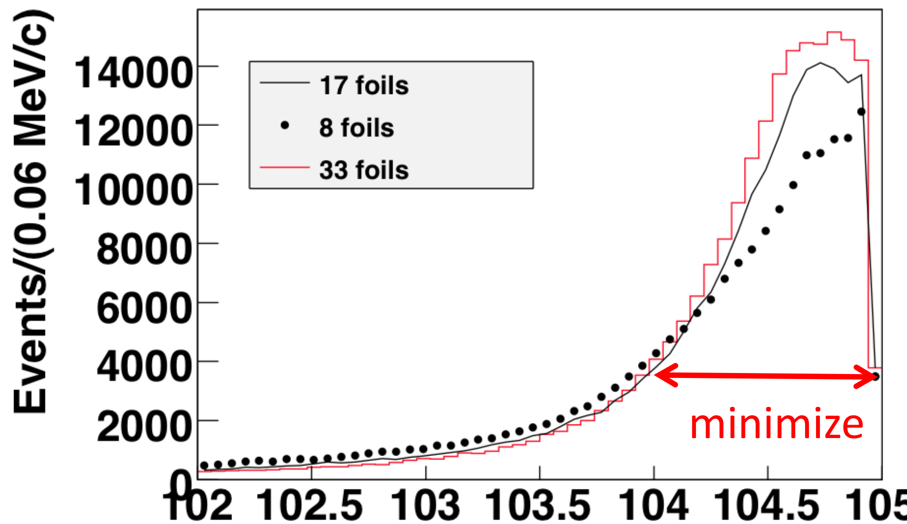

Conversion electron spectrum: p (MeV/c)

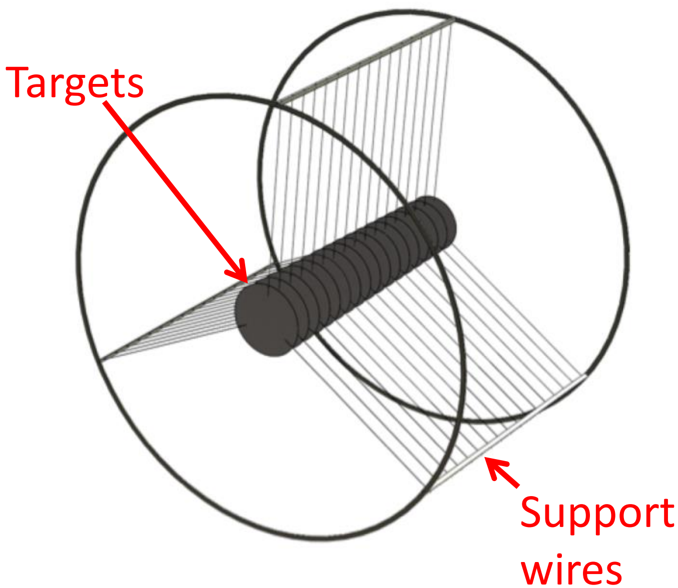

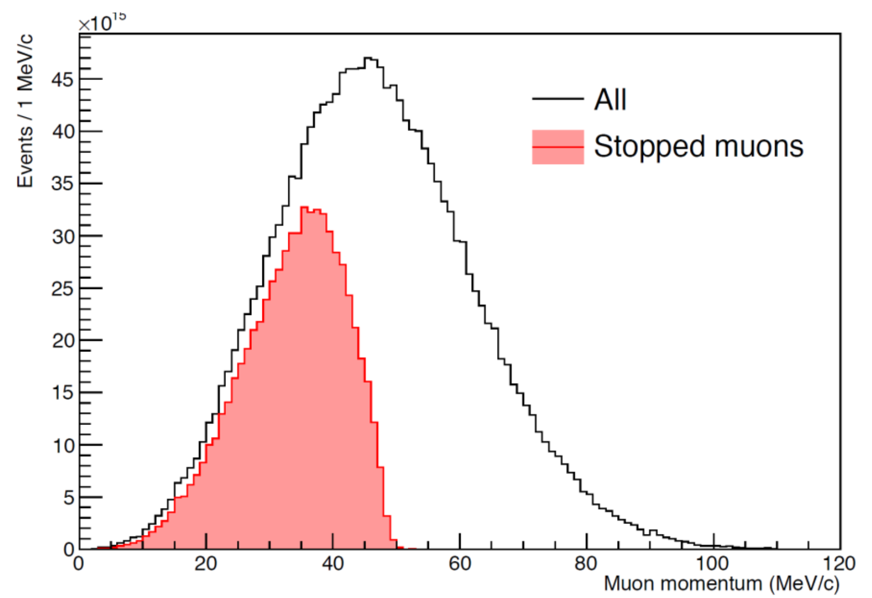

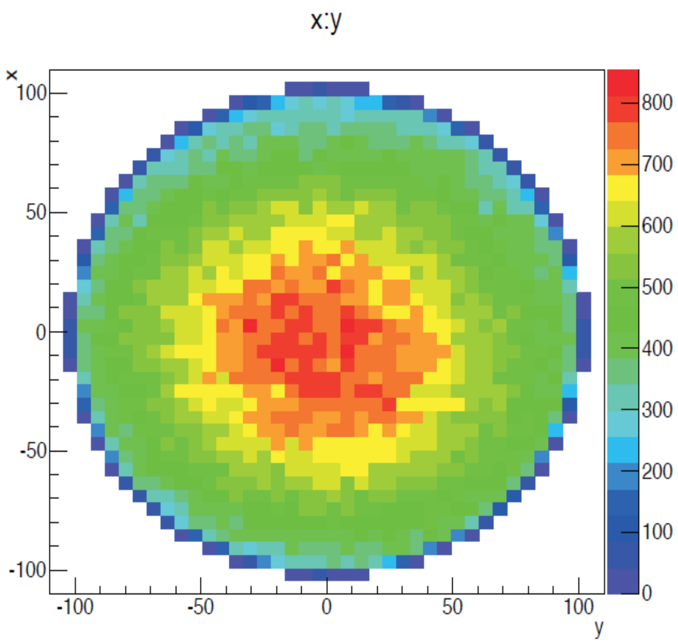

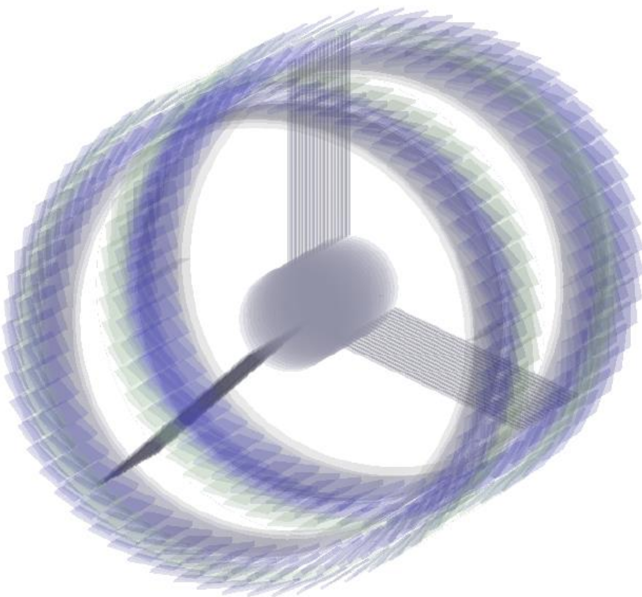

Item	
Material	aluminium
Shape	flat disk
Radius	100 mm disk
Thickness	200 µm
Number of disks	17
Disk spacing	50 mm

Yield (per proton):	After muon-transport section	Stopped in muon target
Muons	5.0×10^{-3}	4.7×10^{-4}
Pions	3.5×10^{-4}	3.0×10^{-6}

- Muon transported in a curved solenoid w/ a dipole field
  - Reduce pions which can produce high momentum secondaries
  - Momentum and charge selection
- Muons stopped inside the series of thin aluminum disks
  - Stopping rate for μ^-/π^- are ~5×10^{-4}/3×10^{-6} / POT

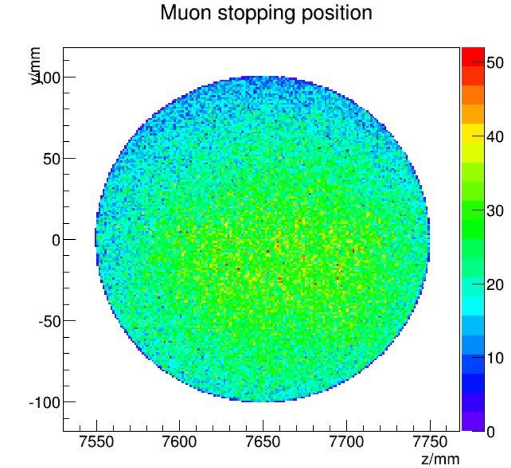

μ- stopping distribution projected on the target plane

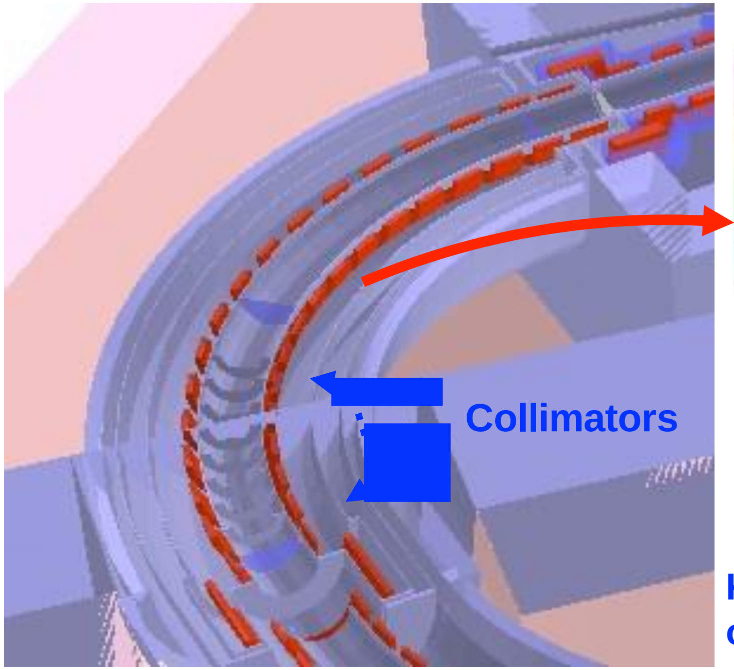

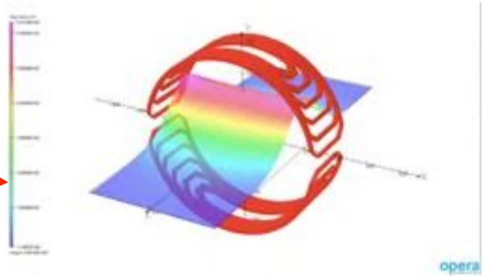

Saddle type coil is put outside of each solenoid coil to generate dipole field

Keep the vertical position of low momentum muons

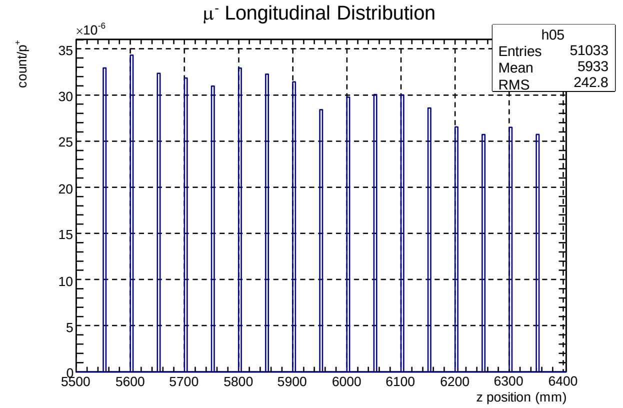

μ- stopping distribution along the beam axis

- Muon stopping target of aluminum
  - Measure acceptance from each disk @TU Dresden
  - Muonic X-ray (2*p*-1*s*) in Al: 346.8 keV
  - Use an isotope of ^{139}Ba: 356 keV
  - Compare with simulations

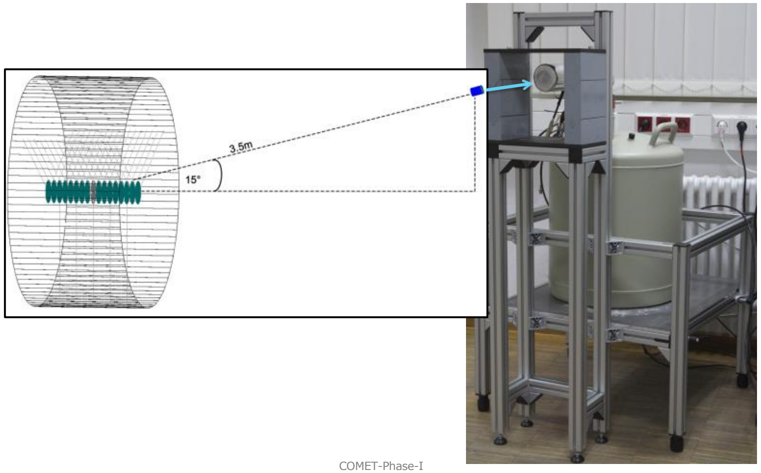

COMET-Phase-I

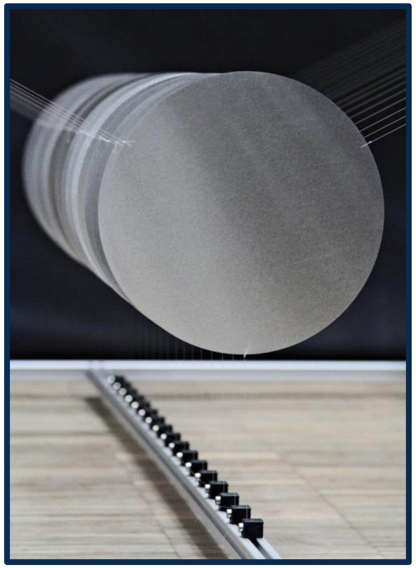

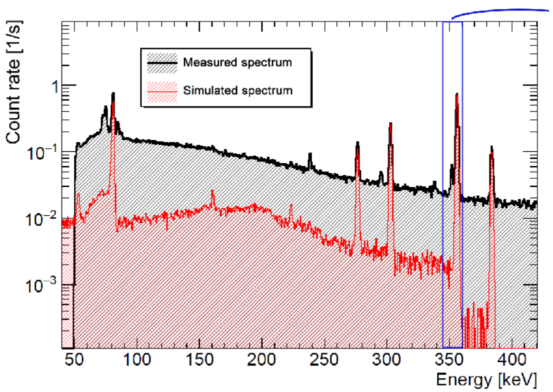

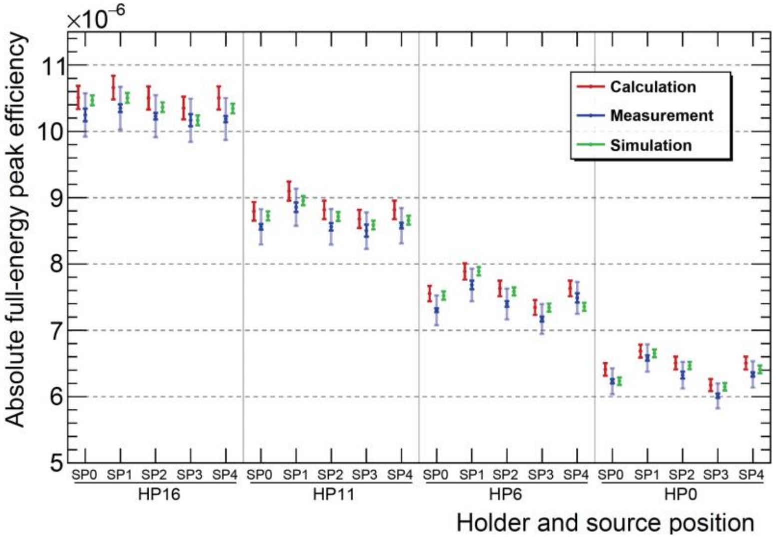

Stopping Target Monitor

Normalization

- The physics quantity we seek is $R_{\mu e} = \dfrac{\Gamma(\mu^- + N \to e^- + N)}{\Gamma(\mu^- + N \to \text{all captures})}$ The numerator is our electron signal
- Generally we do not directly measure the muon capture rate in a conversion search
- The denominator is measured indirectly $\dfrac{1}{\Gamma} = \dfrac{1}{\Gamma_{\text{decay}}} + \dfrac{1}{\Gamma_{\text{capture}}}$
  - Lifetime of the muon – decay or capture
- The lifetime of the muonic atom and the muon capture rate on many nuclei are well-known

  D. Measday, Phys. Rep. 35, 243 (2001)
  - The stopping target for both Mu2e and COMET Phase I is aluminum: ${}^{27}_{13}Al$ abundance is essentially 100% (foils or screens may contain small amounts of other elements)
- There are three clear γ signals produced by μ^- stopping in Al
  - Measure the rate of x-rays from muonic atoms (prompt after a muon stop)
    - **347 keV** 2p-1s transition in Al, 79.8(8)% per muon stop
    - Need good timing to estimate number remaining in the live window
  - Measure a γ resulting from muon capture to an excited nuclear state
    - **1809 keV** γ produced immediately in 51(5)% of captures, 31.1% of stops (confirmed in the AlCap experiment)

      $$\mu^- + {}^{27}_{13}Al \to {}^{26}_{12}Mg^* + n + \nu_\mu \qquad {}^{26}_{12}Mg^* \to {}^{26}_{12}Mg + \gamma(1809)$$
  - Measure γ from decay of longer-lived isotopes produced in muon capture
    - **844 keV** γ 9.2(1.5)% of captures, 5.7% of stops. Need good timing to estimate number remaining in the measurement window

      $$\mu^- + {}^{27}_{13}Al \to {}^{27}_{12}Mg + \nu_\mu \qquad {}^{27}_{12}Mg \to {}^{27}_{13}Al + \gamma(844) + e^- + \bar{\nu}_e \quad \text{(9.5 minute half-life)}$$
- the accepted portion of electrons from DIOs (prompt after capture lifetime)

Normalization - experimental challenges

- The actual normalization for the conversion electron search is to the number of muon stops in the target
- Measuring the 347 keV 2*P*-1*S* x-ray and the 844 keV gamma requires good energy resolution.
- A High Purity Germanium detector (HPGe) is well suited to provide the necessary resolution. However…
  - HPGe is slow and has potential difficulty handling the high anticipated rates
  - HPGe is susceptible to radiation damage from neutrons.
- In Mu2e, the flash of bremsstrahlung photons produced by beam electrons is major background
  - Creates high rates that can damage commercial HPGe
  - To reduce rates, locate HPGe far from stopping target; very small collimators; add absorbers between ST and HPGe: need to reduce rate nominally to 40 K photons above 100 keV/s
- Neutrons produced by muon capture in the stopping target can cause detector damage to HPGe
- Collimators before the HPGe must be carefully aligned so that the detector views the target and little else that could produce backgrounds

Stopping target monitor (STM) placement

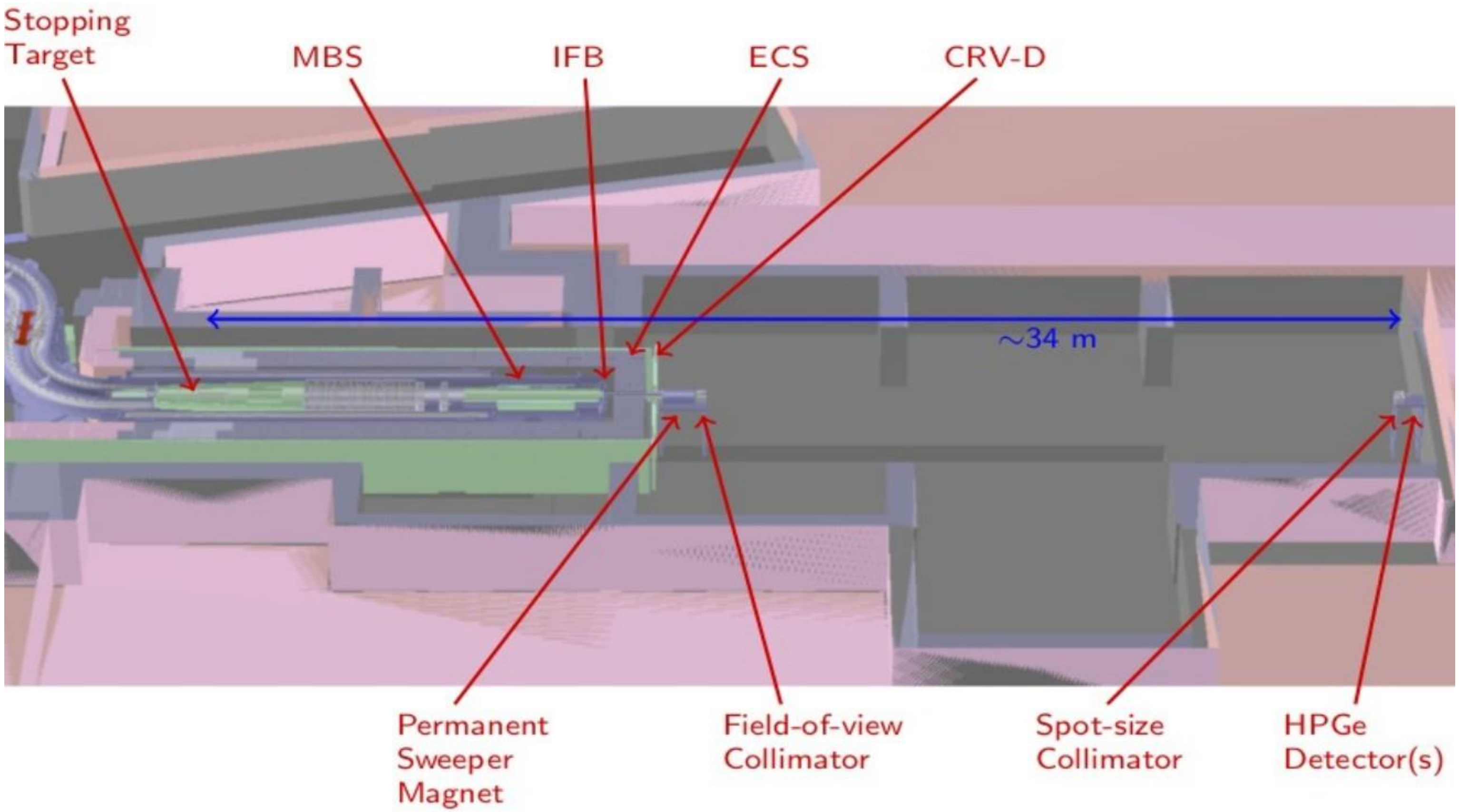

The STM will measure a variety of well understood gamma ray lines … under a high-rate brehmstrahlung background

AlCap spectra with an HPGe detector

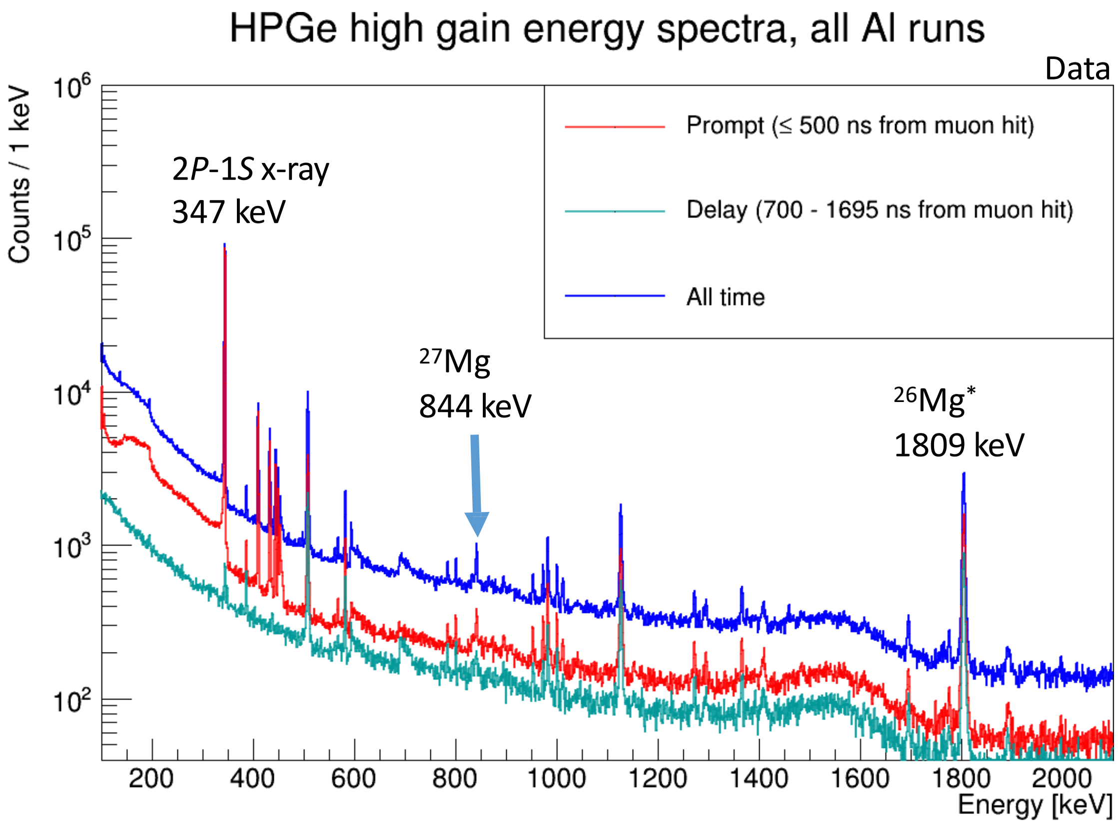

- Excellent energy resolution provided by HPGe is required to isolate signal
  - Radiation damage due to γ flux is not severe
  - Neutron damage is serious: HPGe resolution of ~ 2keV will deteriorate to 3keV after dose of ~1.5×10^{10} neutrons (17 months at full intensity)

Potential background lines

Other materials can generate backgrounds : W, Pb, Ti, SS, mylar, polyethylene

near 347 keV

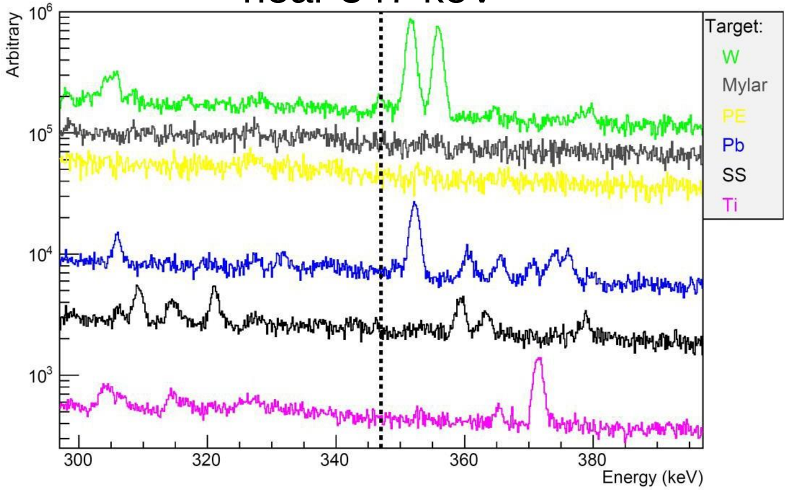

near 844 keV

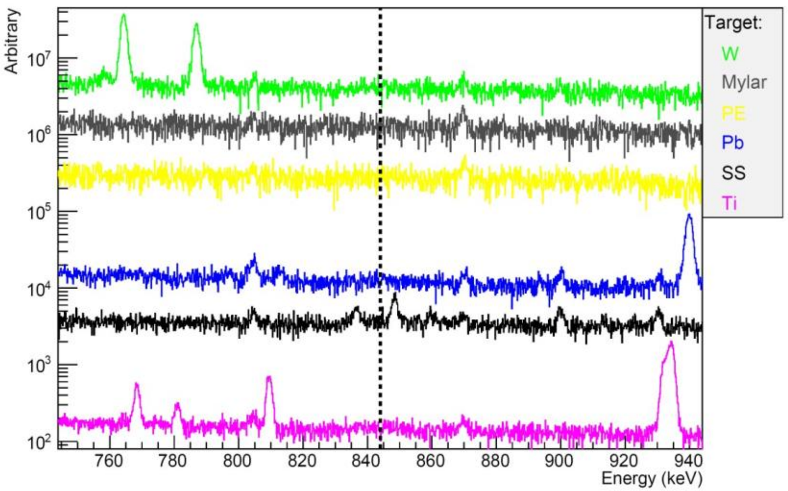

near 1809 keV

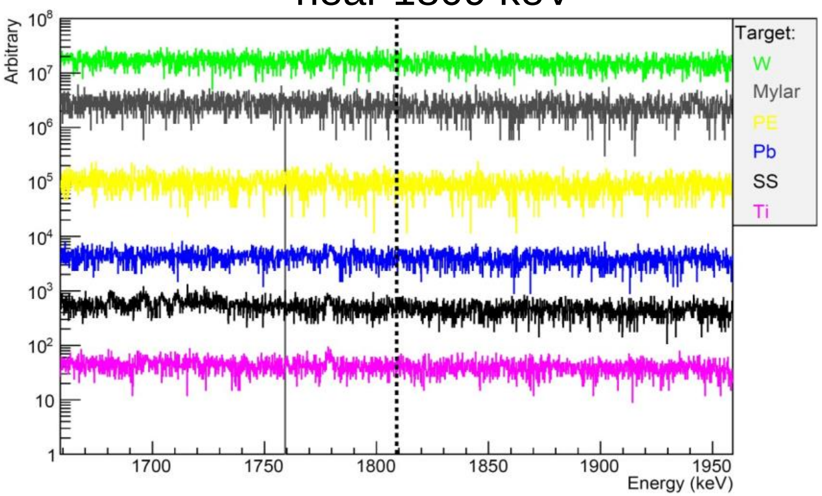

Lanthanum bromide scintillator

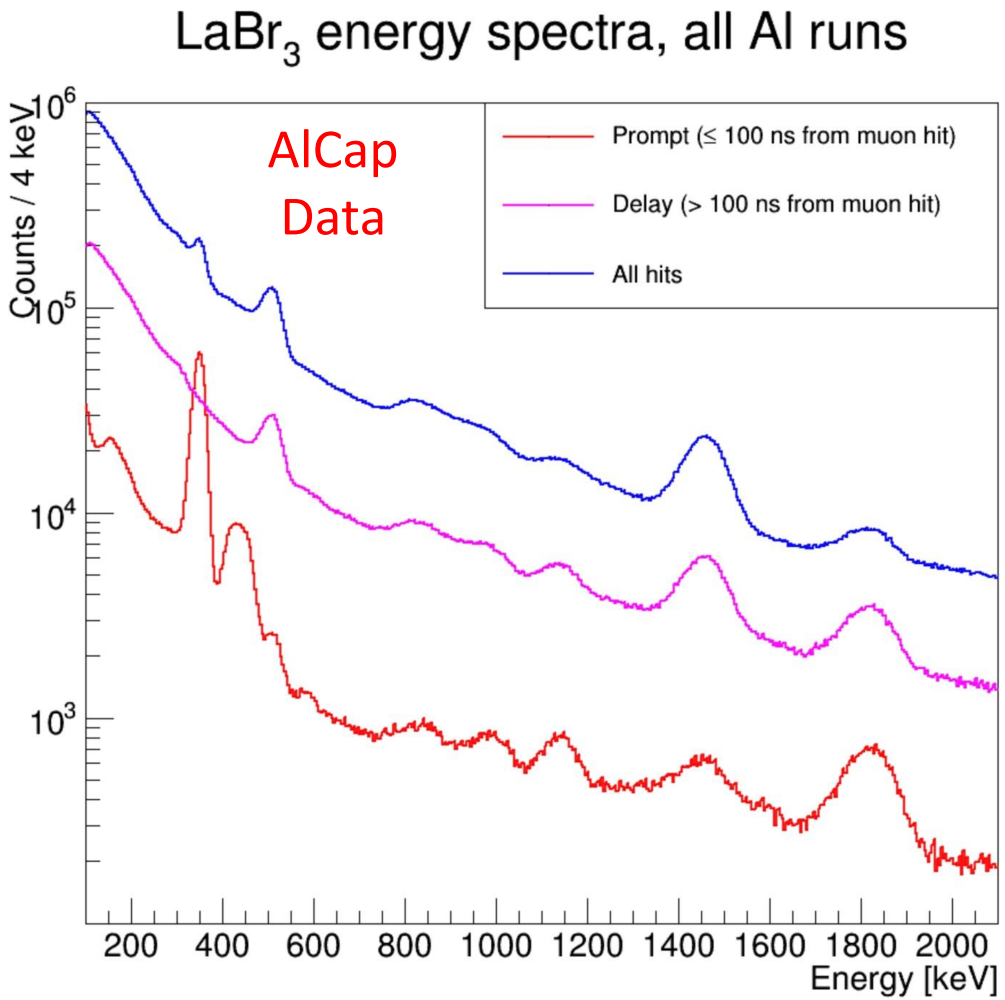

- $LaBr_3$ is a very fast, radiation hard, scintillator that can handle the high rates in Mu2e
  - Energy resolution is an order of magnitude worse than HPGe
- Mu2e is considering incorporating several $LaBr_3$ crystals on periphery of the first crystal annulus

Extinction

We must enforce strict beam extinction between proton pulses

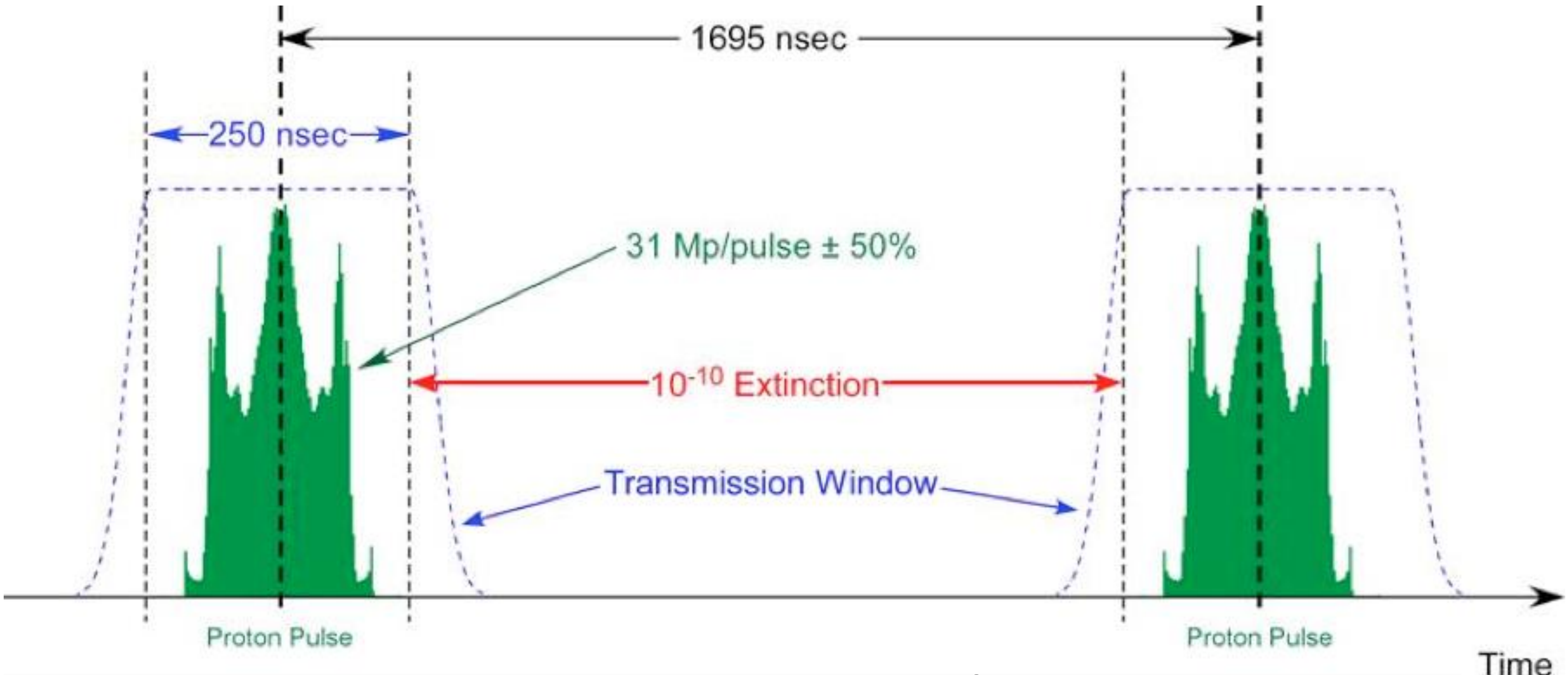

31 Mp = 31,000,000 protons/pulse

$$Extinction = \frac{\#\, protons \text{ not in pulse}}{\#\, protons \text{ in pulse}} \simeq 10^{-10}$$

Allow sufficient time between pulses to reduce backgrounds

Proton beam extinction

Fermilab's Muon Campus Beam Lines

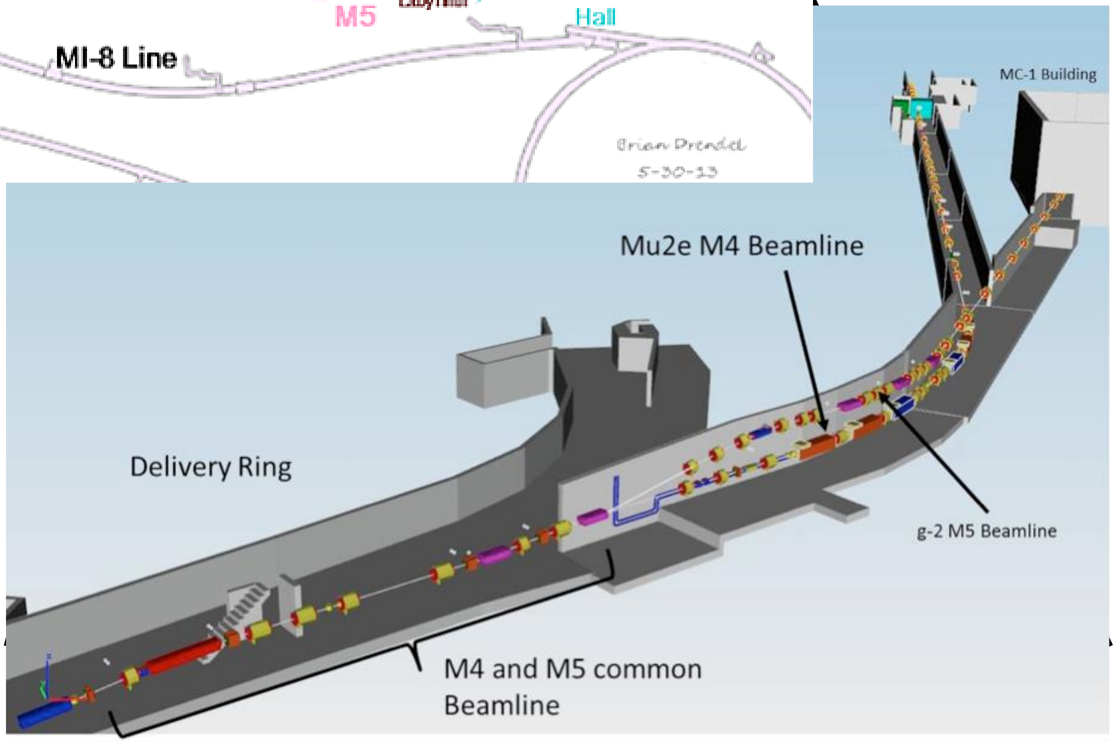

Beam into the M4 beamline from the Recycler + Delivery Ring will already have a between pulse extinction of 10^{-4} or better

Extinction in two steps

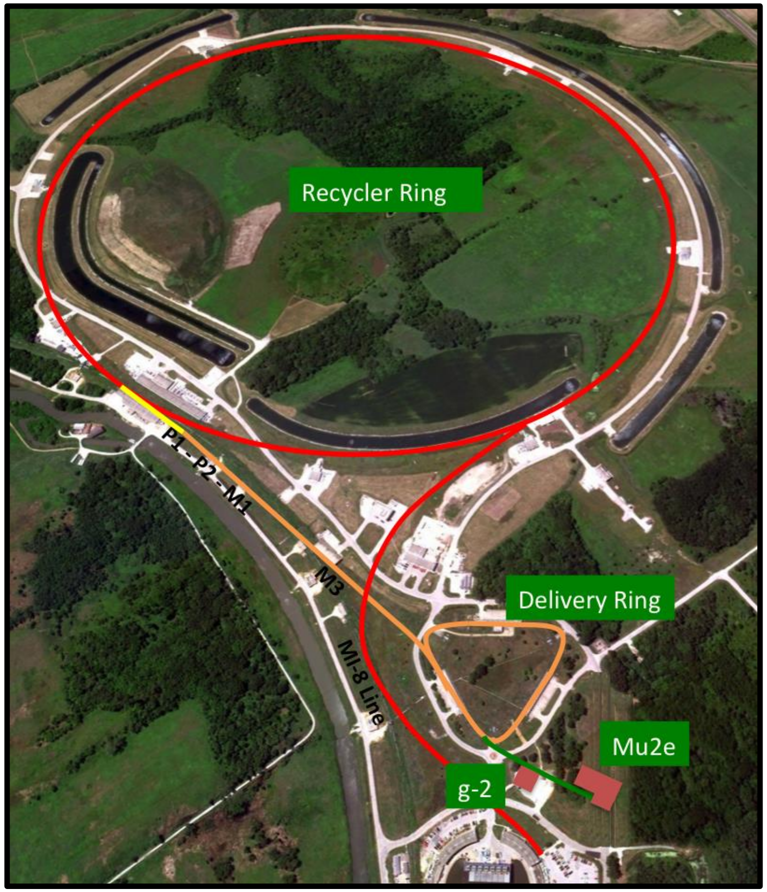

1. Beam formation directs proton pulses to Mu2e production target
   - Extinction factor $\sim 10^{-4}$ or better
2. Oscillating dipoles ("AC dipoles") in beamline deflects out-of-time beam
   - Additional extinction factor $\sim 10^{-7}$ or better

AC Dipole Magnet

External Beamline Extinction Components

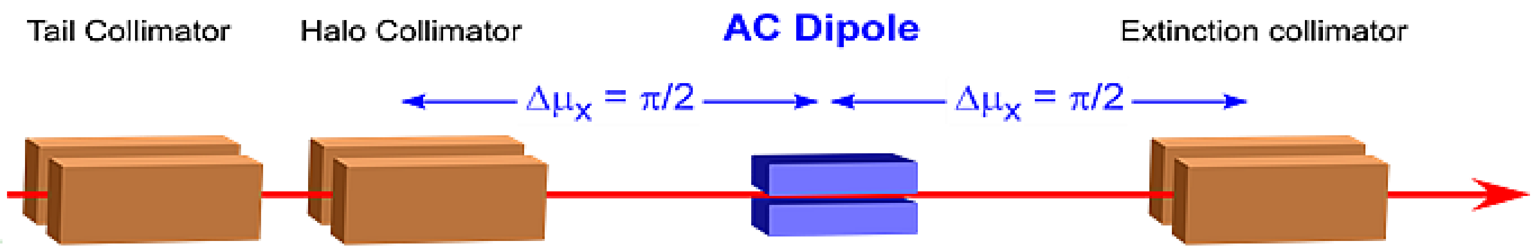

Extinction Level: 2×10^{-5} | Factor of 5×10^{-8} | 1.1×10^{-12}

Normalized Phase Space of Out-of-Time Beam

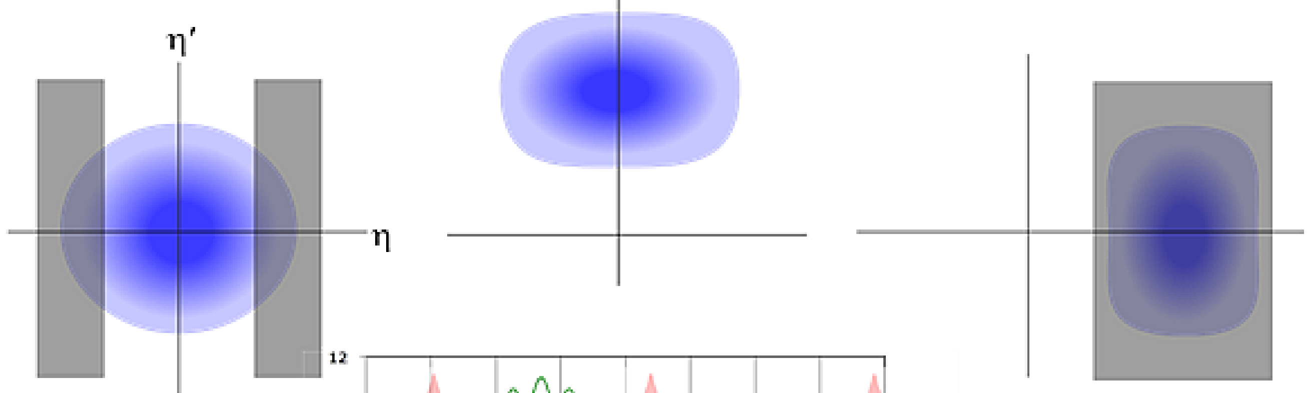

AC Dipole Excitation

The AC Dipole excitation is a superposition of two harmonics: 300 kHz and 4.5 MHz.

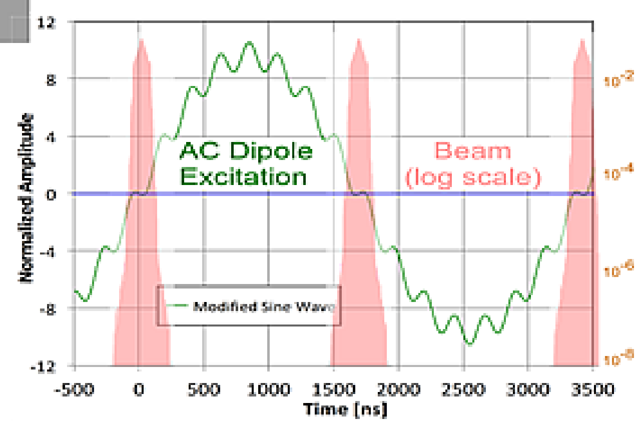

Proton beam pulses shown in pink.

AC Dipole waveform shown in **blue**

Green = ESME simulation of extracted beam from Delivery ring

Black = G4Beamline simulation of external AC dipole + collimators

Blue = Convolution of the two

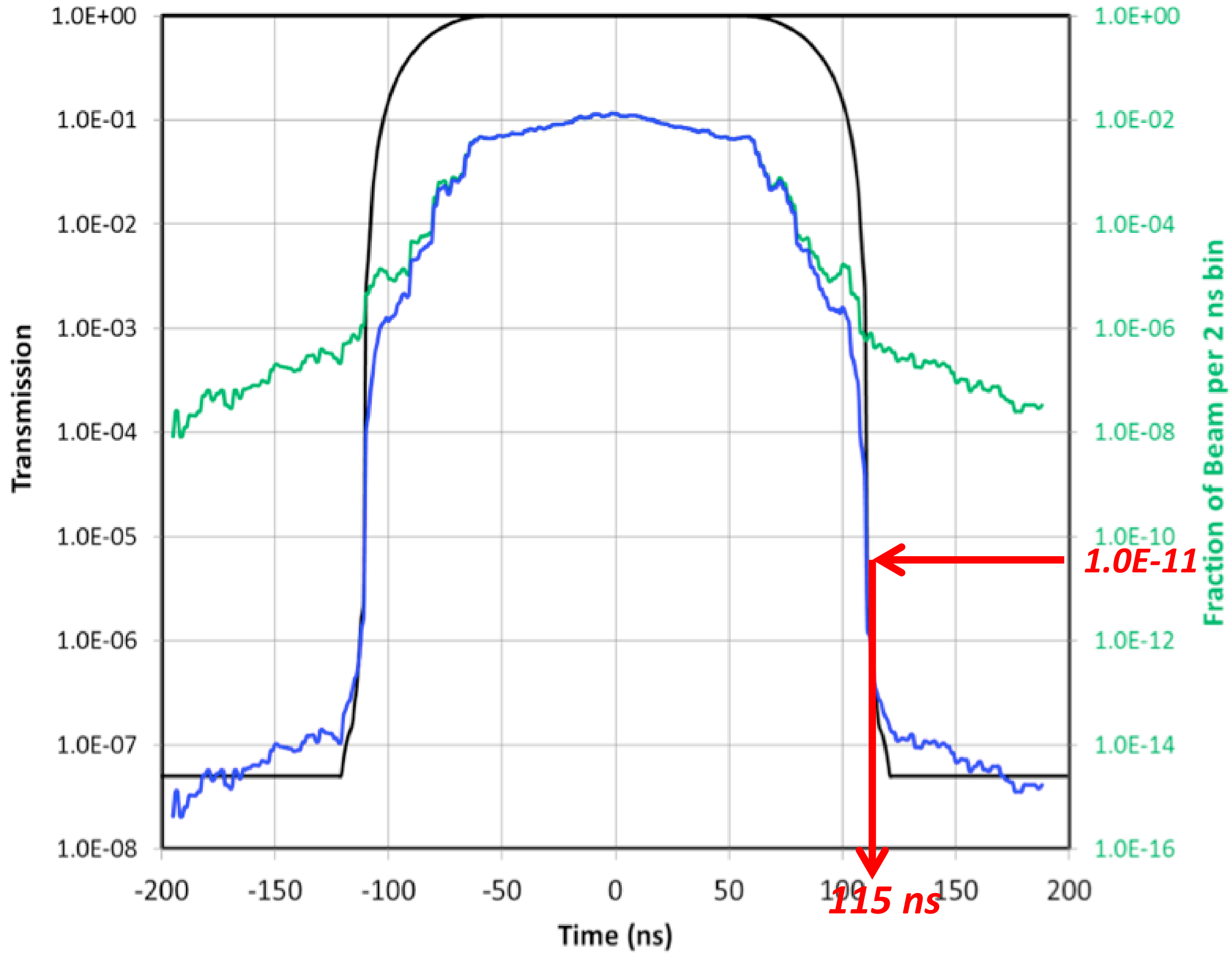

Better than 10^{-11} extinction for beam outside the 230 ns transmission window!

Extinction Monitor

- Achieving 10^{-10} extinction is difficult, but it's not useful unless we can verify it
- We must measure extinction to 10^{-10} @ 95% CL
- Sensitivity roughly 1 proton every 300 bunches!
- A monitor sensitive to single particles is not feasible
  - It would have to be blind to the $3x10^{7}$ particles in the bunch.
- We therefore focus on a statistical technique
  - Design a monitor with good time resolution to detect a small fraction of scattered particles from target: 10-50 per in-time bunch
  - Build up precise statistical profile for in time and out of time beam.
- Goal: Measure extinction to a precision of 10^{-10} in a few hours
- 4×10^{7} protons per pulse
- $\Rightarrow$ 1 out of time proton per 250 pulses
- 6×10^{12} proton/s $= 150{,}000$ pulses/s
- $\Rightarrow$ Extinction measurement time: $10{,}000$ s
- $\Rightarrow 6 \times 10^{16}$ protons on target
- Need 2.3×10^{10} particles to set limit
- $\Rightarrow$ Must count at least $\approx$ **16 particles per pulse**

The Extinction Monitor verifies the degree of extinction between pulses

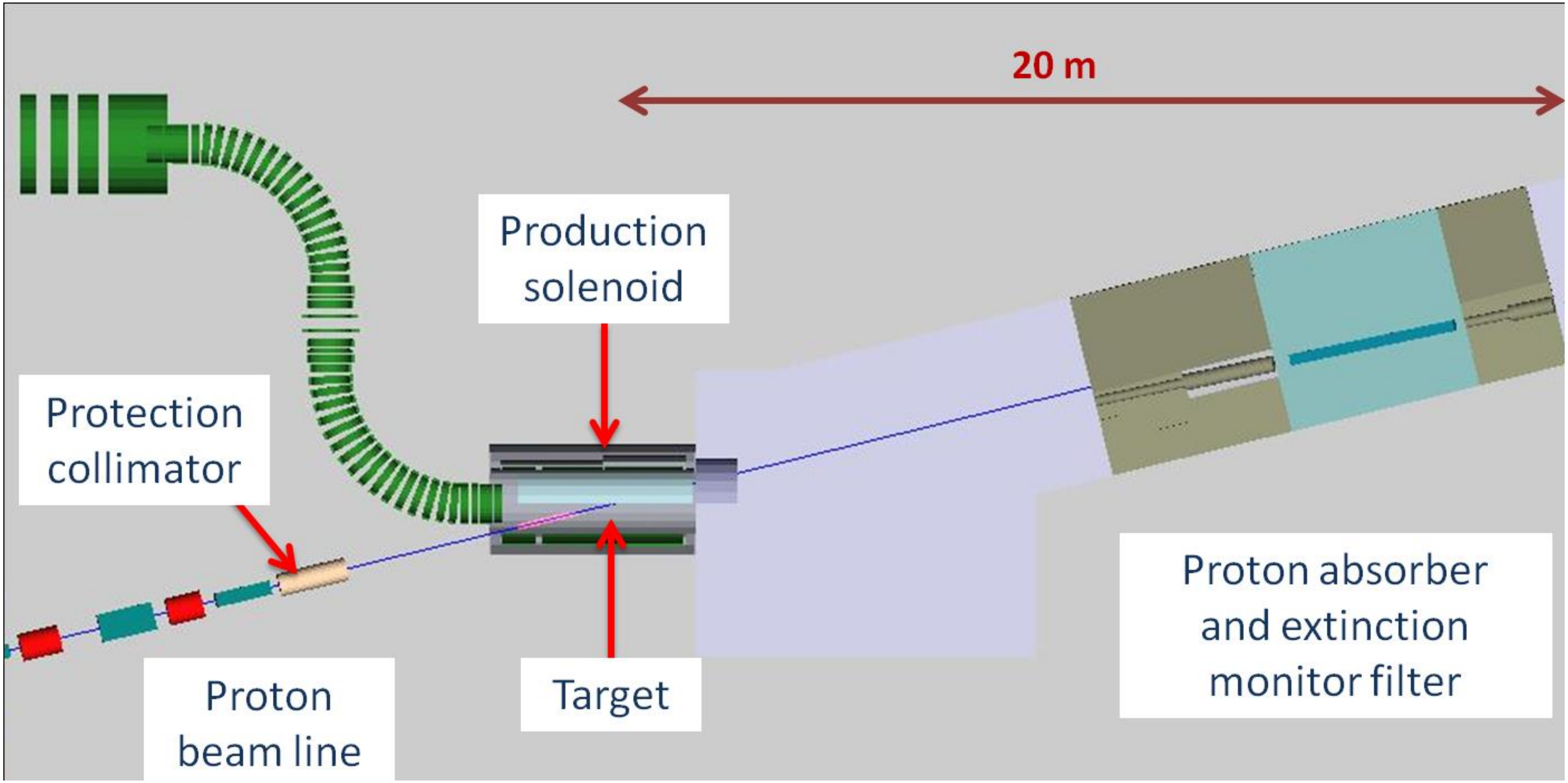

Extinction Monitor Design

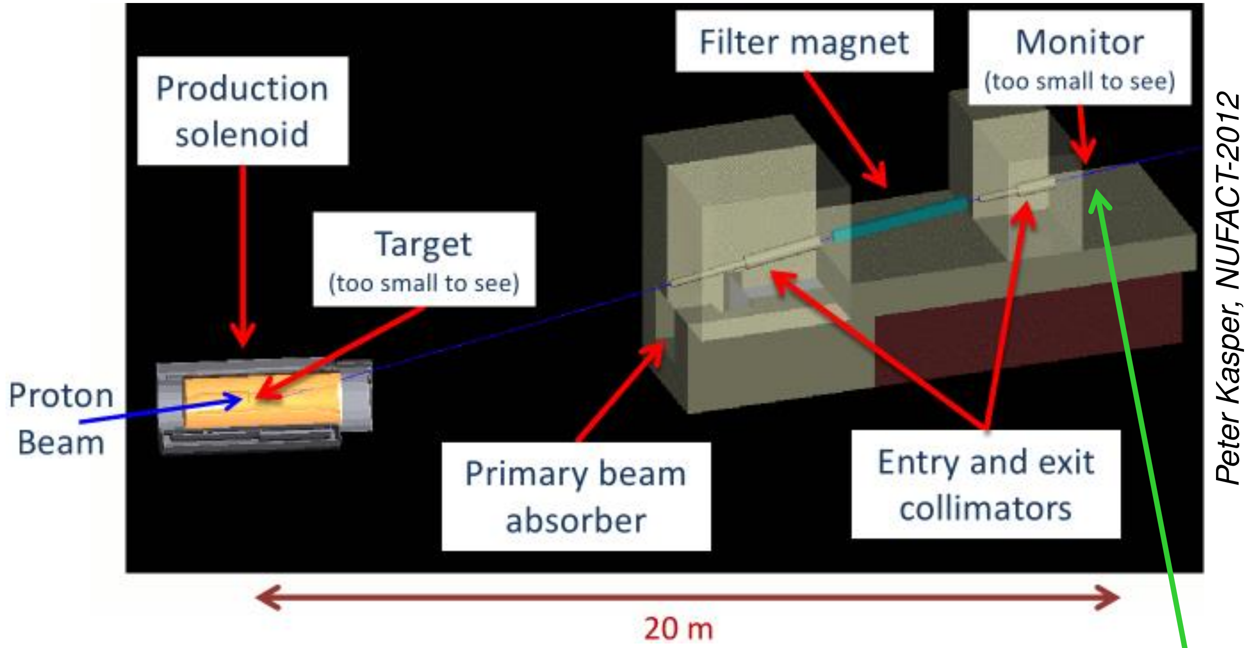

Selection channel built into target dump channel

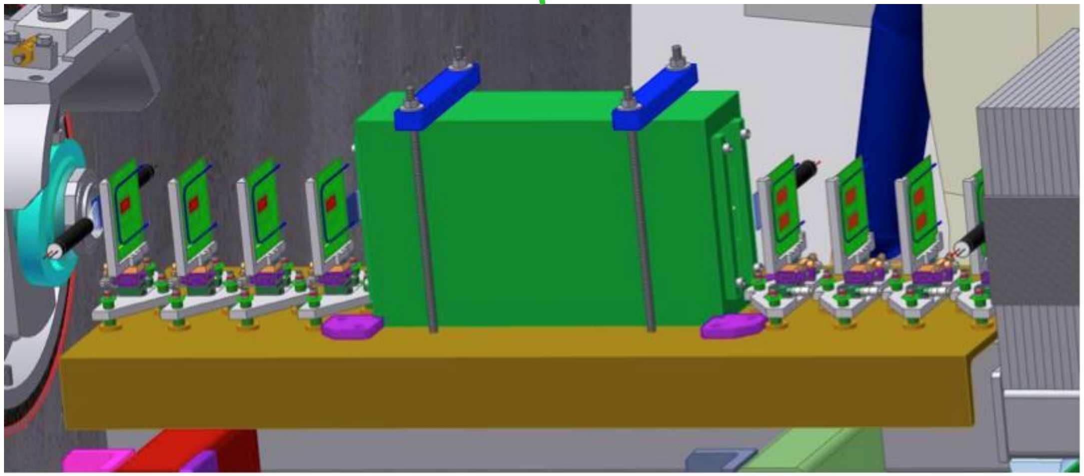

- Spectrometer based on 8 planes of ATLAS pixels
- Optimized for few GeV/c particles

Tracker

Particle trajectories in solenoids

- Particles in a solenoidal field will move in a helical path
- Low momentum particles are effectively "trapped" along the field lines
  - We use this to transport muons
- A particle trapped along a *curved* solenoidal field will drift out of the plane of curvature
  - This is how we will resolve muon charge and momentum in the transport line
- For higher momentum particles, the curvature can be used to measure momentum
  - This is how we will measure the momentum of electrons from the capture target
  - In Mu2e we also use the radius of curvature to keep DIOs out of the main tracker

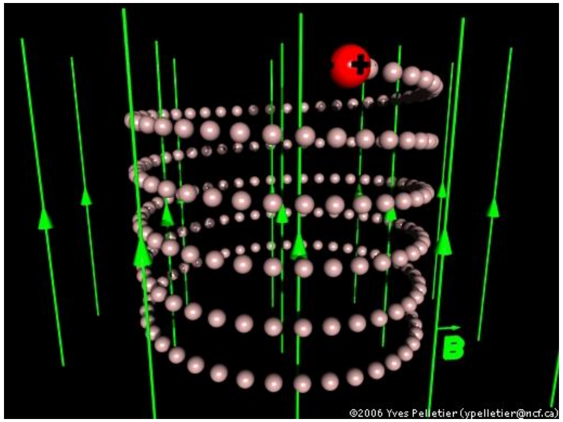

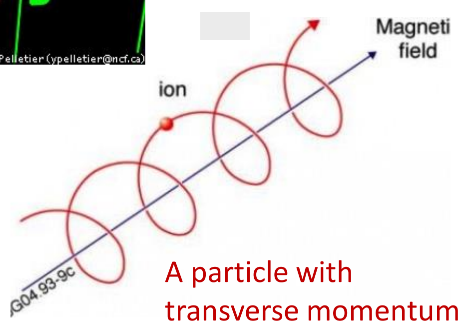

A particle with transverse momentum of 10 MeV/*c* has a radius of 3 cm in a 1 Tesla magnetic field

Mu2e tracker design evolution

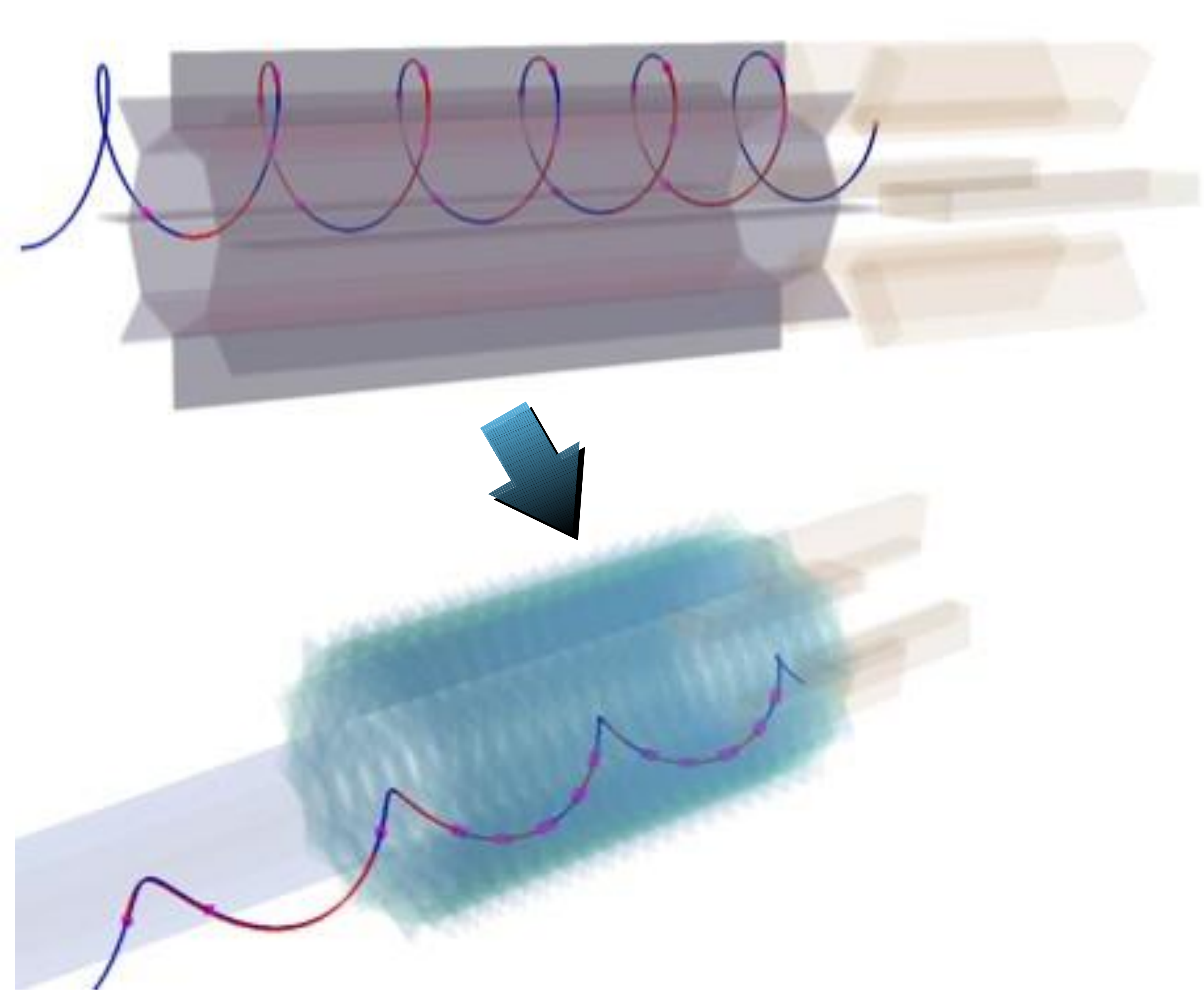

Pattern recognition

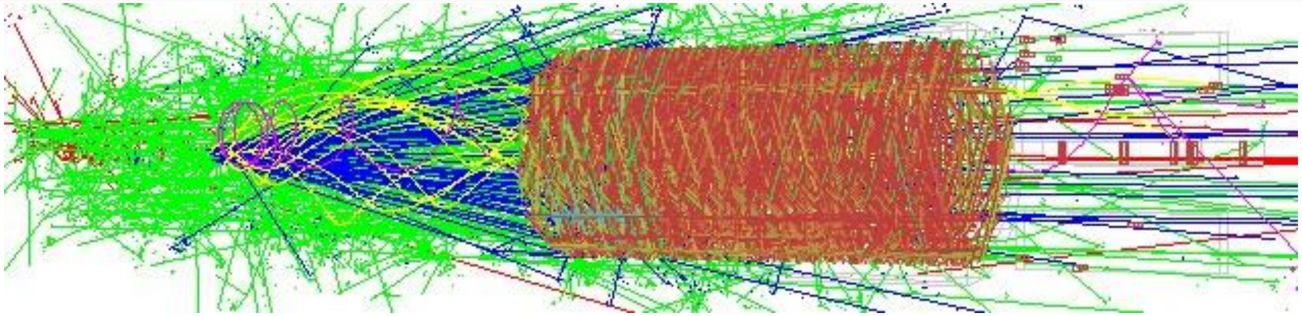

Single proton pulse: particles and hits in 500–1694 ns

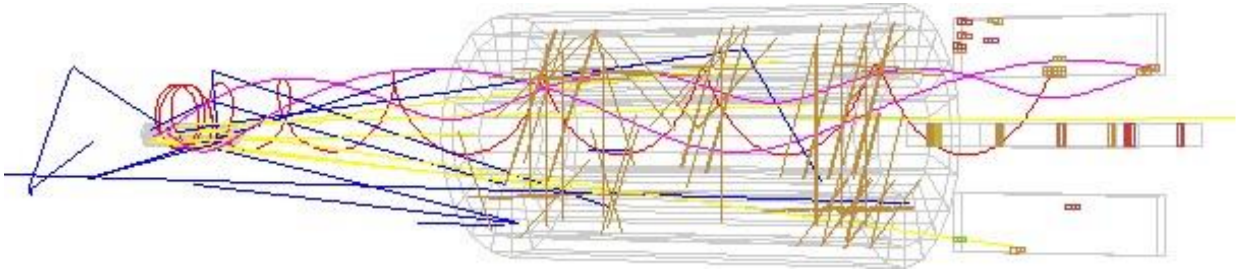

Single proton pulse: particles and hits in ± 50 ns around conversion

- Hit rates
  - From beam flash (0-300 ns): ~1000 kHz/cm
  - The tracker must survive this, but won't collect data in that period
  - Later, near live window (>500 ns)
    - Peak ~ 10 kHz/cm^2 (inner straws)
    - Average ~ 3 kHz/cm^2 (overall)

Helical trajectory

Charged tracking

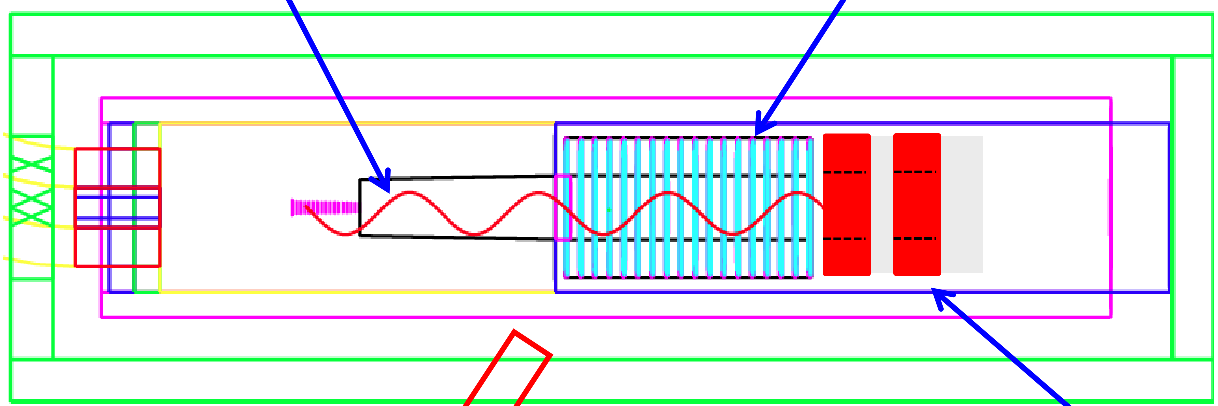

Conversion electrons
hit multiple planes.

Electromagnetic Calorimeter
identifies electrons

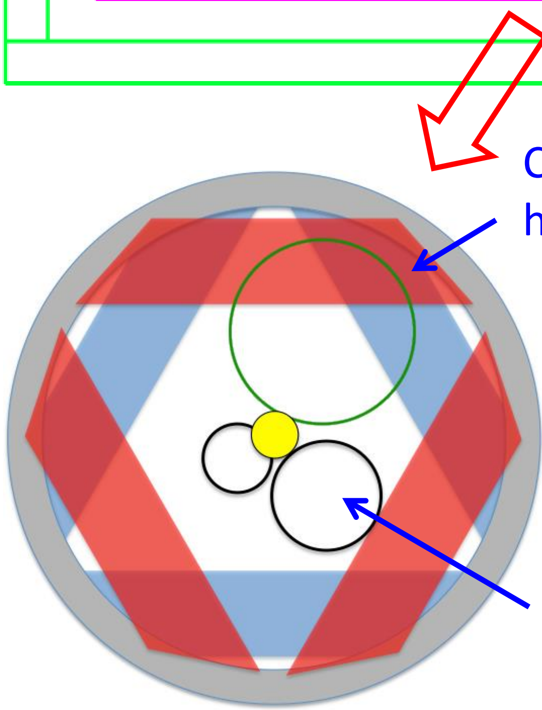

Most muon decays (p_T <53 MeV/c)
go down the middle (vacuum)

Tracker panel structure

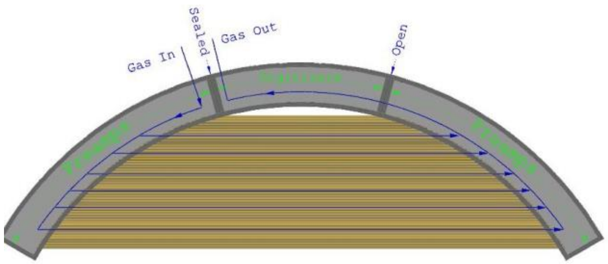

Custom ASIC for time division:
σ ≈ 5 mm at straw center

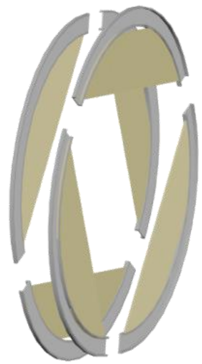

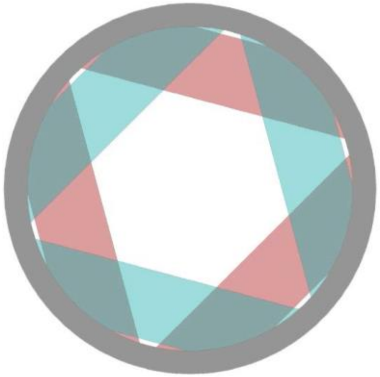

2 planes

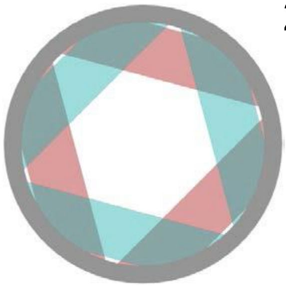

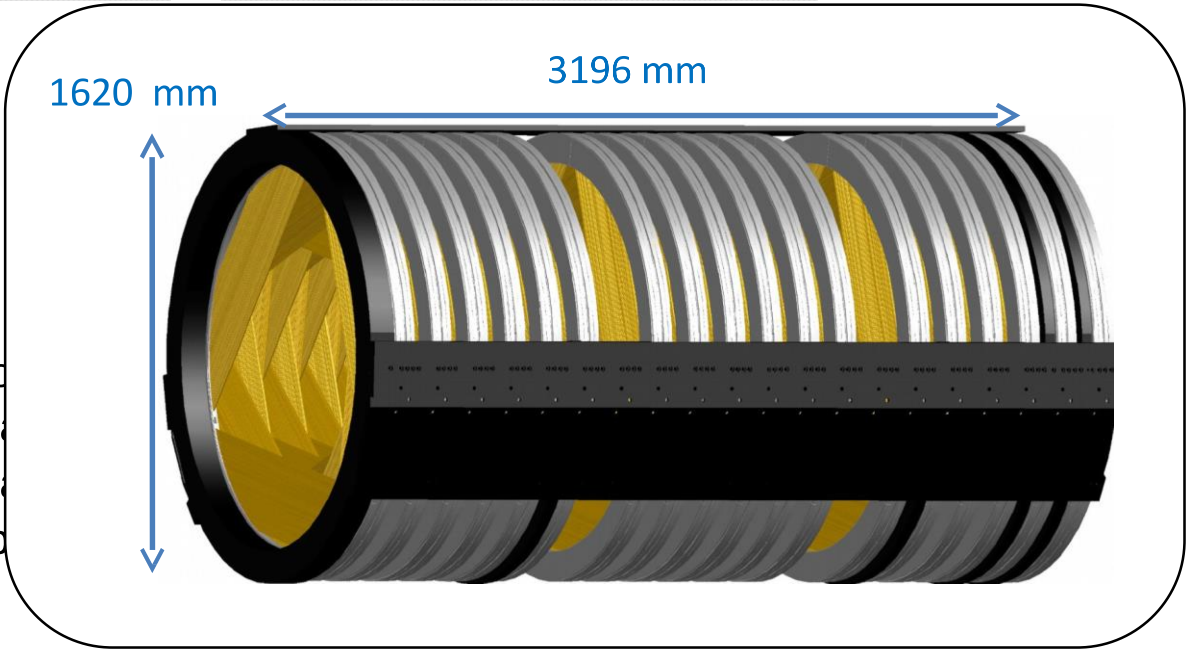

- Each self-supporting panel co
- 6 panels are assembled to ma
- 2 planes are assembled to ma
    - Rotation of panels and p
- The tracker has 18 stations
- >20 k straws total
- Low mass to minimize multiple coulomb scattering (track typically sees ~ 0.25 % X_0)

Particle Tracking Technology

- To achieve the required resolution, we must keep the mass as low as possible to minimize multiple Coulomb scattering
- Design employs transverse planes of "straw chambers" (~20,000 straws)
  - Tracks ionize the gas in each straw tube
  - Charge drifts to sense wire at center
  - Drift time gives precision position
- Advantages
  - Established technology
  - Modular: support, gas, and electronic connections at the ends, outside of tracking volume
  - Broken wires are isolated
- Challenges
  - Straw wall thickness of 15 μm has never been done before
  - Tracker must operate in a vacuum

Straw characteristics

- Straw structure
  - 5 mm diameter, 15 μm wall thickness
  - Material: 2 layers of 6.25 μm mylar each, one coated with 500Å aluminum and one with 200Å gold
- Straw length: 430 – 1200 mm
- Straw tension: 8 N (~800 gm)
- Inside straw:
  - A 25 μm gold plated tungsten wire tensioned @ 0.8N
  - Ar:CO_2, 80:20 gas @ 1 atm
- < 1500V from wire to straw

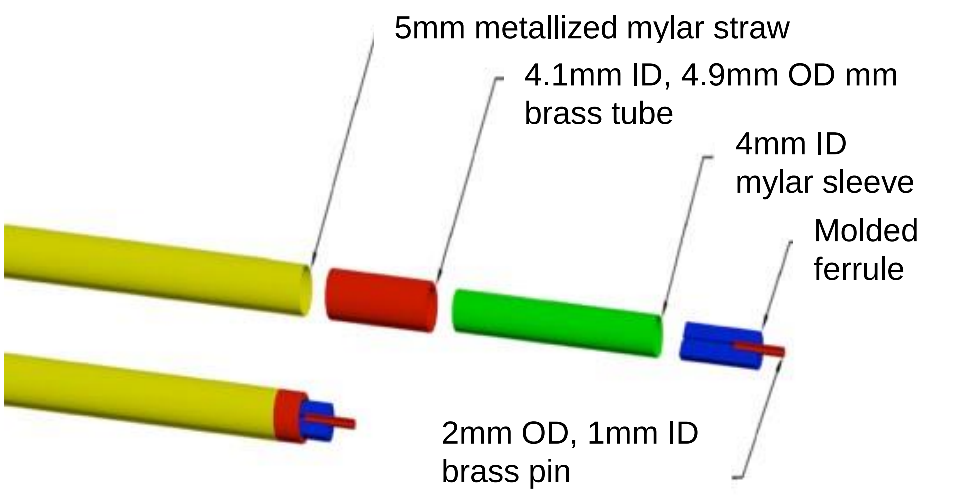

Tracker panel construction



Mu2e track reconstruction

- GHz background rate, single track, no t_0
  - Challenging pattern recognition problem!
  - Tir

- Neec
  resol

- Mult

μ capt
backgı

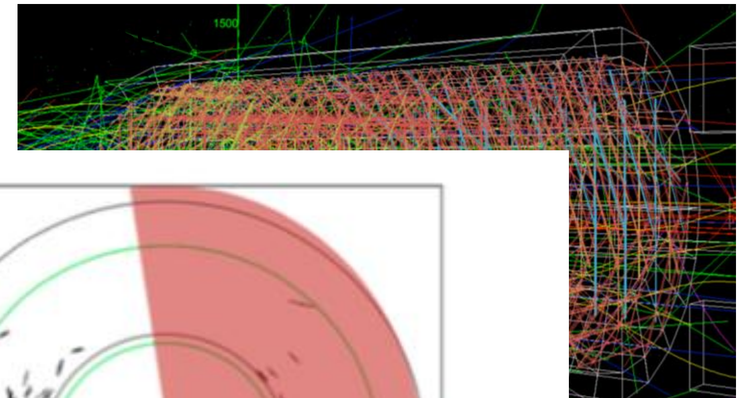

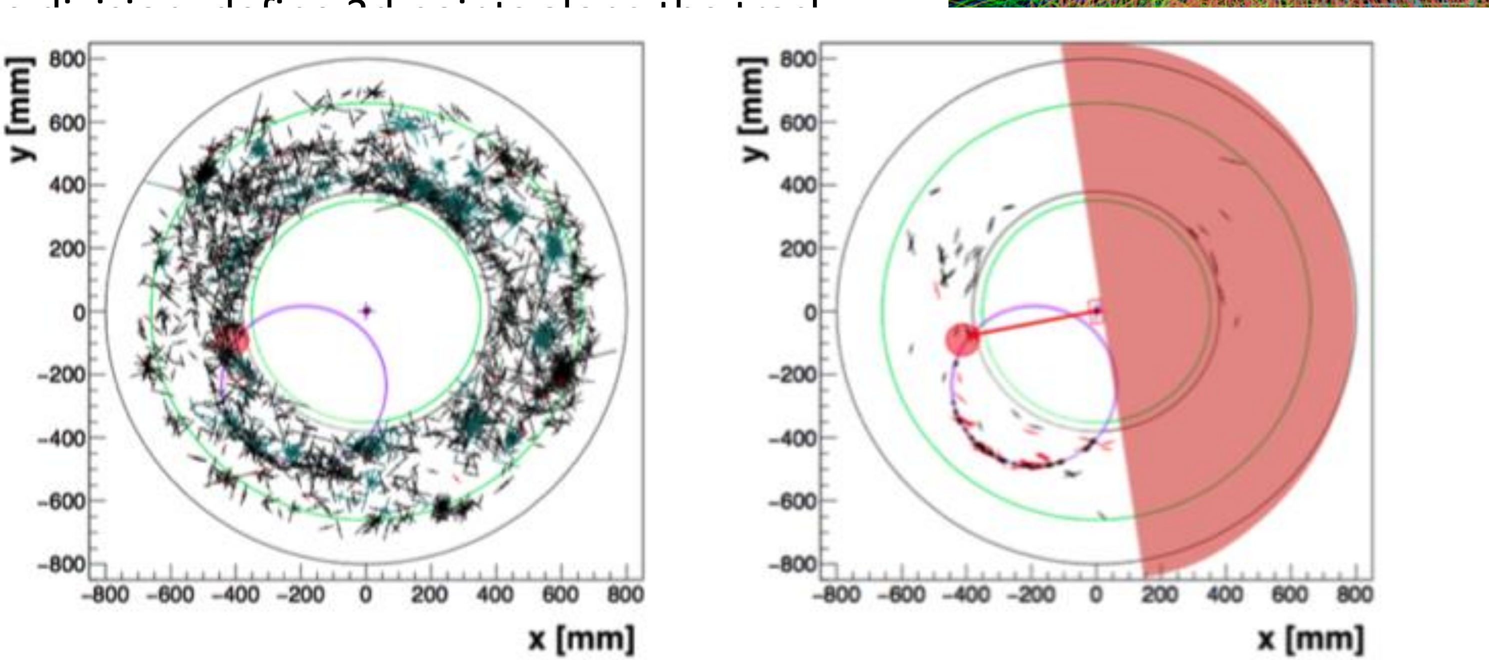

3ABAR)

ɪsolution

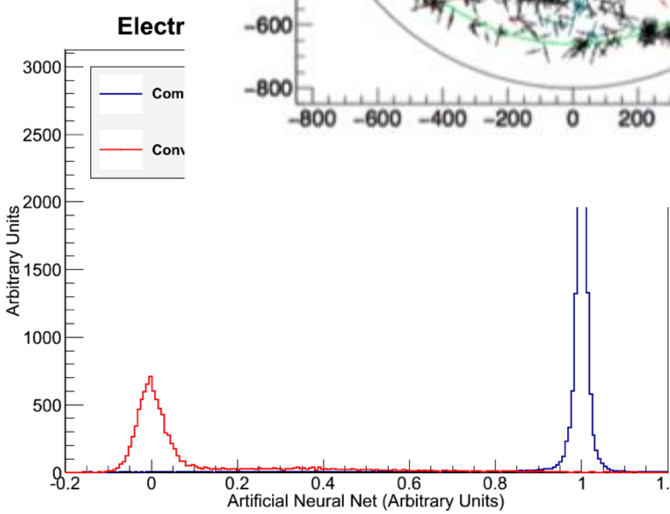

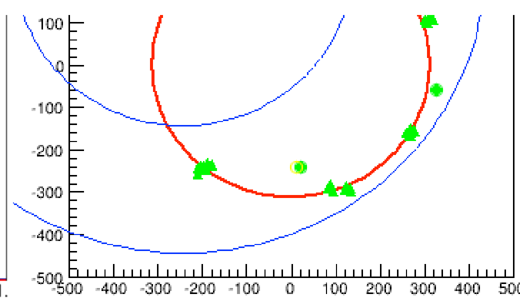

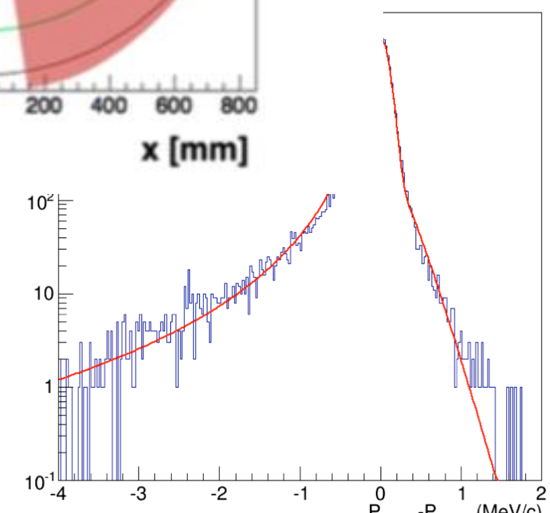

Phase-I detector (CyDet)

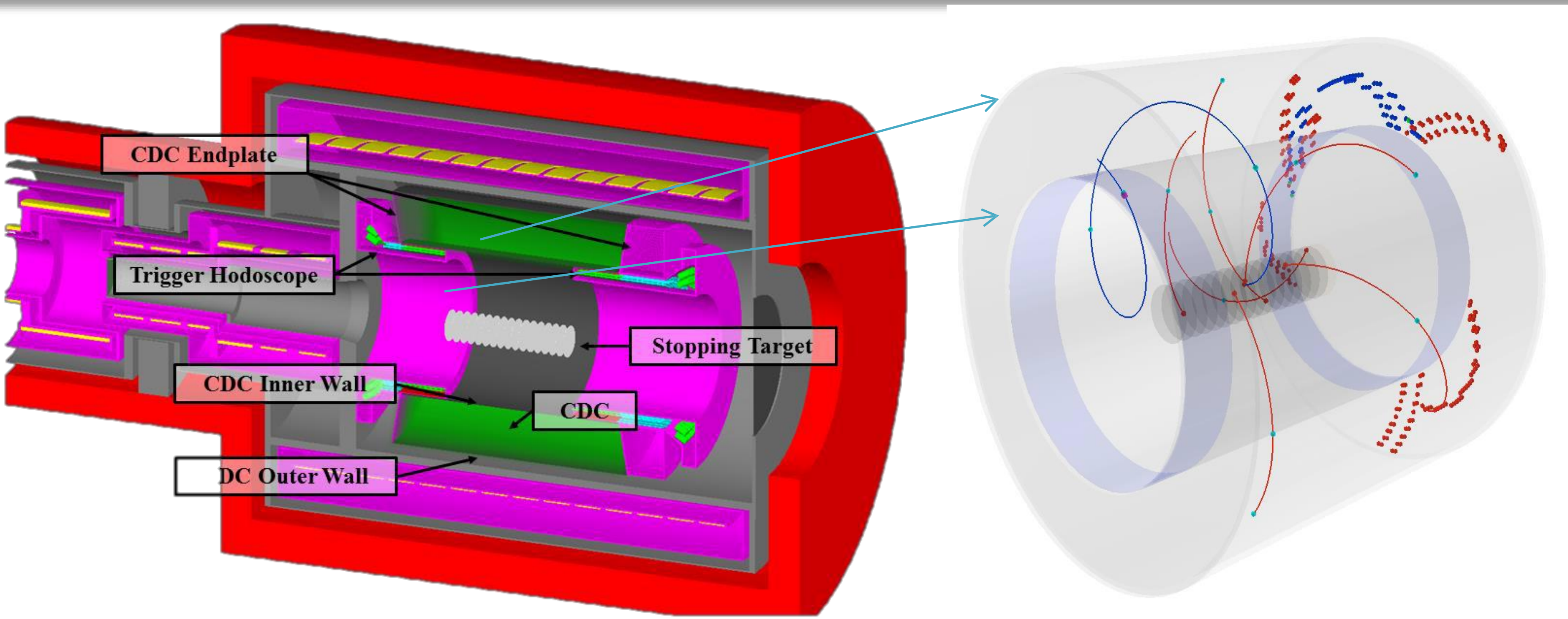

- CyDet is the COMET Phase-I tracking/trigger detector
  - Cylindrical trigger hodoscope:
    - Two layers: plastic scintillator for t0 and Cerenkov counter for PID.
  - Cylindrical drift chamber:
    - All stereo layers: *z* information for tracks with few layer hits.
    - Helium-based gas to minimize multiple scattering.
    - Large inner bore to avoid beam flash and DIO electrons.

CDC

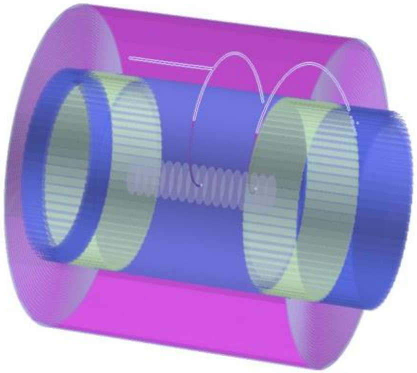

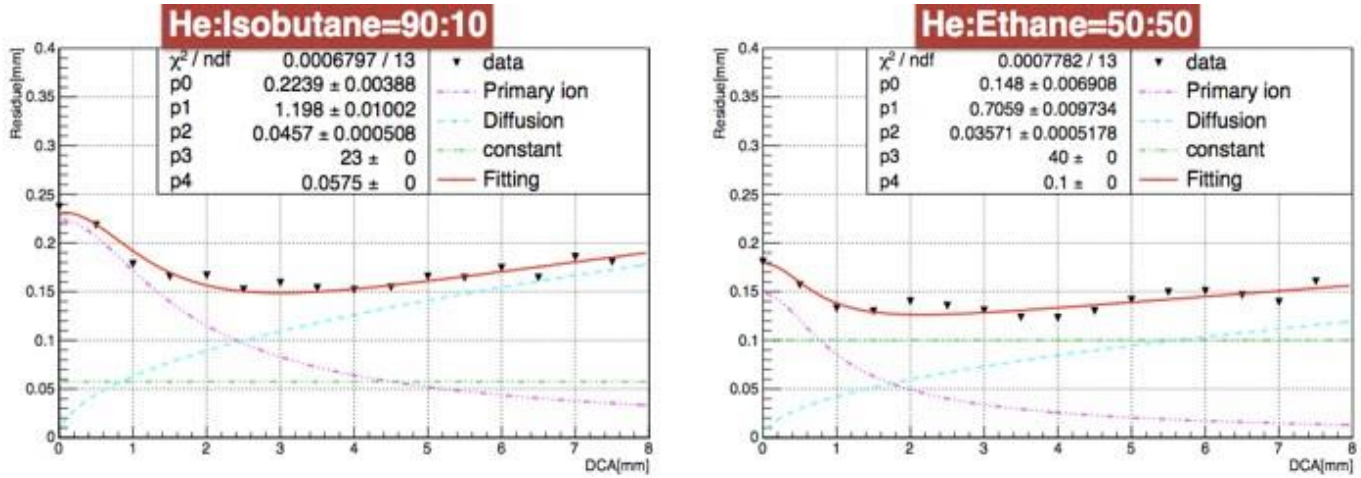

Position resolutions of CDC prototype obtained in the beam test @Spring-8

- **C**ylindrical **D**rift **C**hamber
- Main tracker for Phase-I physics measurement

- All stereo wires enable reconstruction of 3D hit positions
- 20 layers consists of ~5,000 sense wires
- ~1.5T B field
- Gas mixture, He:iC_4H_{10} 90:10 or He:$C_2H_6$50:50

Both gas mixtures show good performance

- Required momentum resolution, σ_p ~ 200 keV/c @p=105MeV/c

RECBE Board Mass Test @IHEP

Detector Construction

- **CDC construction complete**
  - All wires are fine
  - Inner wall installed

Track energy deposit

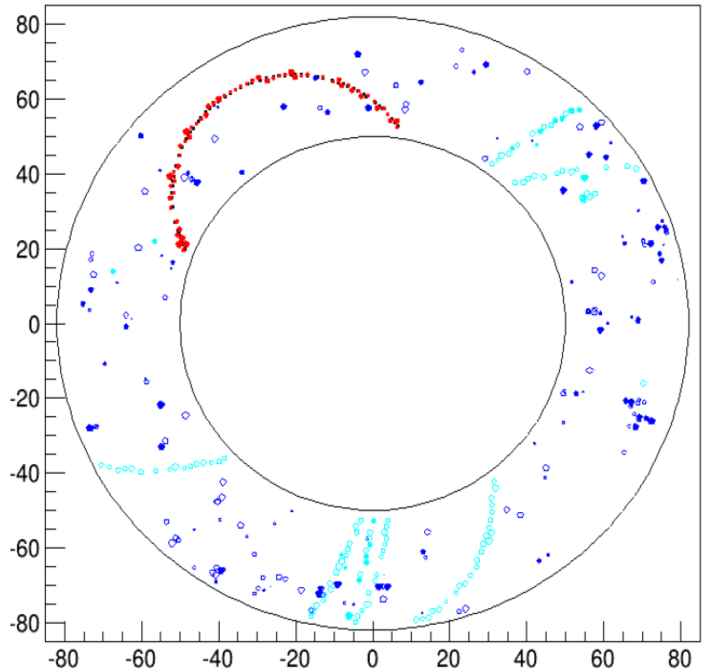

1000 ns after beam flash

- signal
- DIO
- proton/ion (pion capture)
- proton/ion (muon capture)
- other noise

Total energy deposit

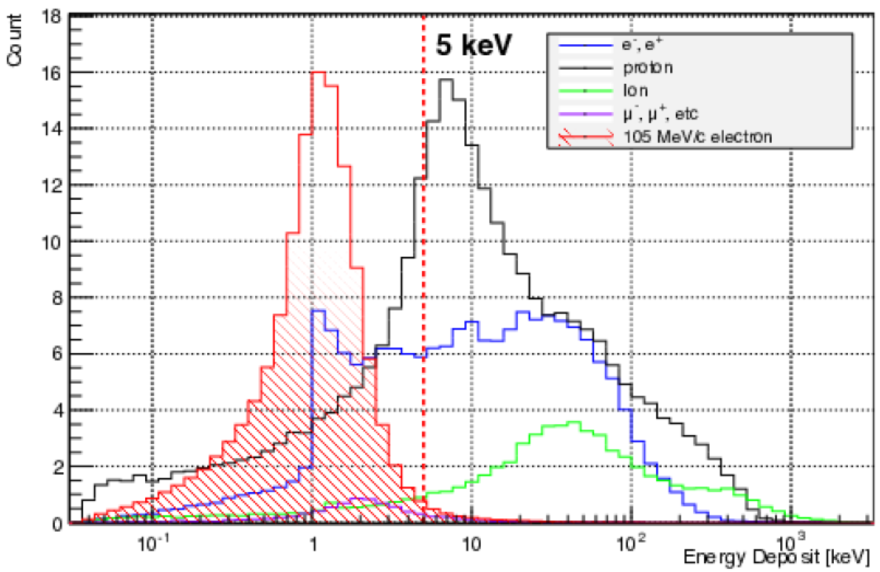

Central Trigger Hodoscope

- **C**herenkov **T**rigger **H**odoscope
  - Each Module consists of an acrylic Cherenkov radiator and a plastic scintillator
  - 64 modules arranged both upstream/downstream sides
  - Require 4 hit coincidence to suppress accidental triggers due to γ rays
  - **Better than 1ns time resolution** obtained by using the prototype detector for 100MeV/c electrons
  - Preamplifier prototype produced and irradiation tests to be done

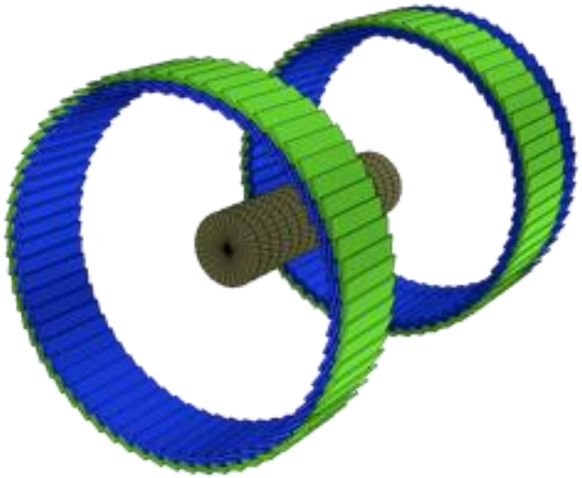

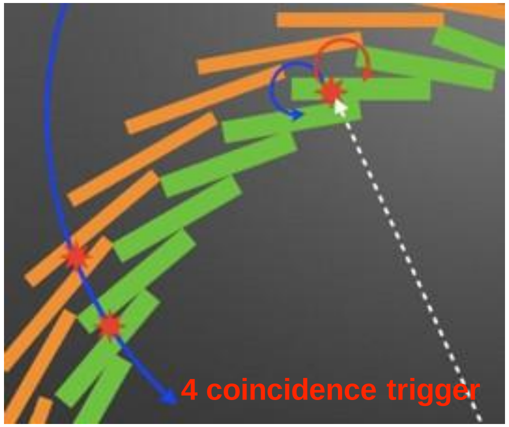

Fine mesh PMT

TOP: Plastic Scint.
Bottom: Acryl

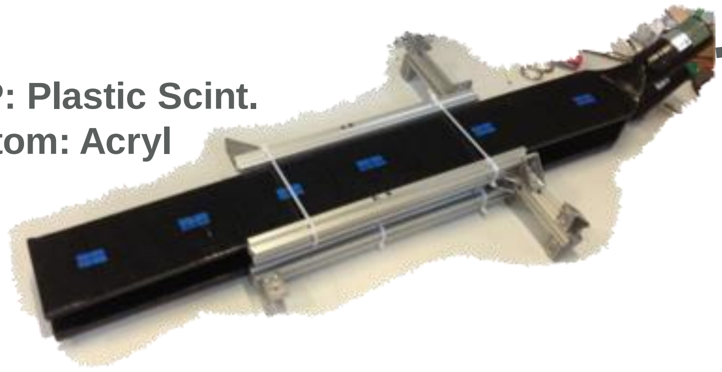

Analog FE prototype

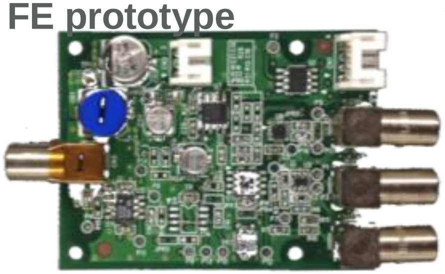

To digitizer

Timing hodoscope CTH

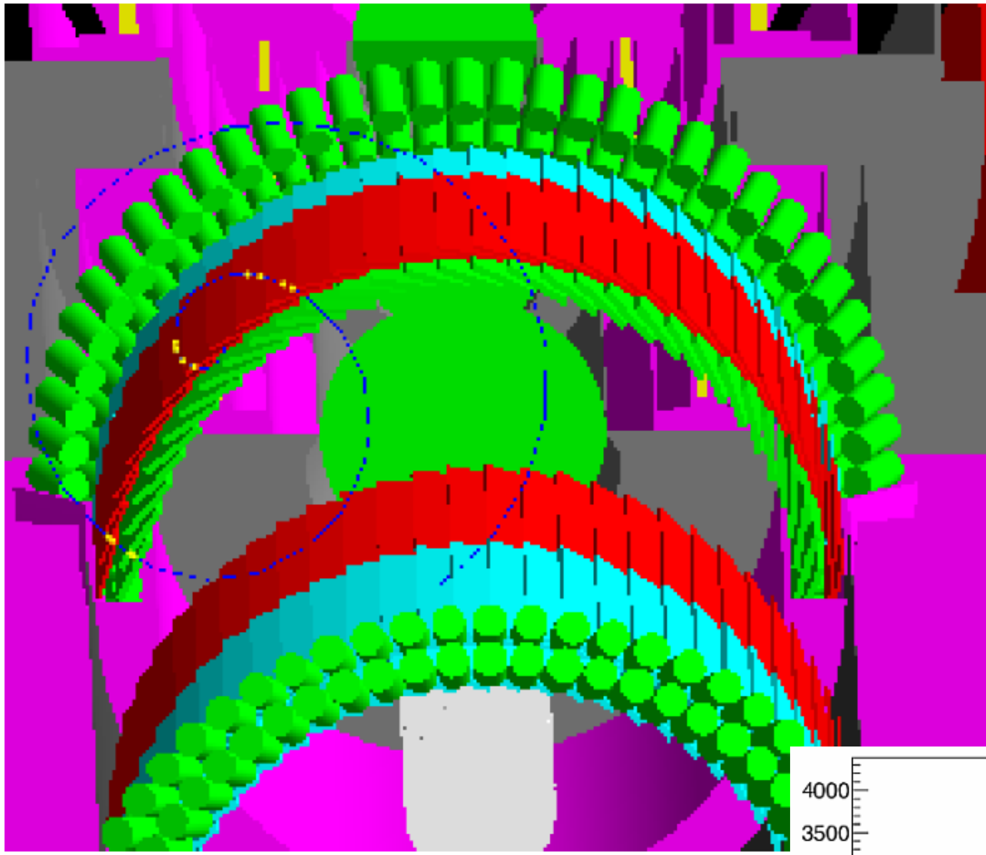

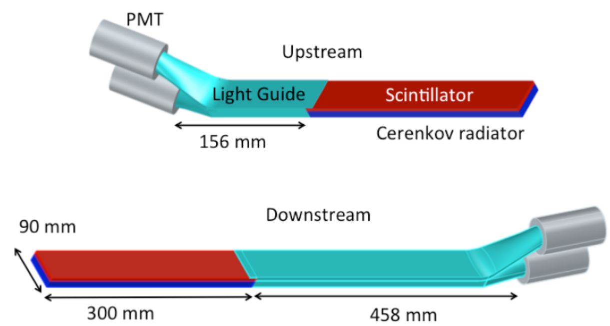

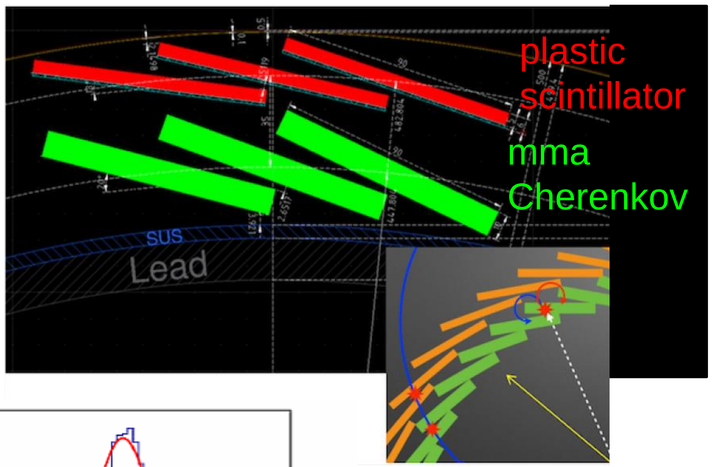

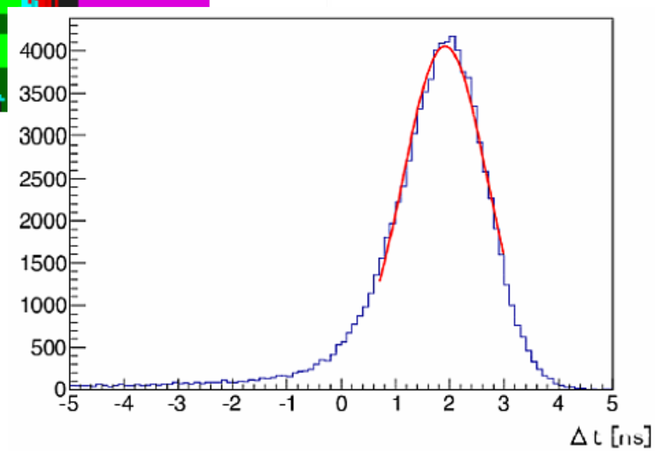

StrECL in COMET Phase I

An apparatus to measure the muon beam in Phase I and a prototype for Phase II

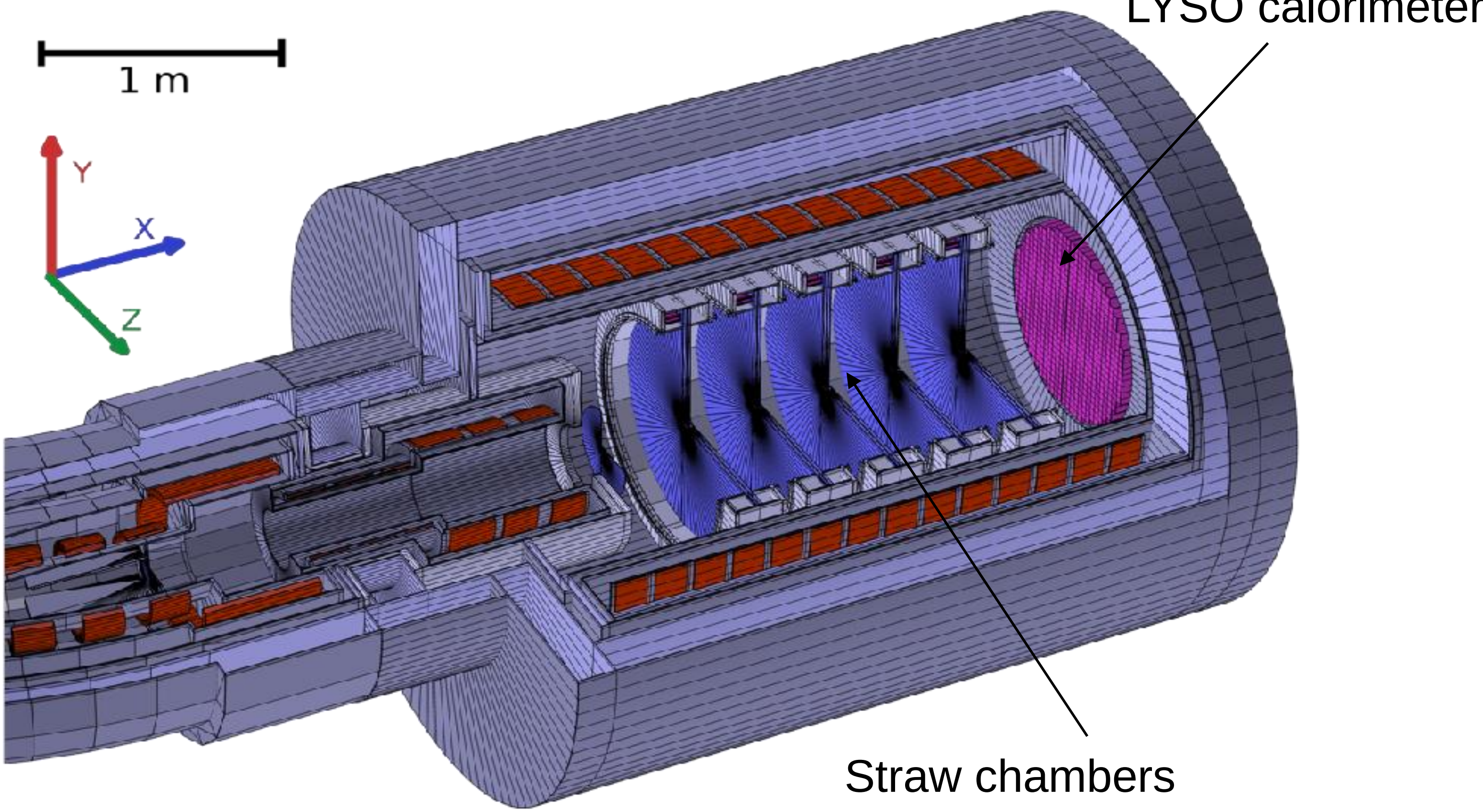

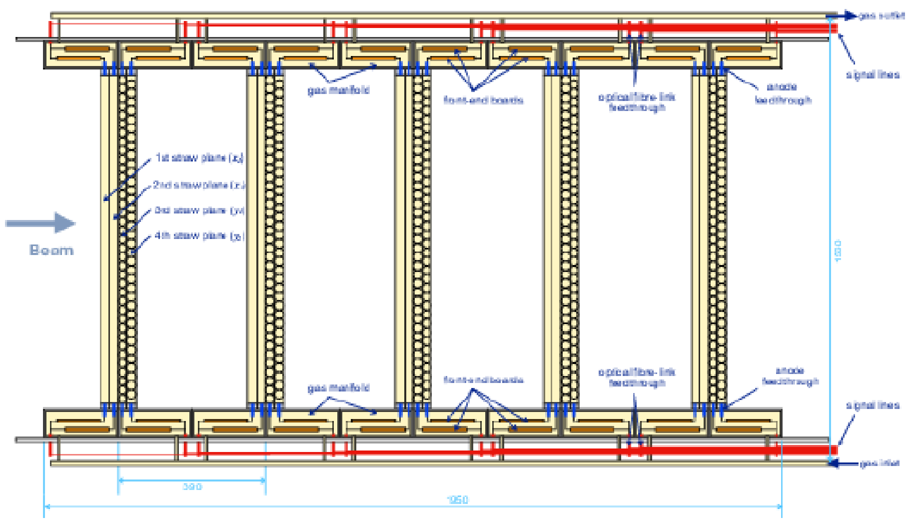

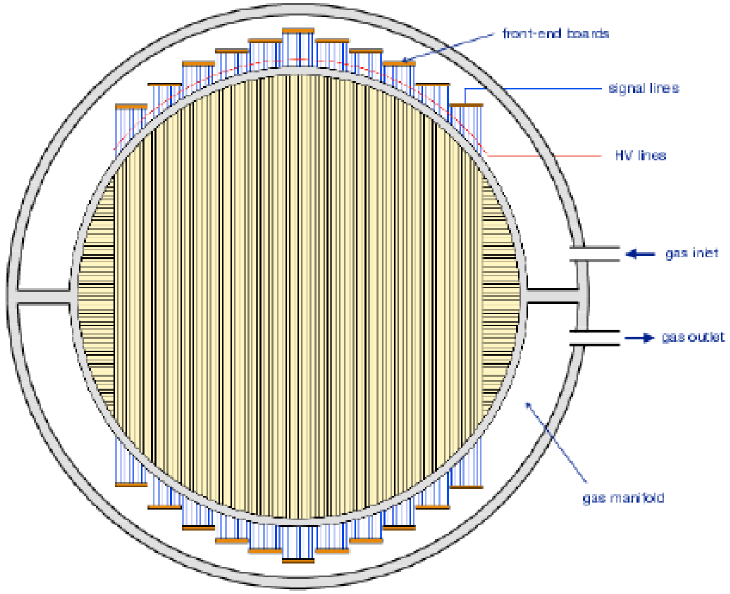

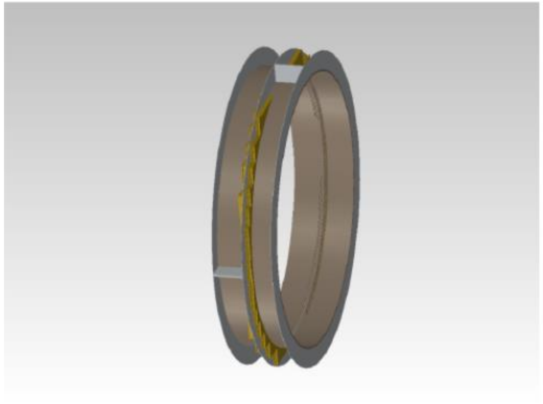

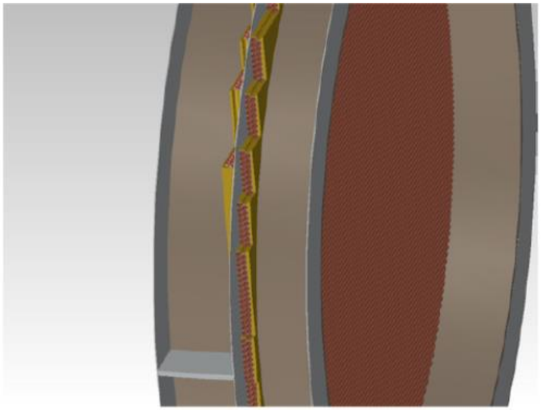

Straw tube material is PET (polyethylene terephthalate)
Straw dimensions in drawing are scaled by a factor of three

Straw tubes
Taped, not spiral-wound
20μm walls with 70nm Al layer

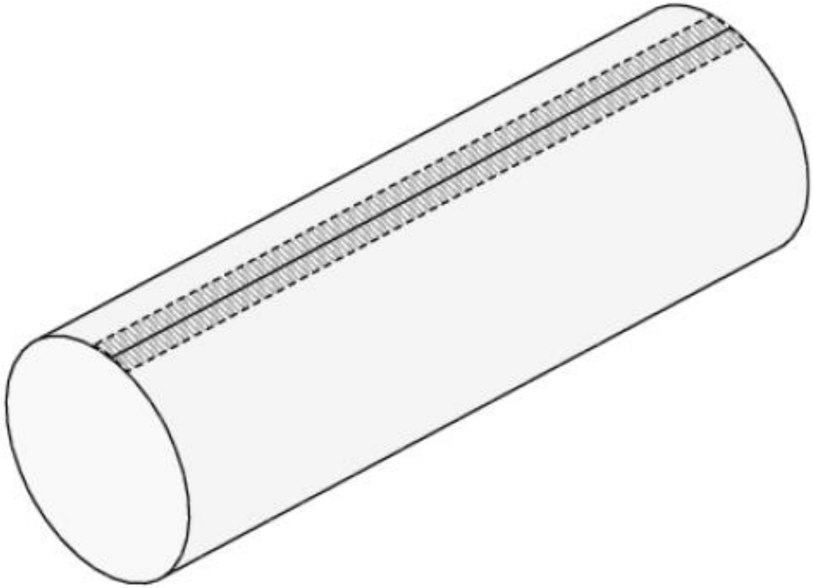

Straw tube measured and simulated performance

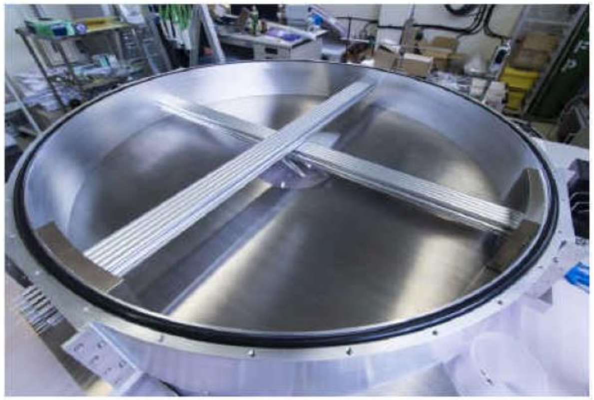

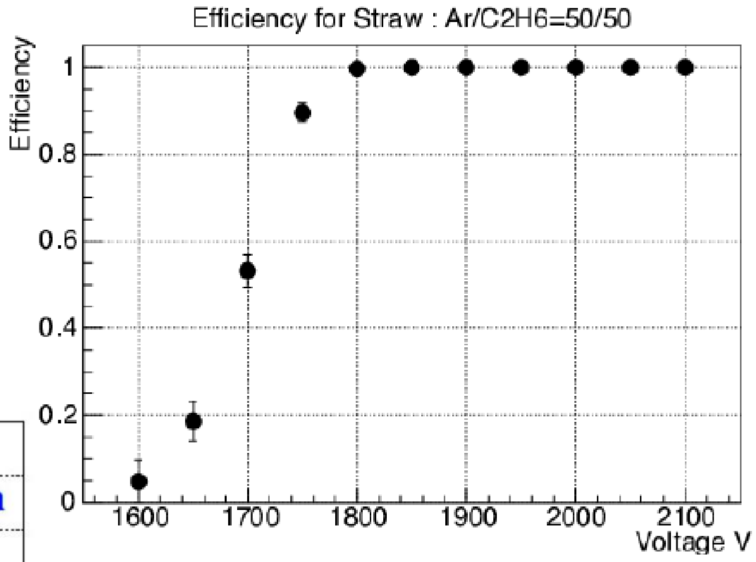

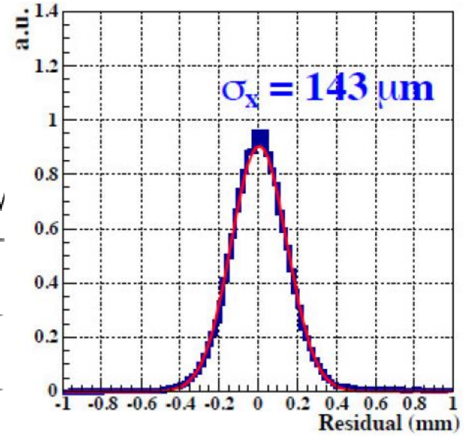

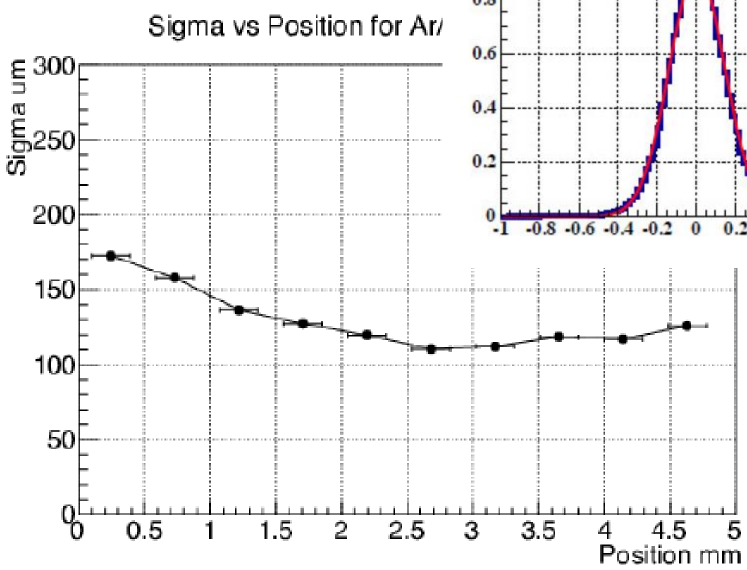

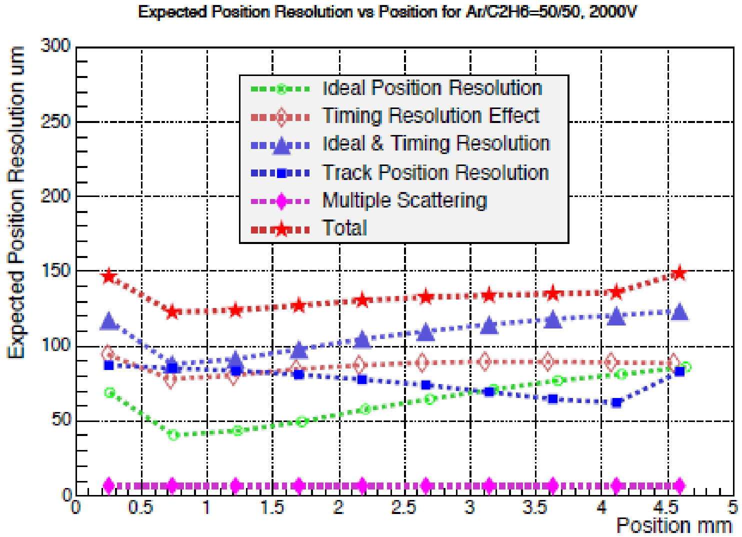

Calorimeter

Original Mu2e Calorimeter

- Four vanes
- Each vane consists of 12x44 crystals 3x3x13 cm^3

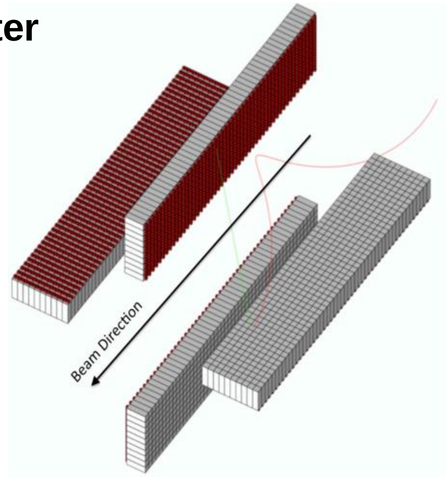

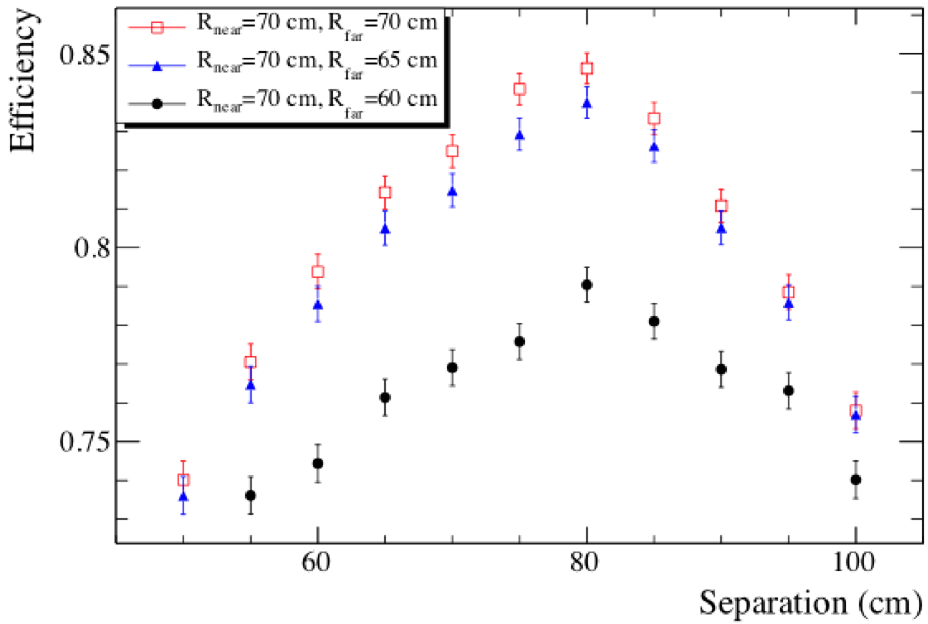

Replaced by two discs separated by ~1/2 wavelength of CE helix

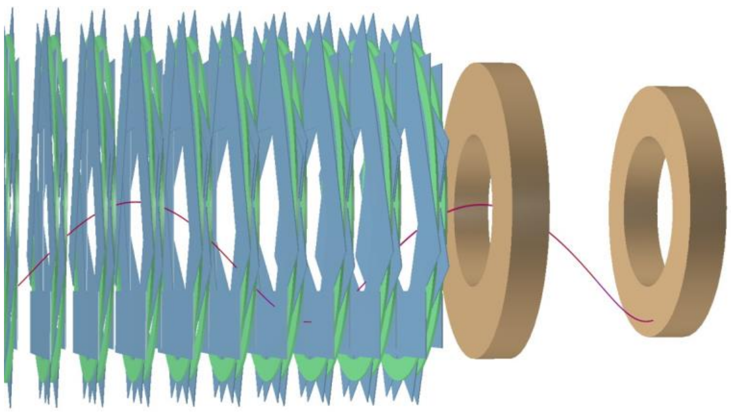

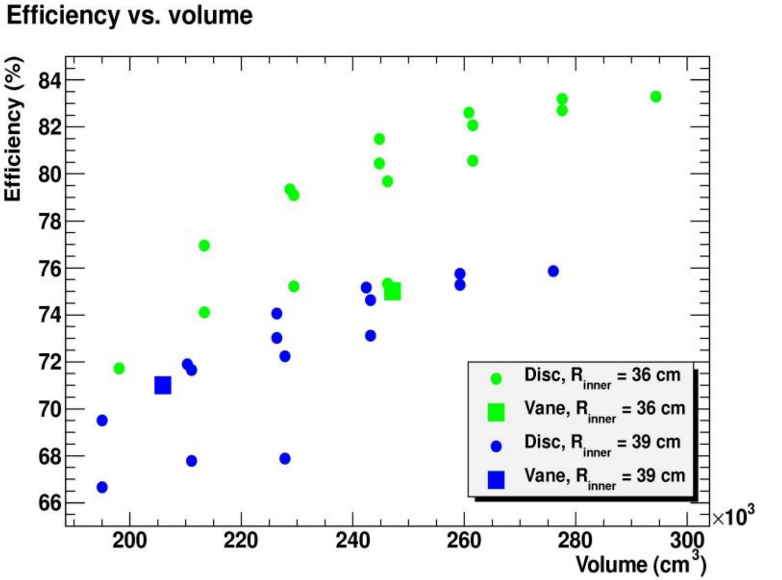

Calorimeter design

- The central hole region in the tracker and calorimeter allows us to be largely insensitive to DIO and beam flash backgrounds
- The calorimeter consists of two identical annuli, spaced apart by 700 mm (½ λ of the helical trajectory of the conversion electron)
- *r_{inner} = 374 mm*
  r_{outer} = 660 mm
  depth = 10 X_0 (200 mm)
- Each annulus contains 674 square CsI crystals with dimensions 34x34x200 mm^3
- Each crystal is read out by two large area (14x20 mm^2) six element UV-extended SiPMs

  The analog front end electronics is directly mounted on the SiPM

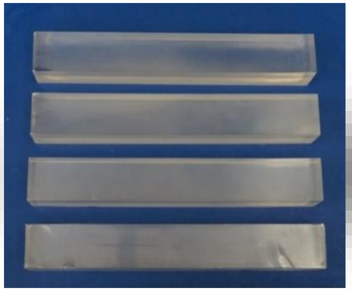

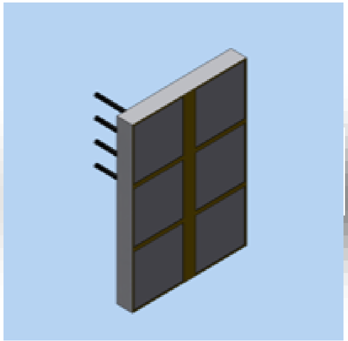

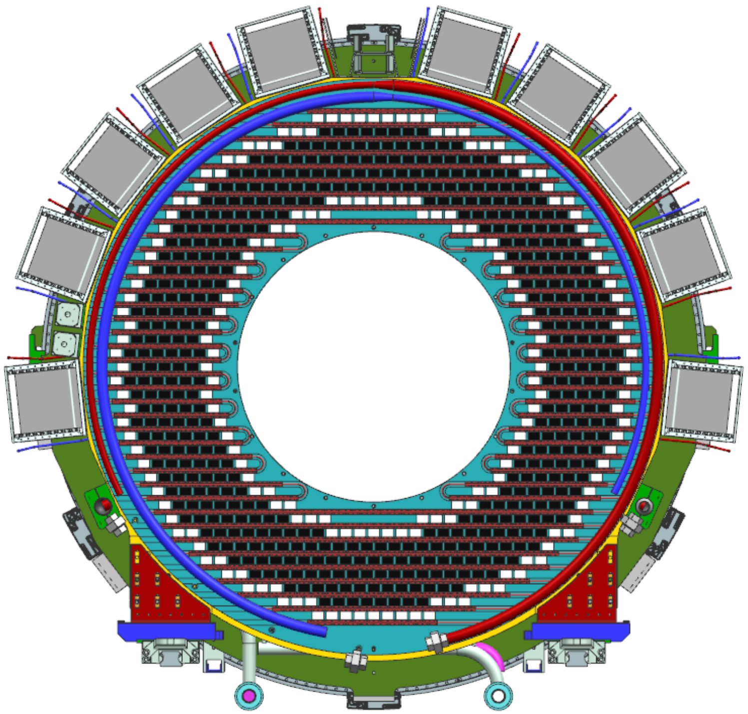

- The digital electronics and voltage regulators are located in electronics crates mounted on the periphery
- Calibration and monitoring are provided by a 6 MeV radioactive source and a laser system

Calorimeter crystal choice

	LYSO	BaF_2	CsI
Radiation length X_0 [cm]	1.14	2.03	1.86
Light yield [% NaI(Tl)]	75	**4**/36	3.6
Decay time τ [ns]	40	**0.9**/650	20
Photosensor	APD	**R&D APD/SiPM**	SiPM
Peak wavelength [nm]	402	**220**/300	315

LYSO

- Radiation hard
- Not hygroscopic
- Excellent LY
- τ = 40ns
- Peak 420 nm,
- Easy to match to APD.
- High cost 30- 40$/cc

Barium Fluoride (BaF_2)

- Radiation hard, not hygroscopic
- Very fast (220 nm) scintillating light
- Larger slow component at 300 nm. must be suppressed for high rate capability
- Photosensor must have extended UV sensitivity and be "solar"-blind
- Medium cost 10$/cc
- Develop for Mu2e-II

CsI (pure)

- Not as radiation hard
- Slightly hygroscopic
- 20 ns emission time
- Peak 315 nm.
- LY comparable to fast component of BaF_2.
- Inexpensive(6-8 $/cc)

Energy resolution

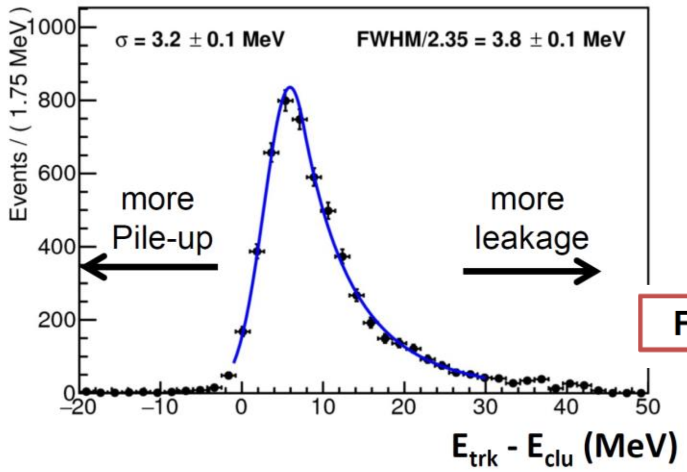

Simulation includes full background and digitization and cluster-finding, with split-off and pileup recovery

FWHM / 2.35 = 3.8 ± 0.1 MeV

Dependence on LRU and photostatistics

Specification is LRU<5%

Nominal photoelectron yield is 30 pe/MeV, Dropping to 20 pe/MeV after irradiation

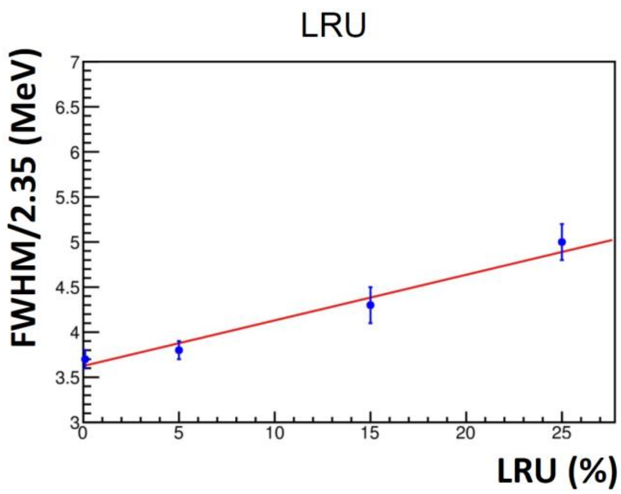

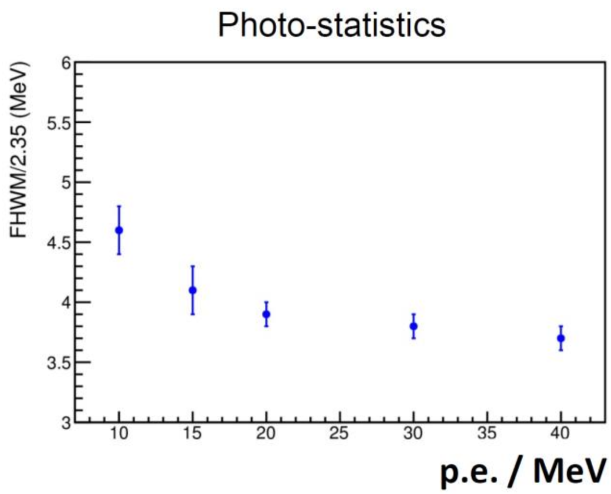

Mu2e Crystals: un-doped CsI

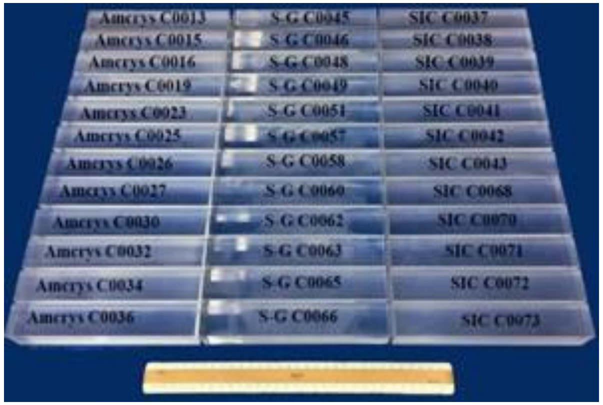

Density (g/cm3)	4.51
Radiation length (cm)	1.86
Moliere Radius (cm)	3.57
Refractive index	1.95
Peak luminescence (nm)	310
Decay time (ns)	26

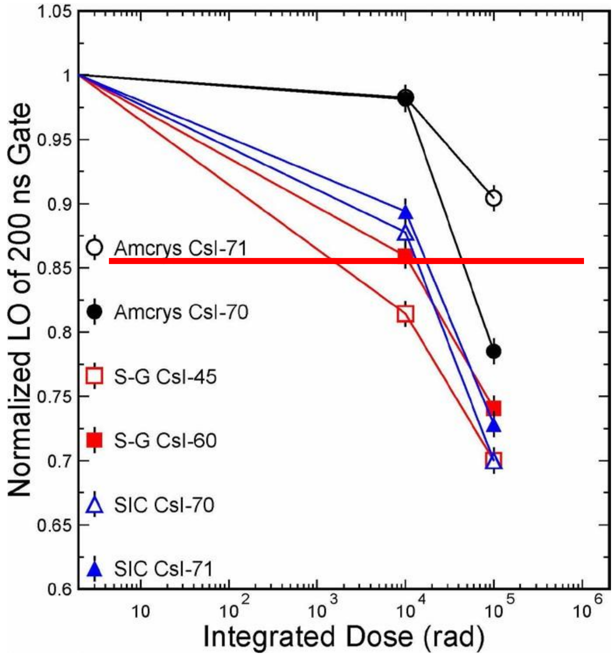

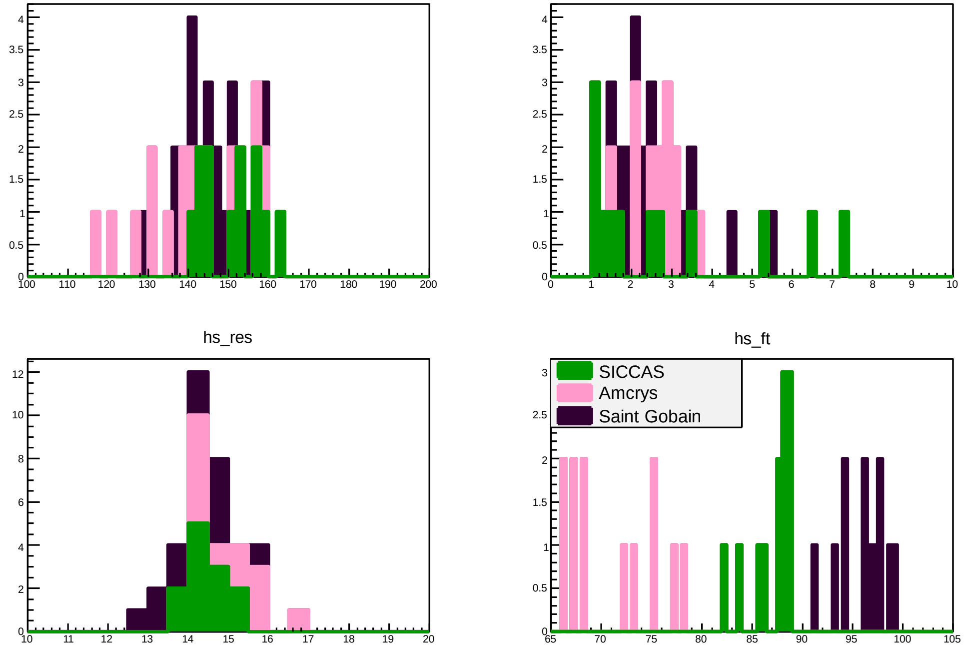

Two disks required for complete acceptance

- Large acceptance for $\mu \rightarrow e$ events
- Particle Identification capabilities
- An independent trigger

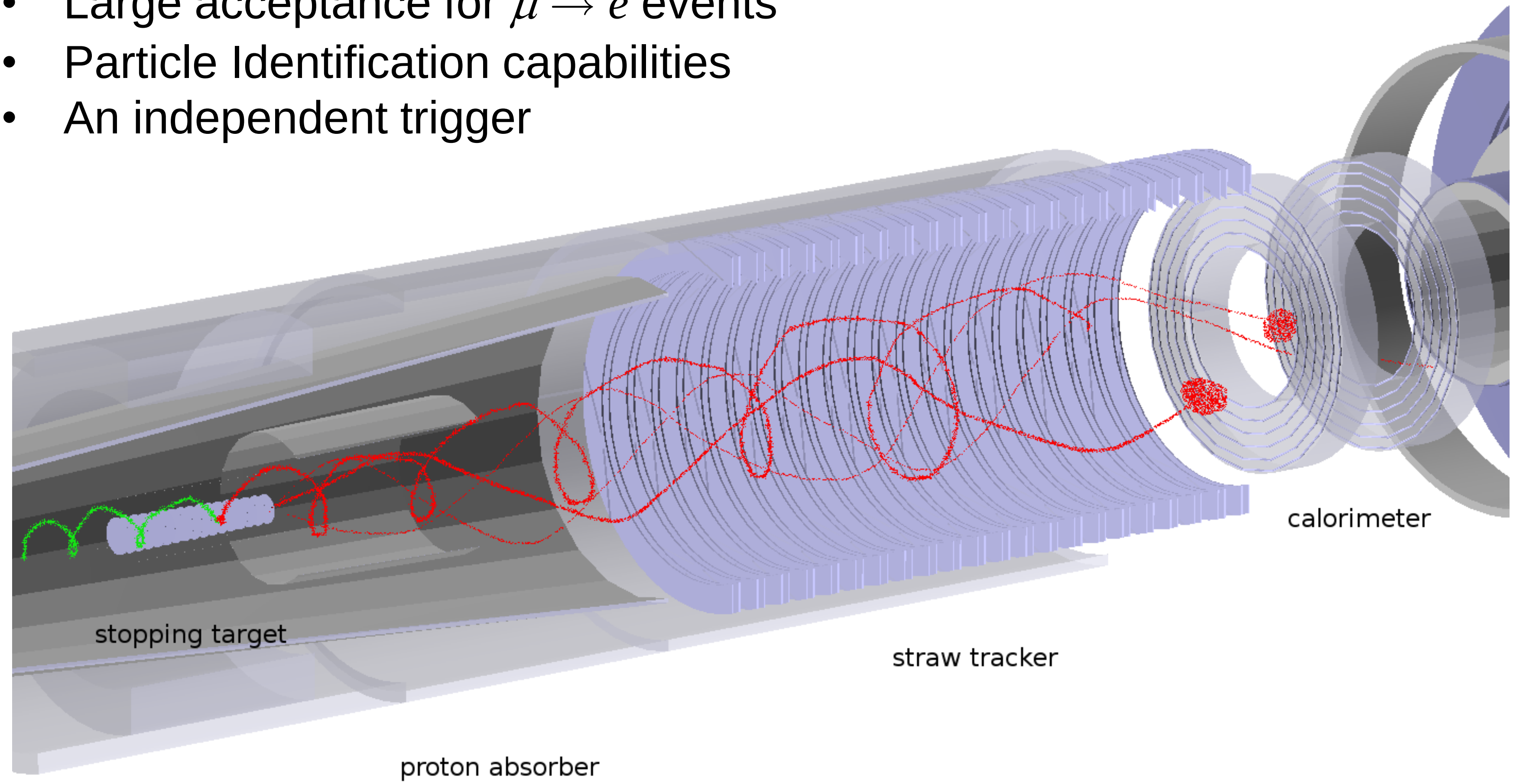

- Provides “seeds” to improve track finding efficiency at high occupancy

PID – Requirement #1

- Cosmic Ray Veto (CRV) studies show:
  - with a CRV inefficiency of 10^{-4} we would have < 0.1 “fake” events from atmospheric particles

a cosmic ray μ rejection factor ~ 200 is needed

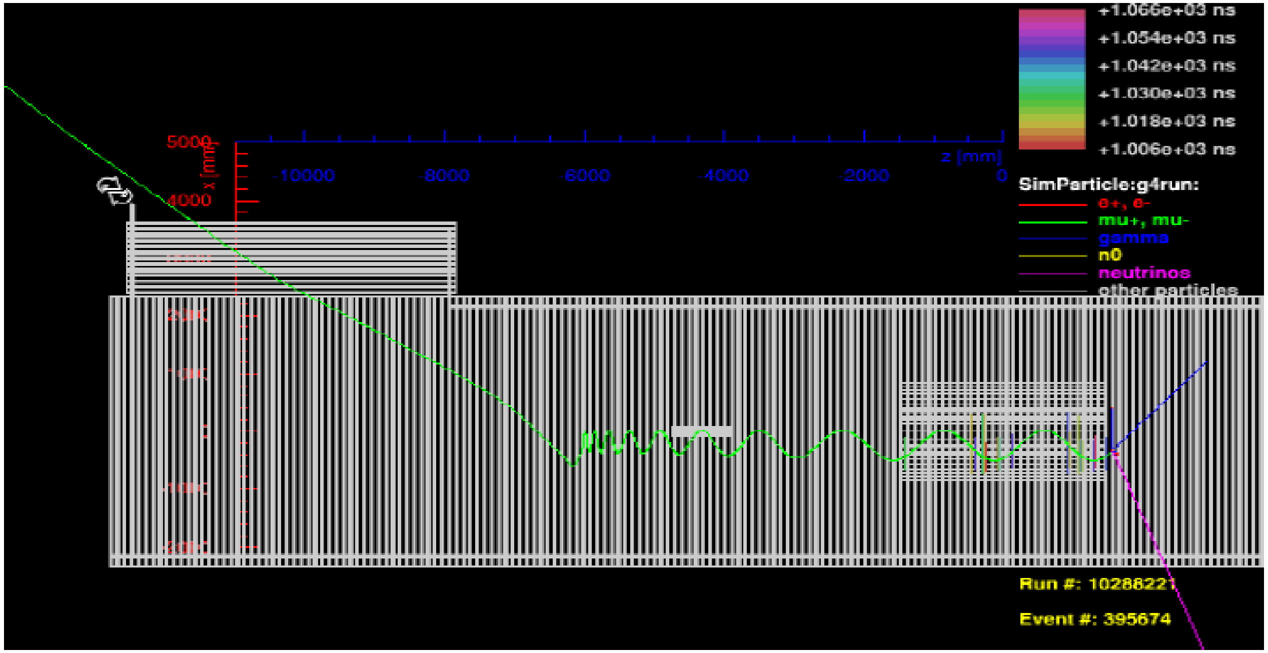

Event display: μ^- mimicking conversion electron signal

PID calorimeter-tracker – the basic idea

$$\beta = \frac{p}{E} \sim 0.7, \;\; E_{kin} = E - m \sim 40 \text{ MeV}$$

- Compare the reconstructed track and calorimeter information:
  - $E_{\text{cluster}}/p_{\text{track}}$ & $\Delta t = t_{\text{track}} - t_{\text{cluster}}$,
  - Build a likelihood for e^- and μ^- using E/p and Δt distributions
  - Use the likelihood ratio: $\ln L_{e/\mu} = \ln \frac{L_e}{L_\mu} = \ln L_e - \ln L_\mu$

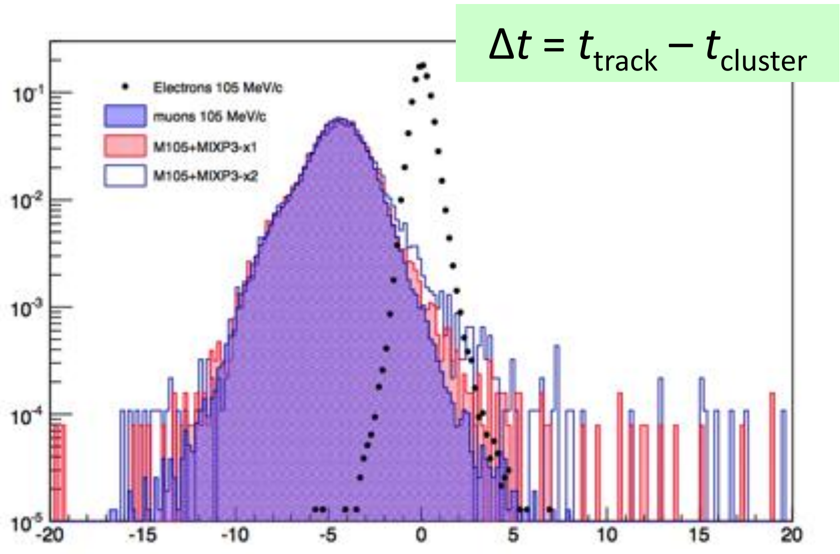

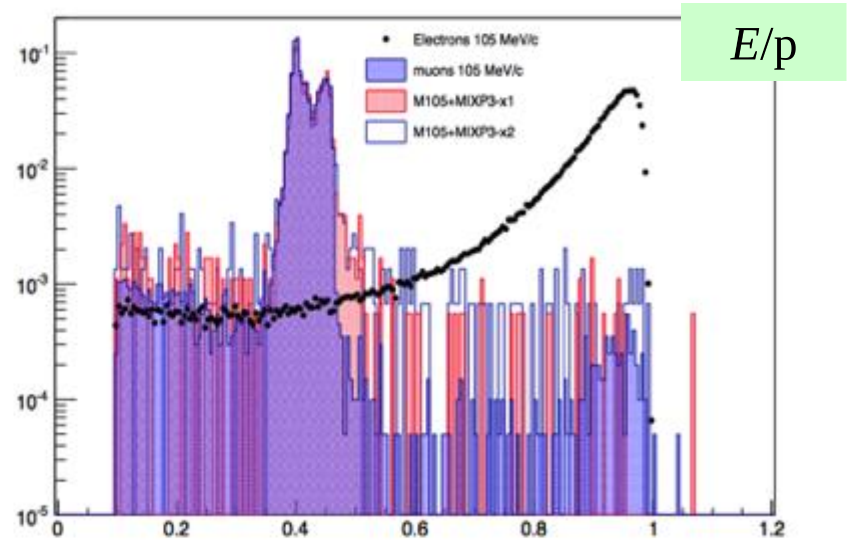

Particle identification – μ/e discrimination

E/p: electrons vs muons

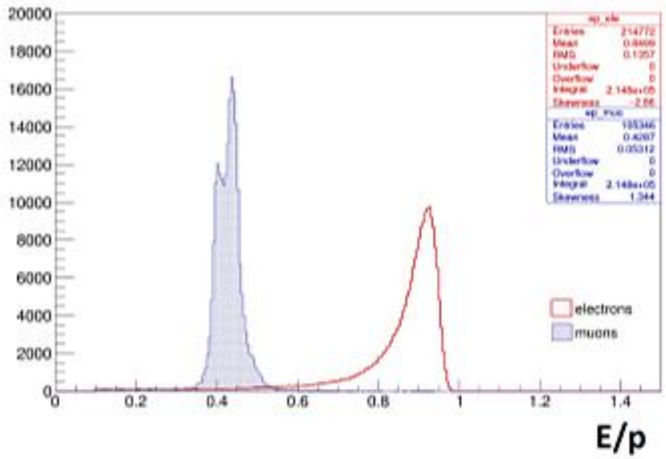

Δt electrons vs muons

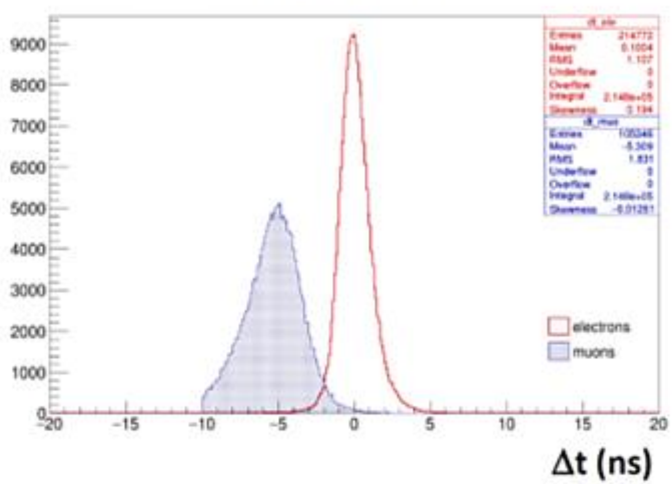

Electron ID efficiency vs muon rejection

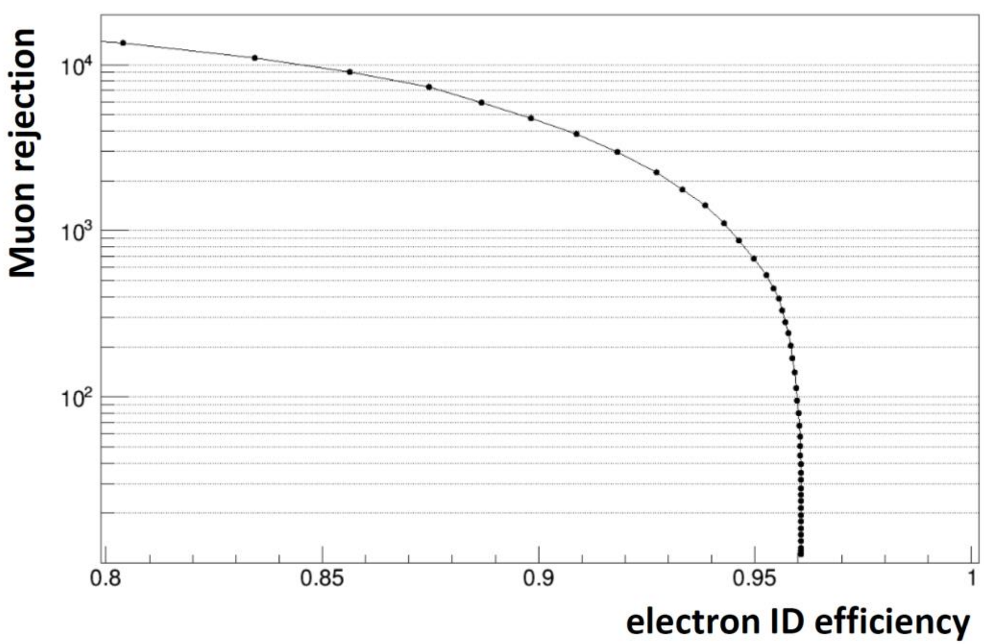

μ rejection of ~10^3 for 95% e^- efficiency

Track seeding

The speed and efficiency of tracker reconstruction is improved by selecting tracker hits compatible with the time ($|\Delta t| < 50$ ns) and azimuthal angle of calorimeter clusters ⇨ simplification of the pattern recognition.

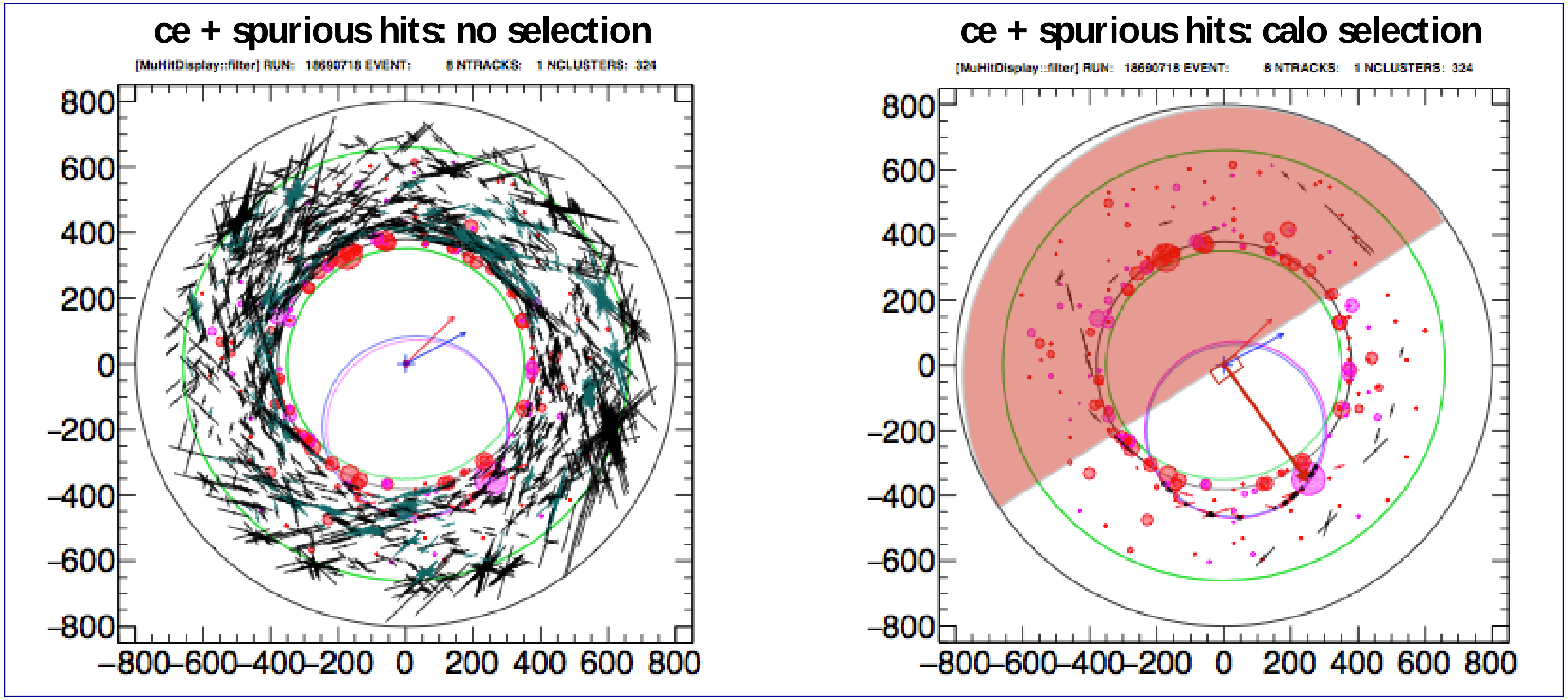

Fitting a helix to the selected tracker hits and calorimeter cluster increases the relative tracking efficiency by ~ 10%

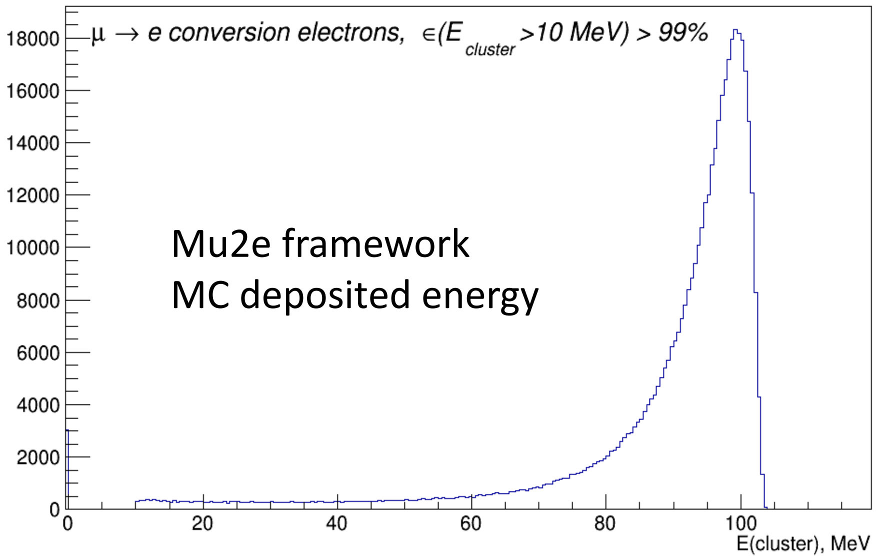

Ecut = 1.0 MeV

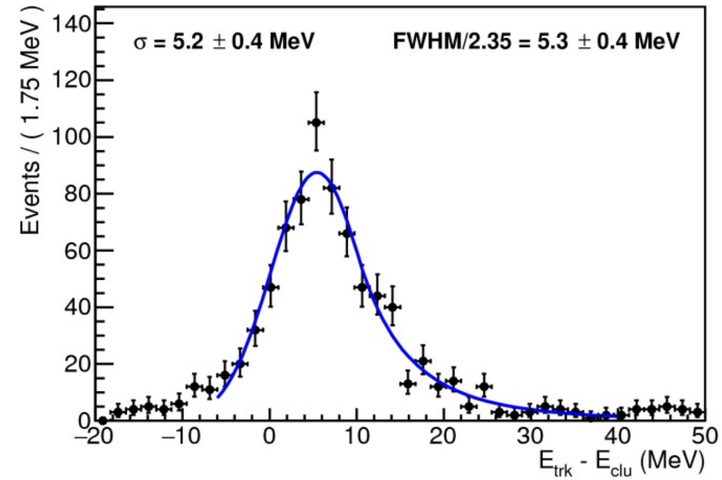

- ~ 99% acceptance of events with good tracks have a cluster *E* > 10 MeV
- Calorimeter-seeded track trigger can increase the trigger acceptance by 10%
- A standalone calorimeter-based online trigger can be used for efficiency and background studies.

Simulation of CsI+SiPM performance

Pileup recovery

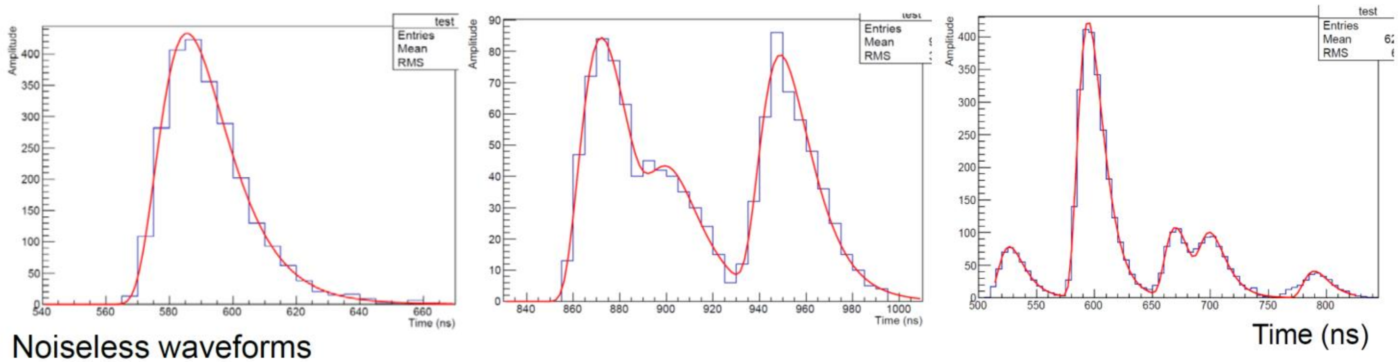

Noiseless waveforms

Position resolution (at face of disk)

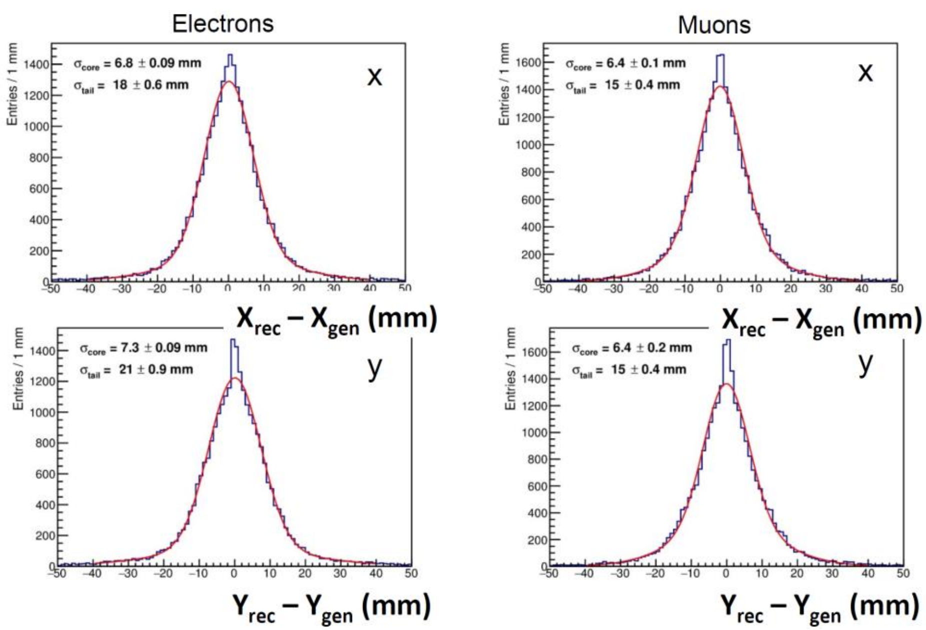

Geometric efficiency

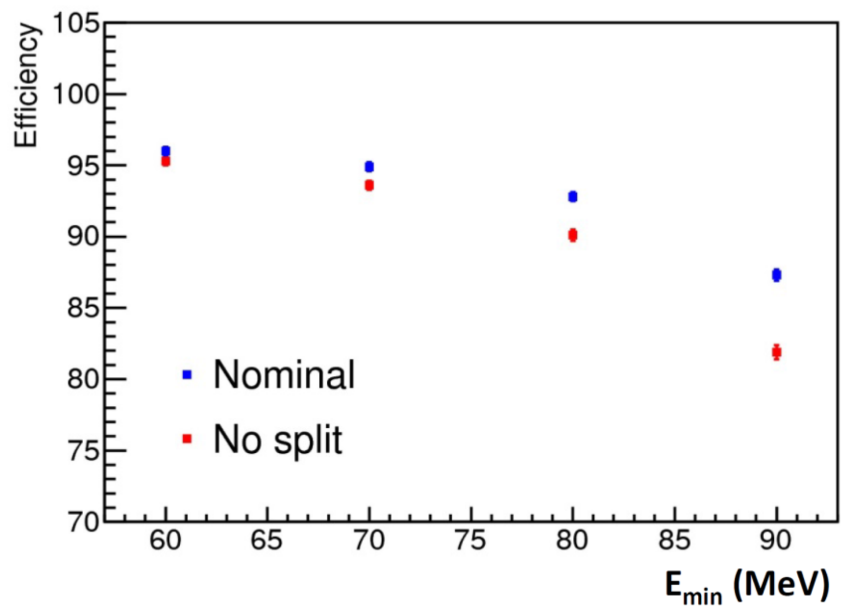

Prototyping/testing

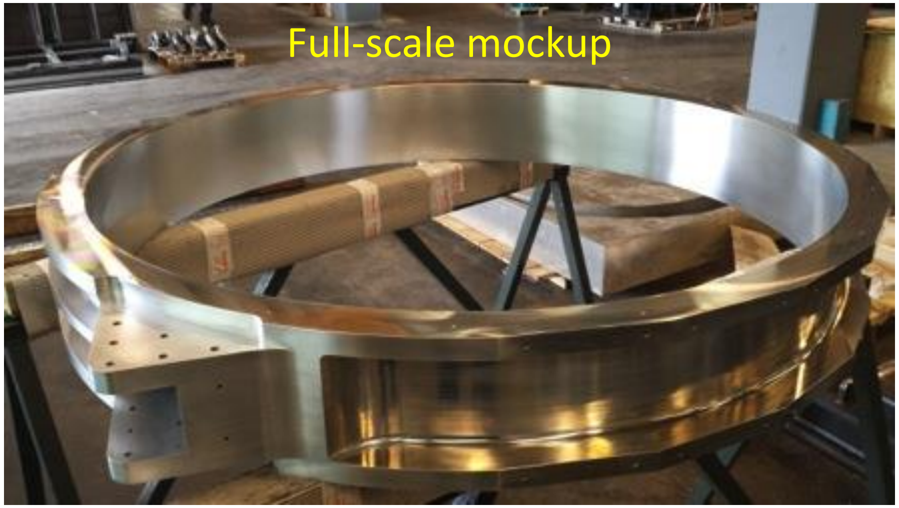

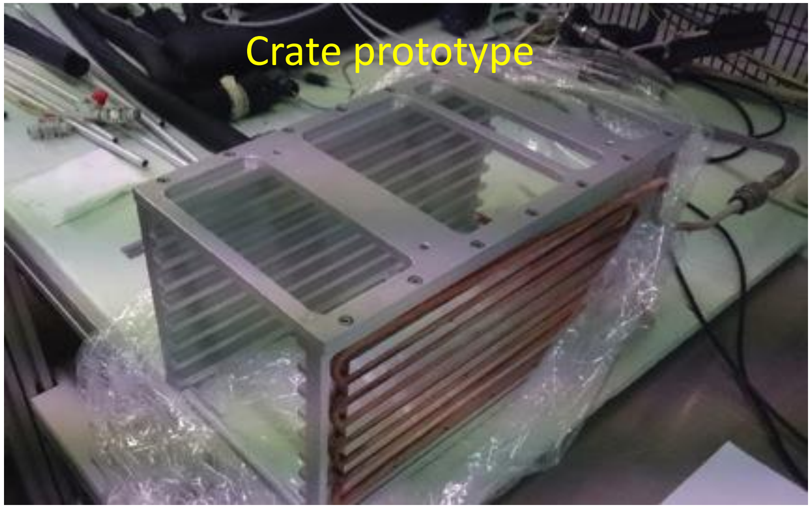

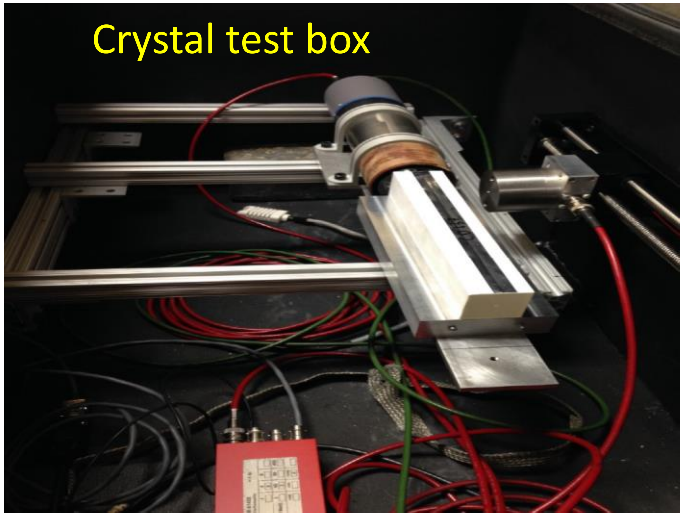

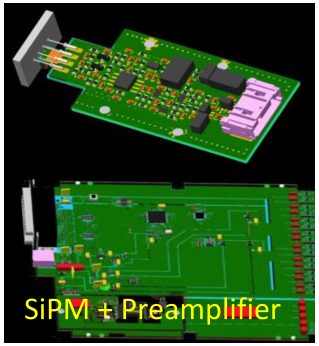

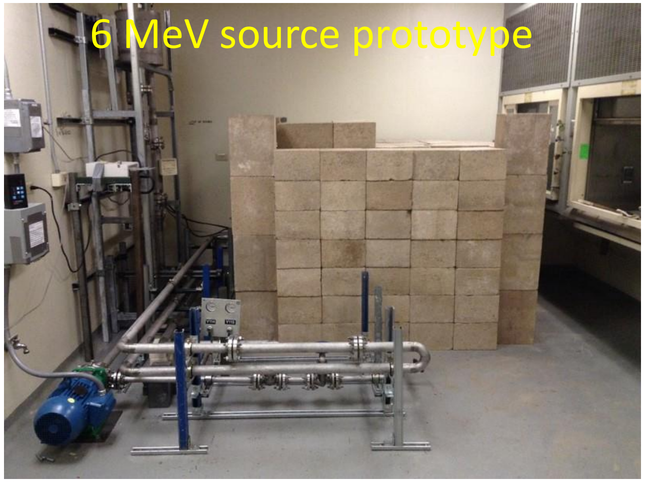

Calorimeter Module 0

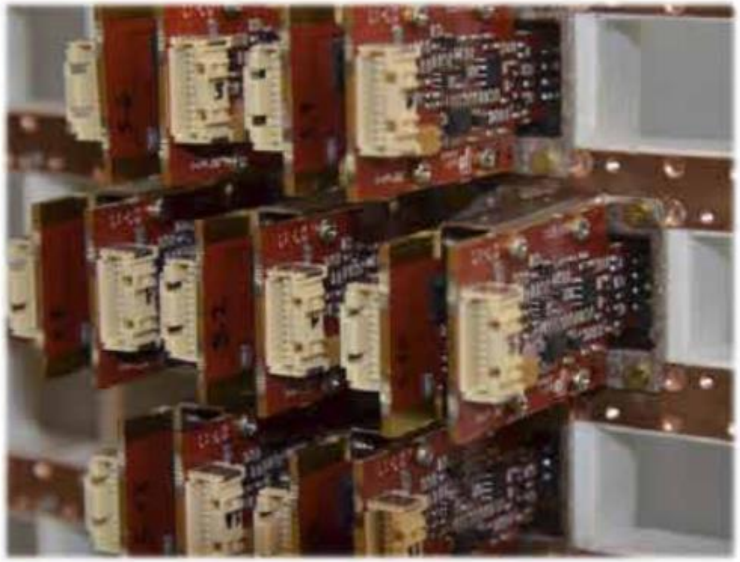

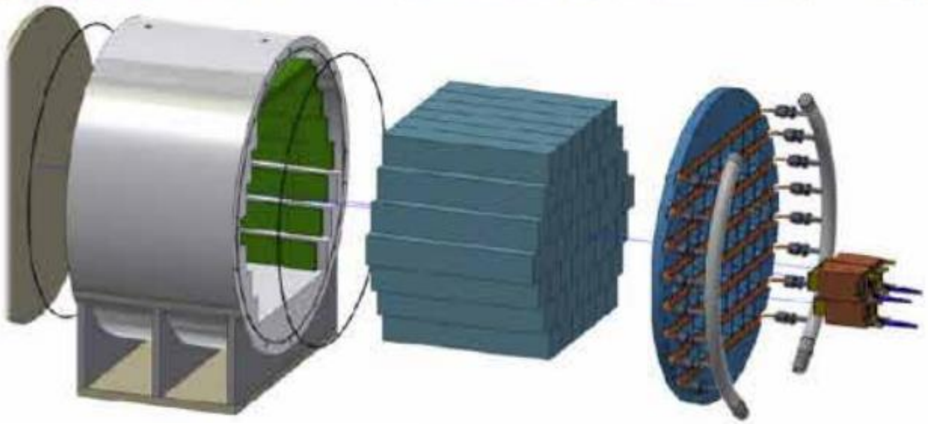

Calibration and monitoring

1) The *BABAR* calibration source has been rebuilt to provide 6.13 MeV γ s on demand

$$^{19}F + n \rightarrow {}^{16}N + \alpha$$
$$^{16}N \rightarrow {}^{16}O^{*} + \beta \quad t_{1/2} = 7\ \mathrm{s}$$
$$^{16}O^{*} \rightarrow {}^{16}O + \gamma(6.13\ \mathrm{MeV})$$

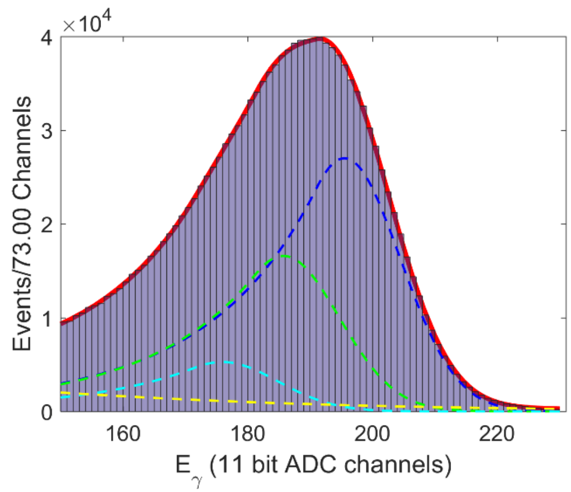

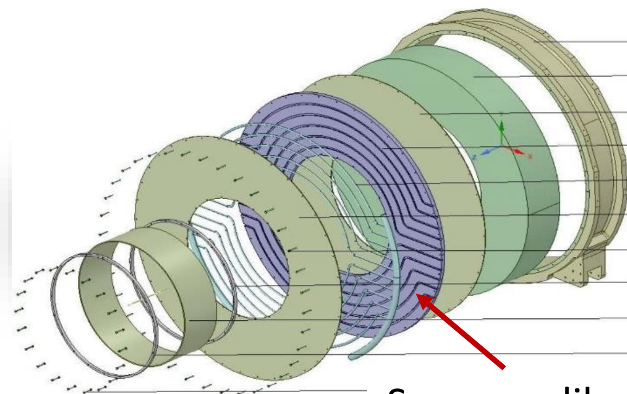

Source calibration tubes

2) Laser system to monitor SiPM performance

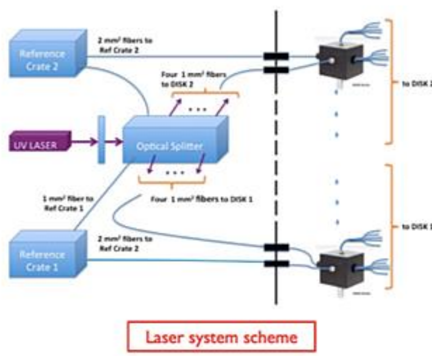

3) Cosmics + E/p for DIOs at reduced B field

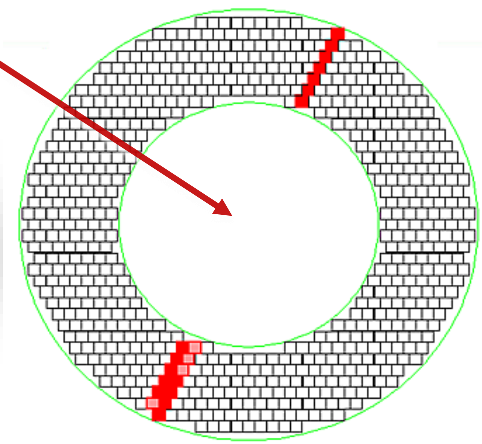

Radiation hardness

- Radiation levels for COMET Phase-I
  - at detector area by PHITS/Geant
  - neutron: 10^{12} n/cm^2 (1MeV eq)
  - gamma-rays: 2 kGy
- Radiation issues
  - electronics components (RECBE, CTH, Roesti)
    - regulators and SFP (optical transceiver)
  - FPGA
- Irradiation tests made
  - gamma irradiation: Osaka U.
  - neutron irradiation: Kobe U.

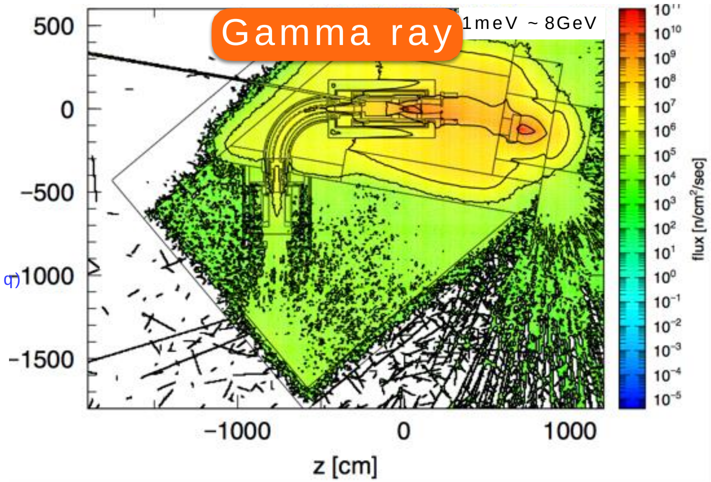

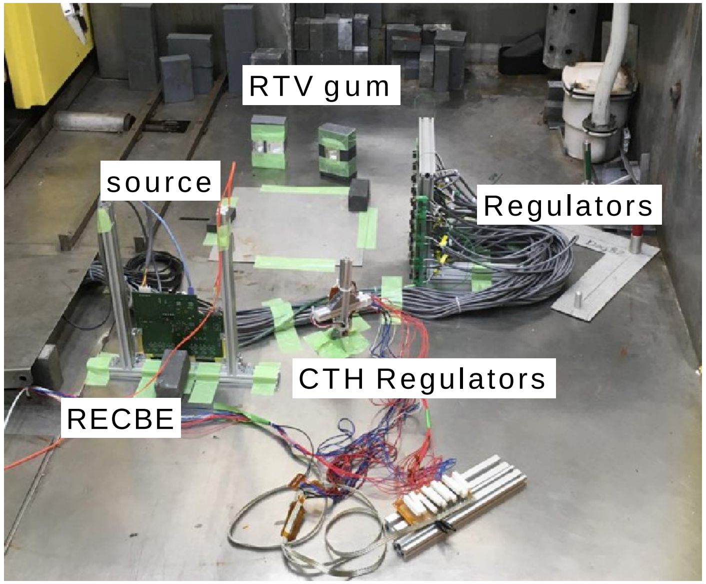

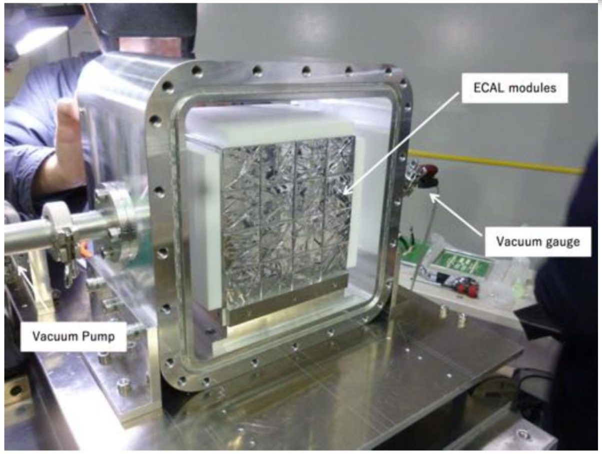

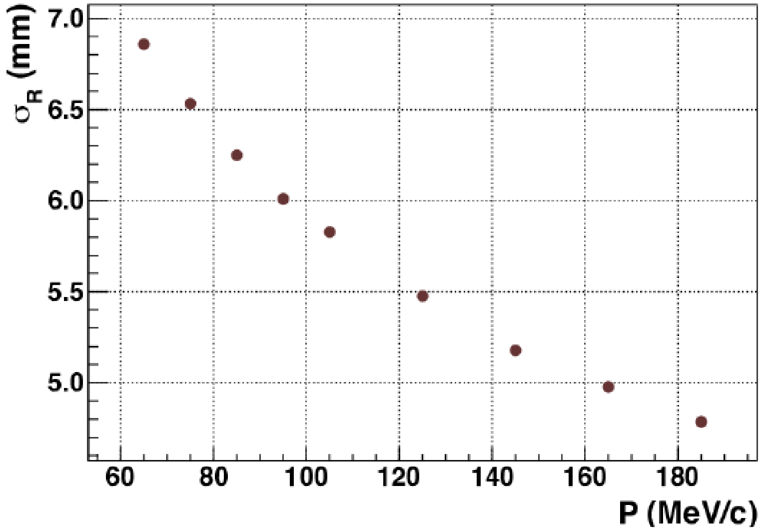

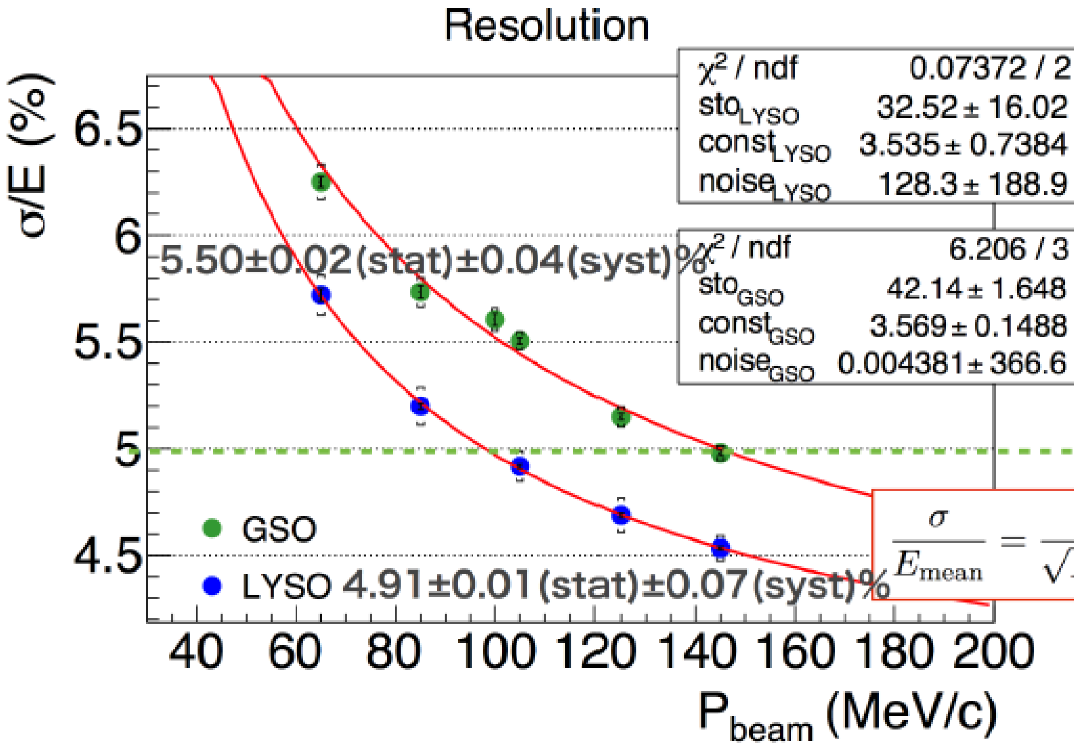

$$\frac{\sigma}{E_{mean}} = \frac{\text{sto.}}{\sqrt{P_{mean}}} \oplus \text{const.} \oplus \frac{\text{noise.}}{P_{mean}}$$

LYSO calorimeter

GSO and LYSO crystals were tested
Preliminary resolutions were 5.7% and 4.6%
LYSO was chosen as final option

(a) 1 crystal

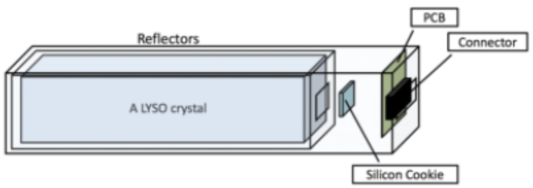

(b) 2x2 module
4 crystals

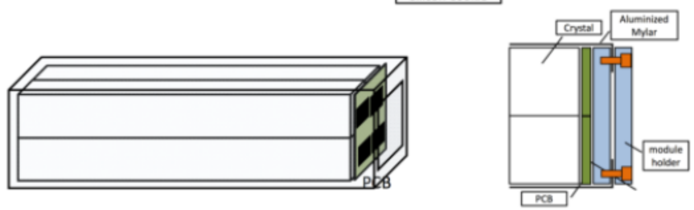

(c) 4x4 super-module
16 modules = 64 crystals

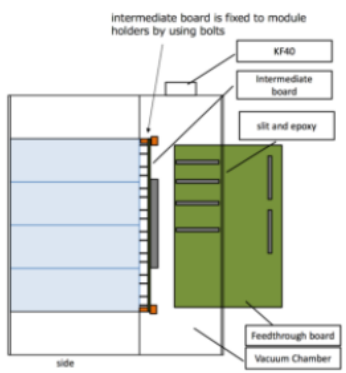

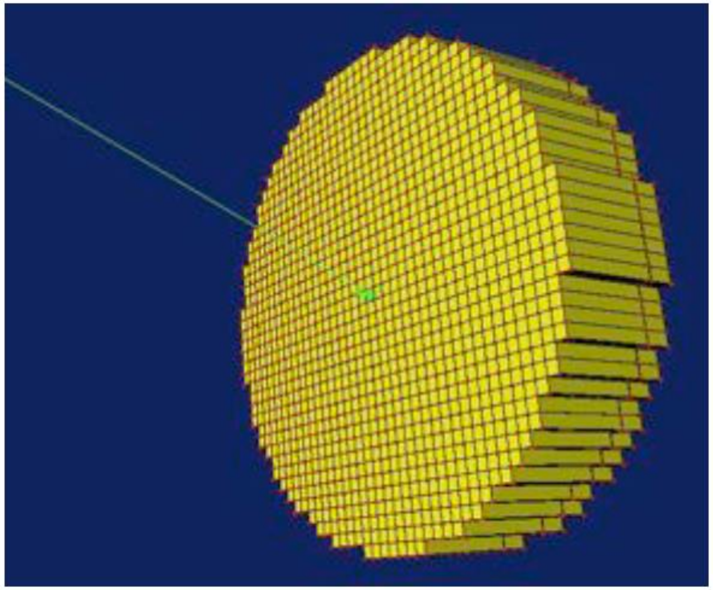

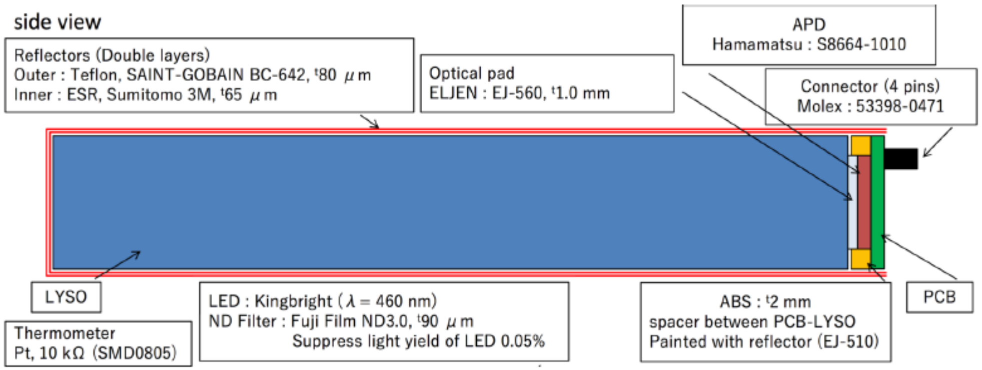

Improving S/N in the CyDet

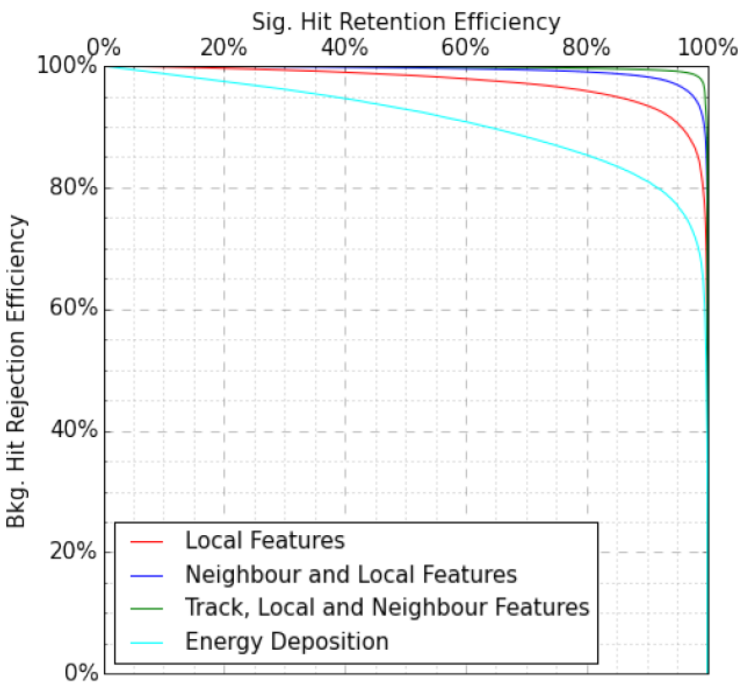

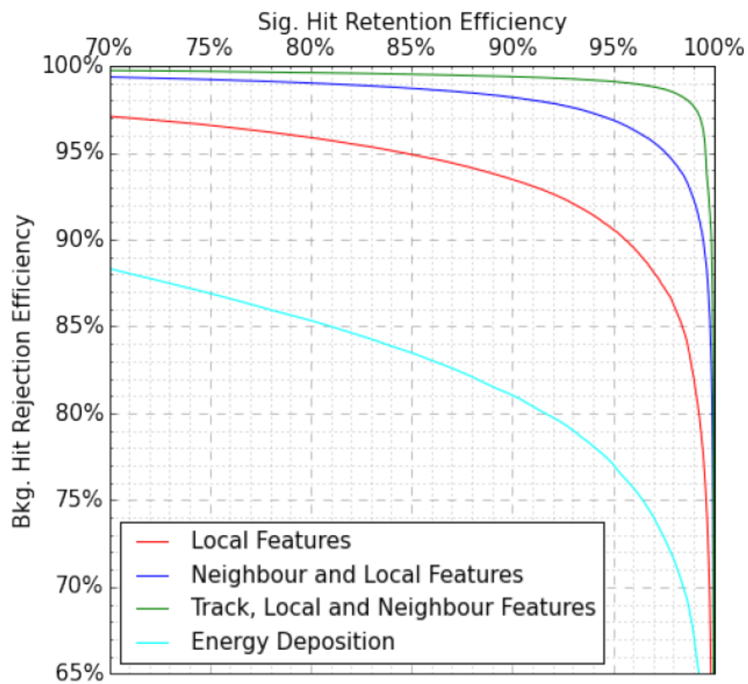

Cosmic Ray Veto

Cosmic Ray Background

- The total background from all sources in the three-year Mu2e conversion electron sample is 0.4 events
- Cosmic rays produce 1 signal-like event per day by interacting with detector components to produce a 105 MeV electron, resulting in $\mathcal{O}(10^3)$ potential background events

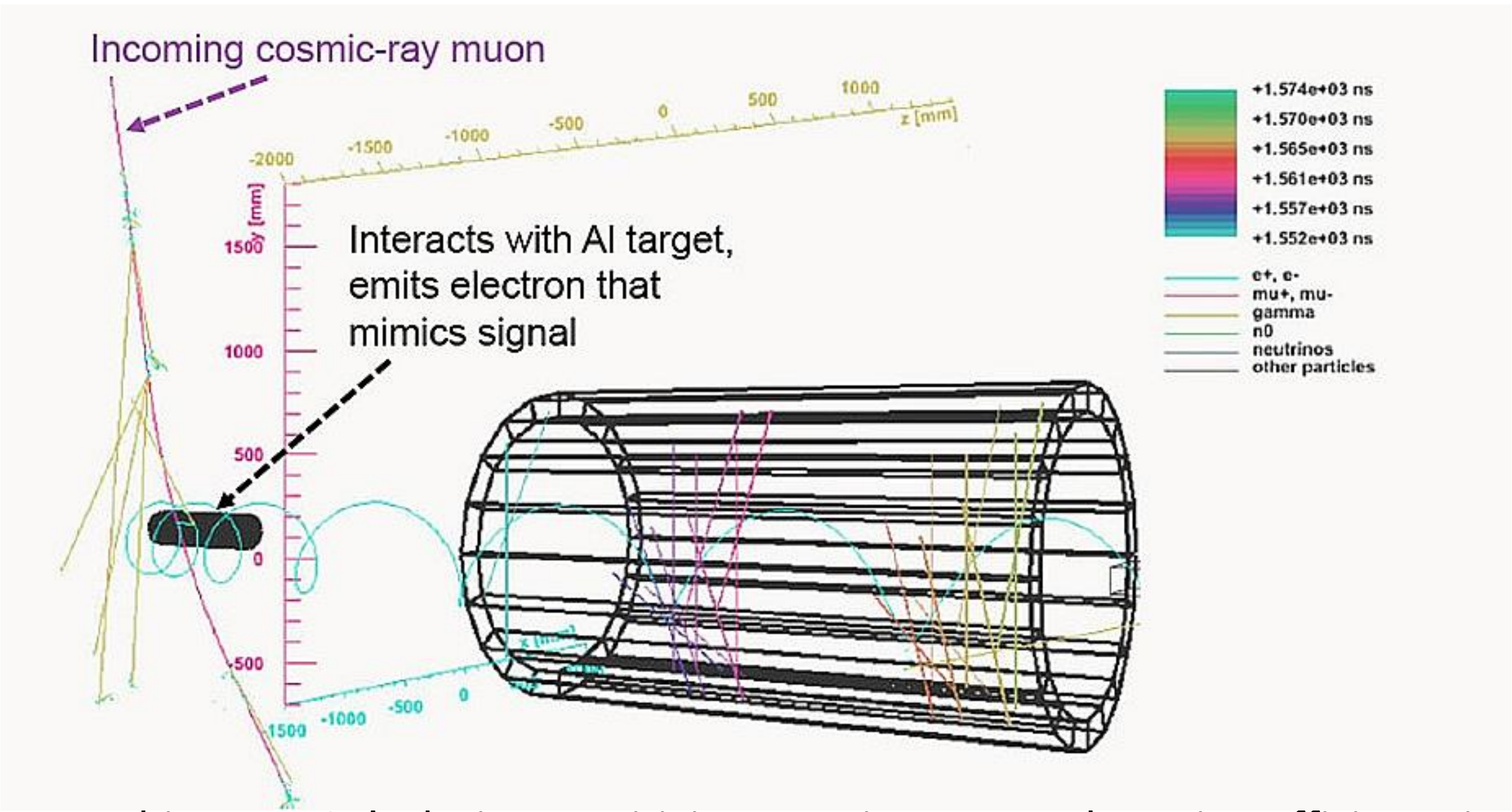

- Thus, to achieve Mu2e's design sensitivity, cosmic ray veto detection efficiency is required to be > 99.99%

Active Cosmic Ray Veto

- Cosmic Ray Veto(CRV) consists of 4-layer scintillating 5x2 cm^2 counters, readout through wavelength-shifting fibers by 2x2 mm^2 SiPMs
- All counters except CRV-U and CRV-TST are read out on both sides
- Require hit coincidence in at least 3 out of 4 layers localized in time and space for a cosmic ray muon track
- Veto 125 ns from a signal window after each coincidence in the CRV

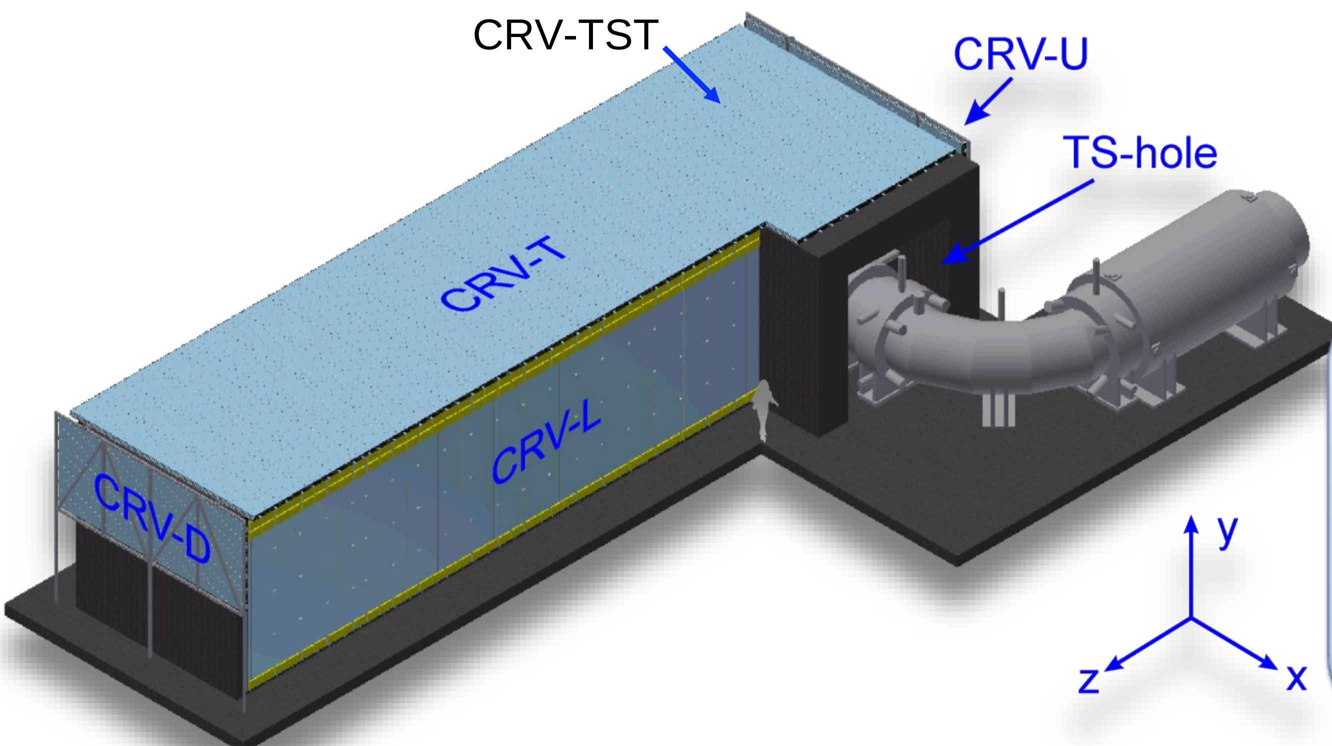

CRV details:

- Area: 323 m^2
- 82 modules
- 55 tons of counters
- 50 km of fibers
- 18,944 SiPMs

Cosmic Ray Veto (CRV)

- Multiple layers of scintillator panels surround detector to veto cosmic rays

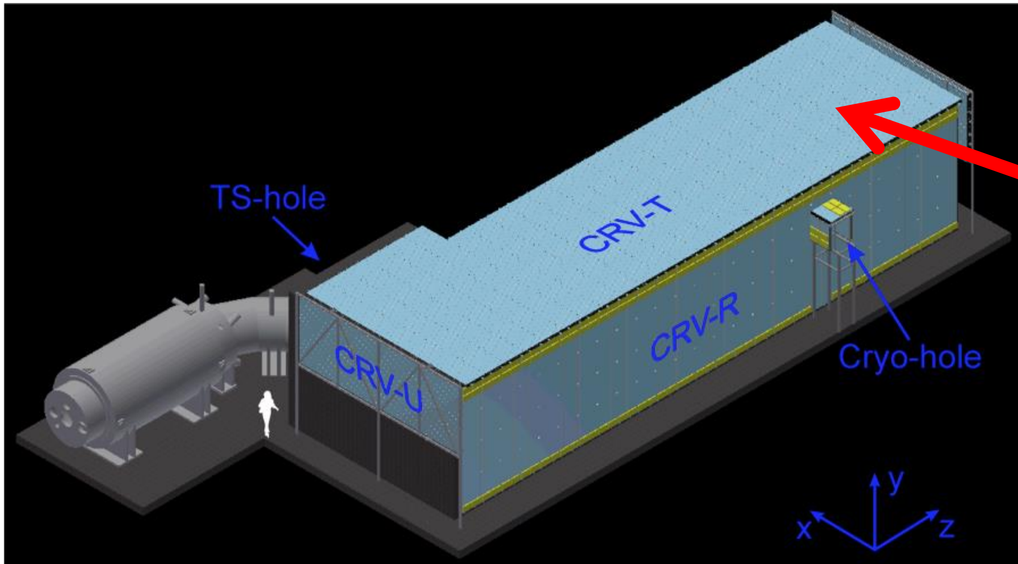

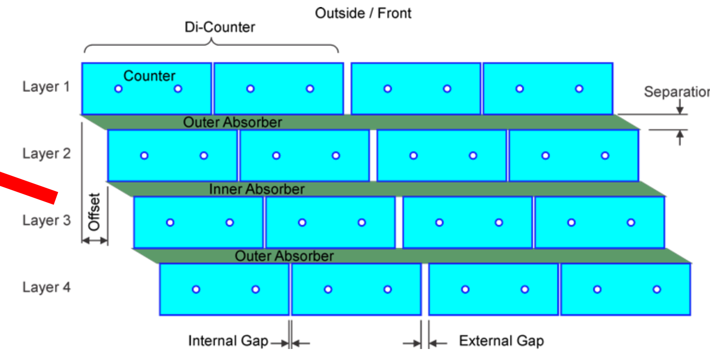

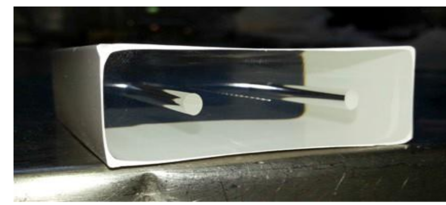

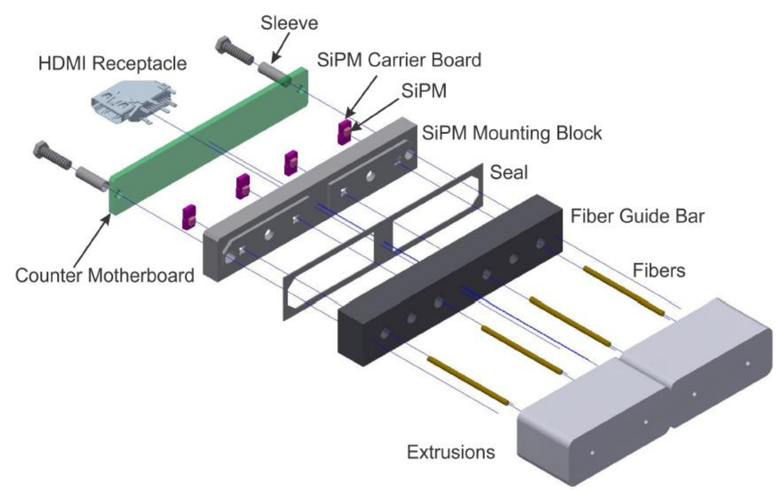

Neutrons and gammas at the CRV

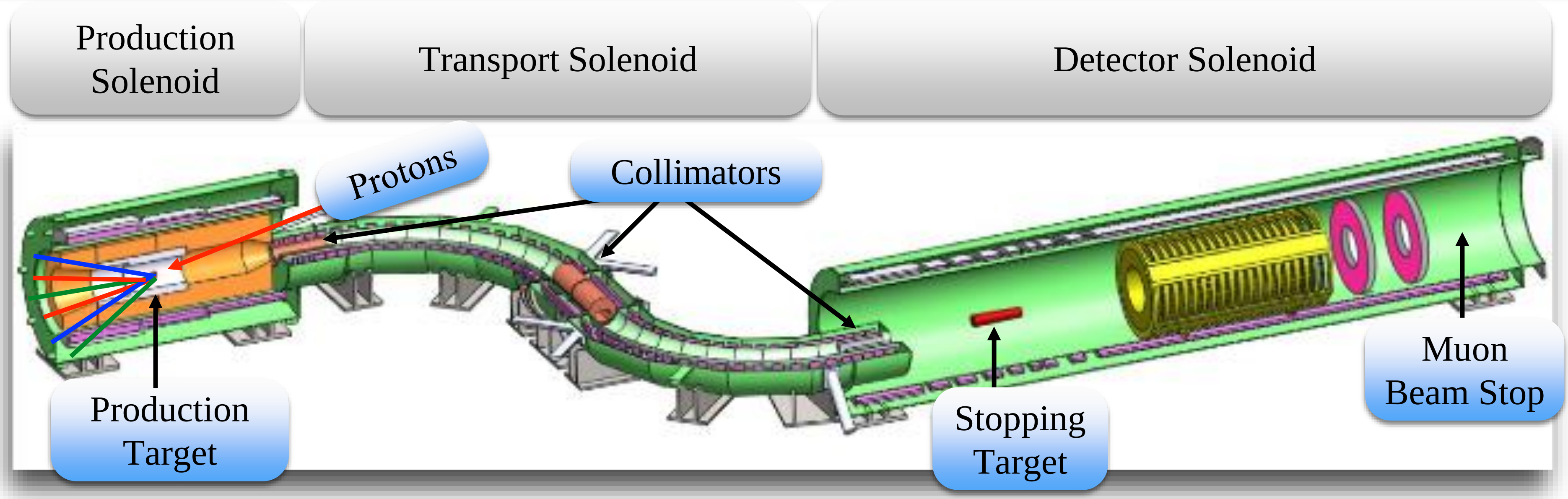

- Neutron and gamma fluxes from beam interactions are challenges to the CRV
  - Hits in the CRV fake cosmic ray muons and increase the dead-time
- The largest source of neutrons originate from the Production Solenoid after the beam flash
  - This source is prompt; it is reduced after 700 ns
- Neutrons are thermalized, captured and produce delayed γs
  - Other sources of γs : bremsstrahlung from electrons from μ decays
- Source of delayed neutrons originate from μ captures on collimators, beam-line and stopping target

CRV shielding

- CRV needs to be shielded from the beam-induced radiation backgrounds
- Therefore the CRV is mounted on ~1 meter of concrete walls
- T-shaped concrete blocks are designed to avoid direct cracks
- Region close to PS/TS is enhanced with heavy barite-enriched concrete

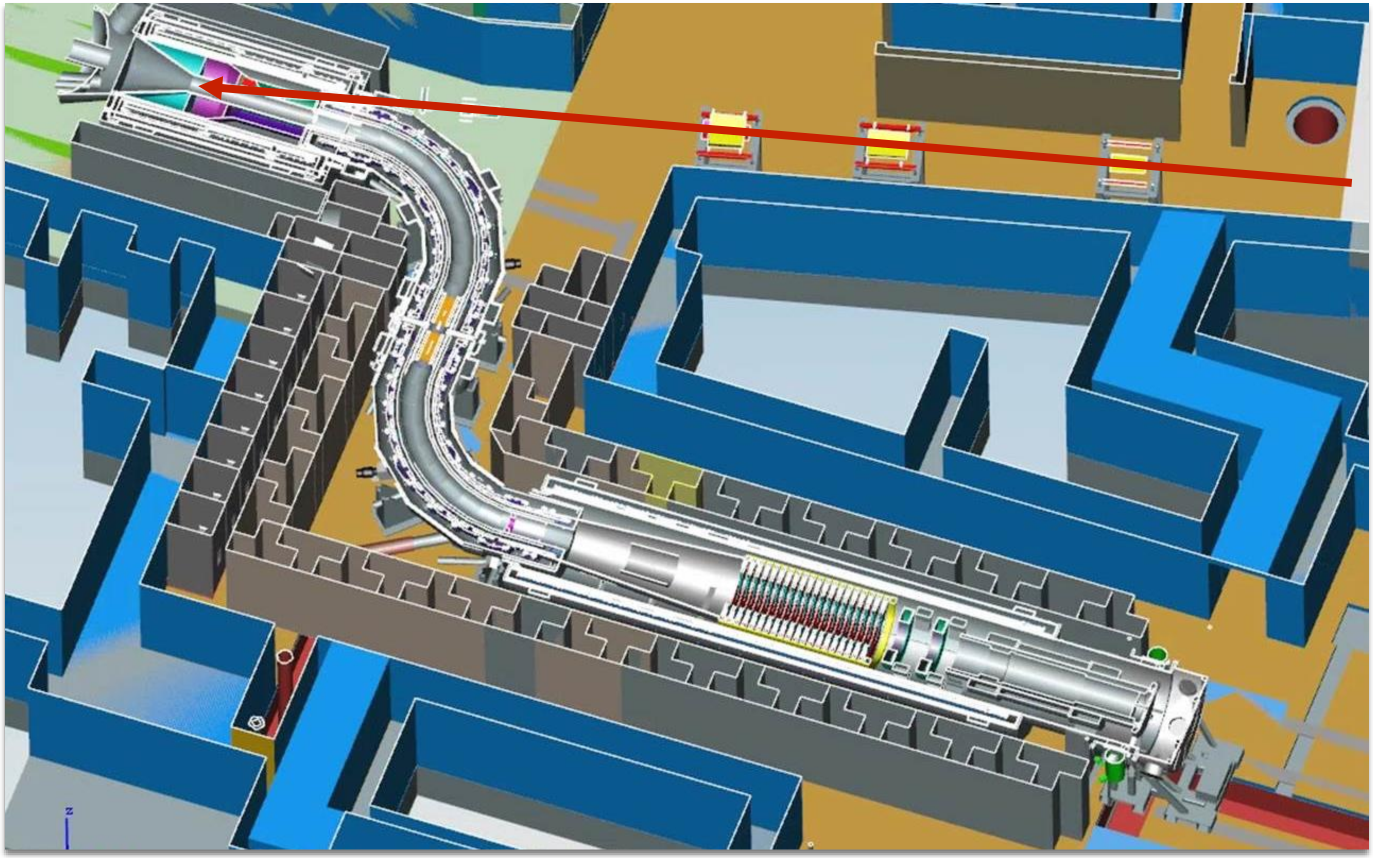

- COMET CRV uses scintillator slabs with embedded fiber and SiPM readout,
- Radiation tolerance is important
  - 5 walls, each wall composed of panels
  - readout ASIC from LHCb from LPC
- Resistive Plate Chamber (RPC)
  - used in high neutron yield area.
  - LPC design, radiation tolerance

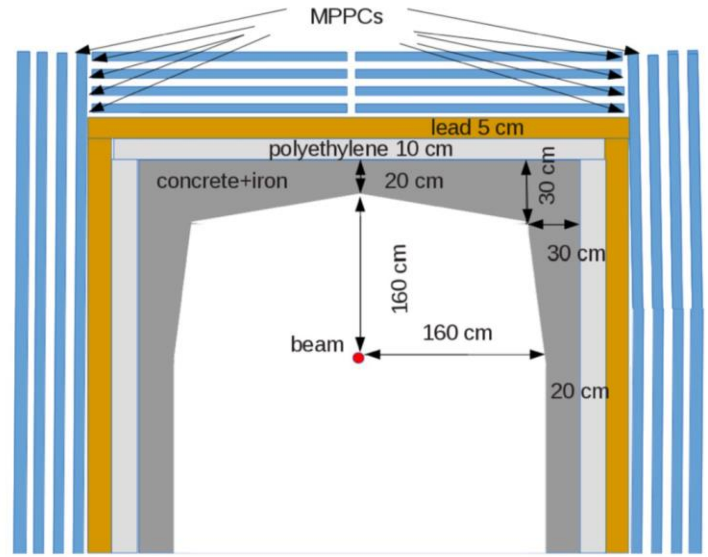

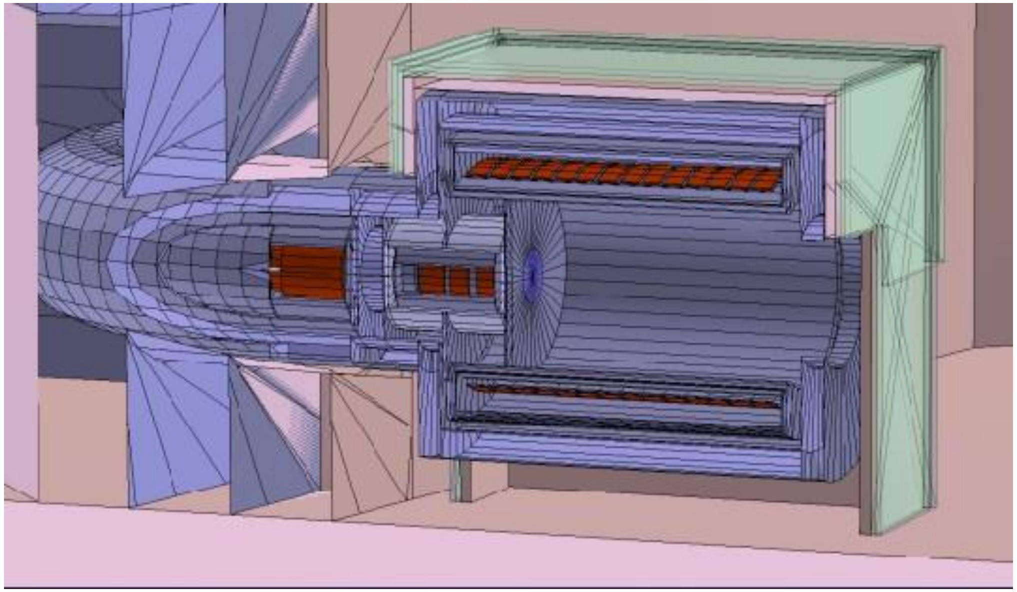

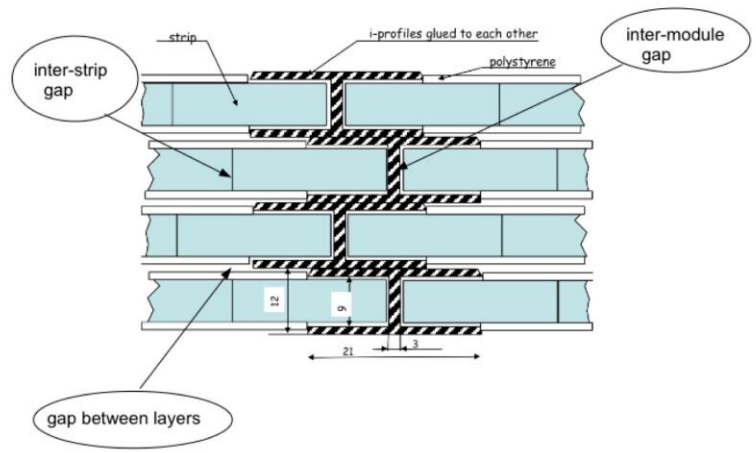

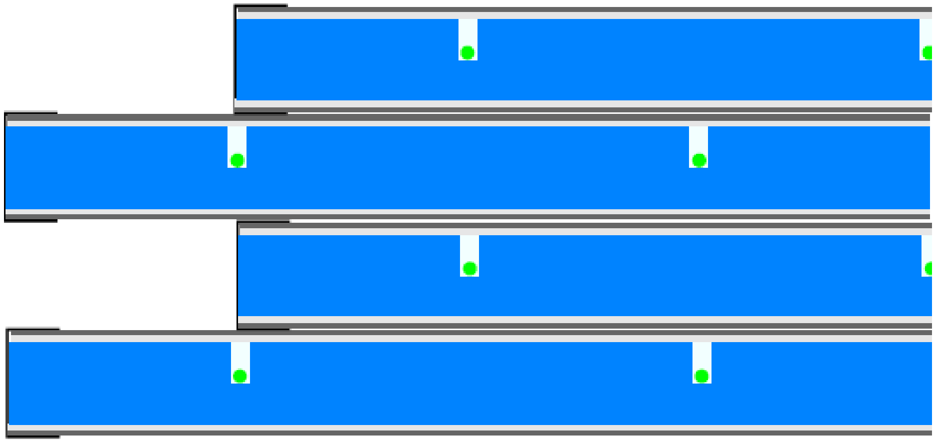

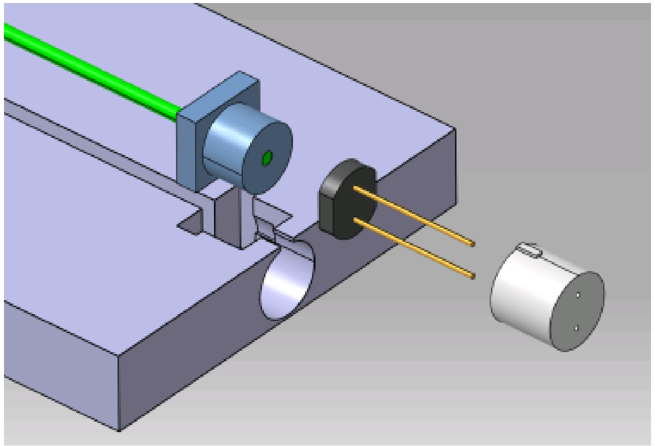

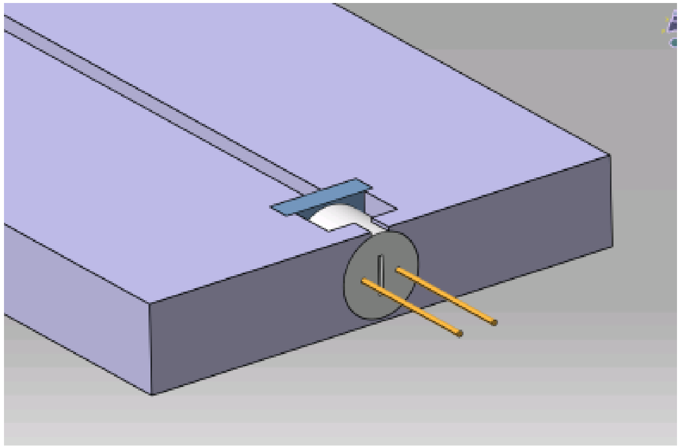

Schedule

The CLFV landscape

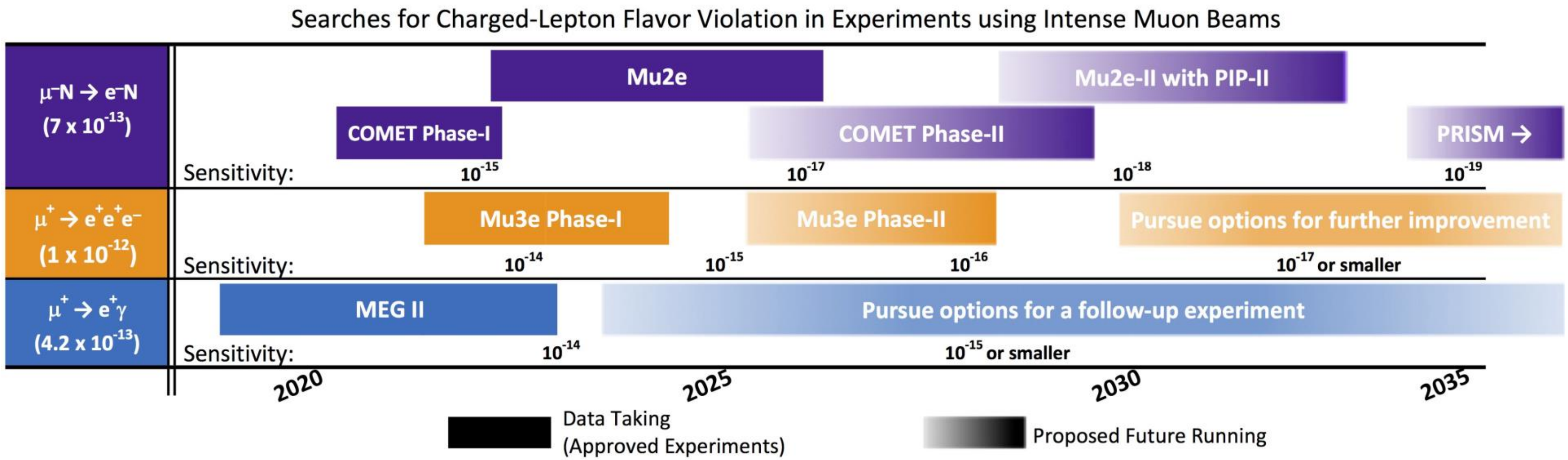

After COMET and Mu2e

$$R_{\mu e} = 10^{-16}$$

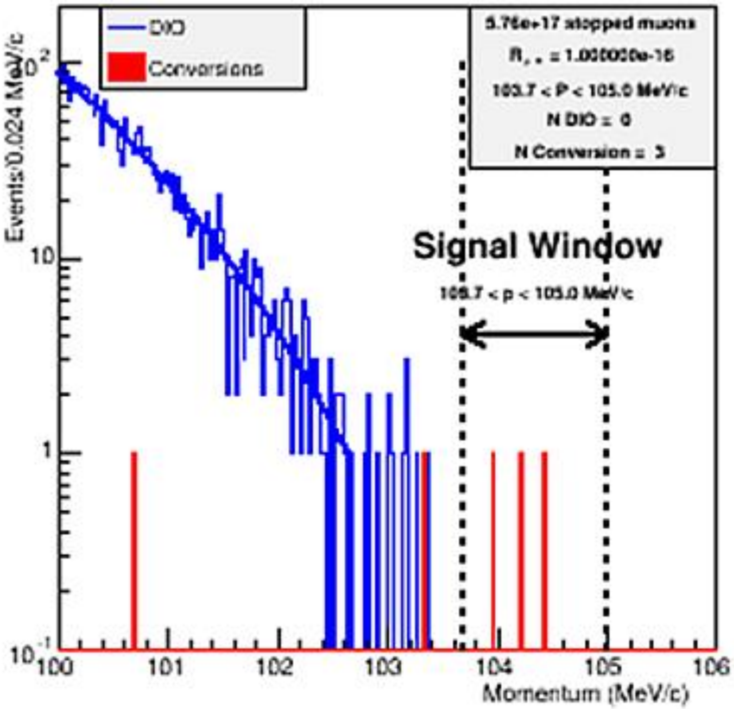

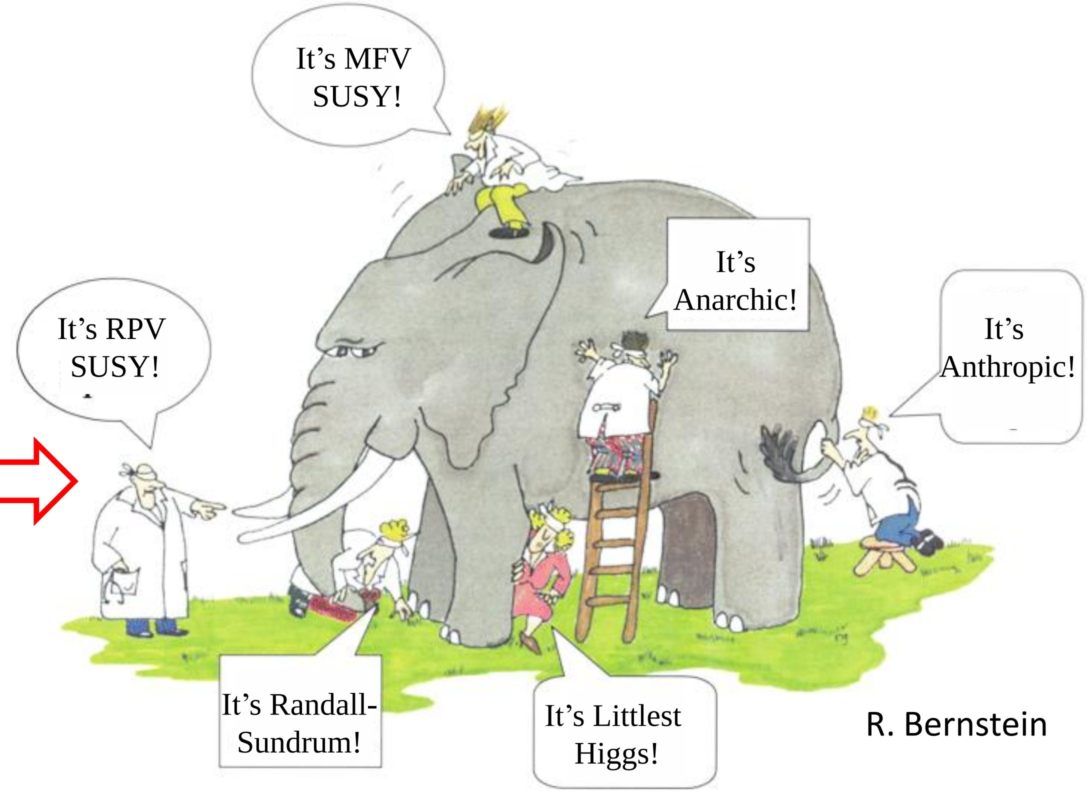

R. Bernstein

- What's the $\mu \to e\gamma$ signal (if any)
- What's the target dependence?

Upgrade scenarios

Mu2e Signal?

No

- Both prompt and DIO backgrounds must be lowered to measure

  $R_{\mu e} \sim 10^{-18}$

- Must upgrade all aspects of production, transport and detection

Yes

- Must compare different targets
- Optimize muon transport and detector for short bound muon lifetimes
- Backgrounds might not be as important.

Target dependence of conversion

- Different models predict different target dependence as well as different relative rates for μ N $\rightarrow e$ N and $\mu \rightarrow e\,\gamma$
- Caution is advised

$$B_{\mu\rightarrow e}(Z) \equiv \frac{\Gamma_{conv}(Z,A)}{\Gamma_{capt}(Z,A)}$$

- Sources of structure vs Z
  - Nuclear shell structure
    - r = $r_0 A^{1/3}$ <u>on average</u>
  - Normalization to μ capture which is a process that has coherent and incoherent components that vary with nuclear structure

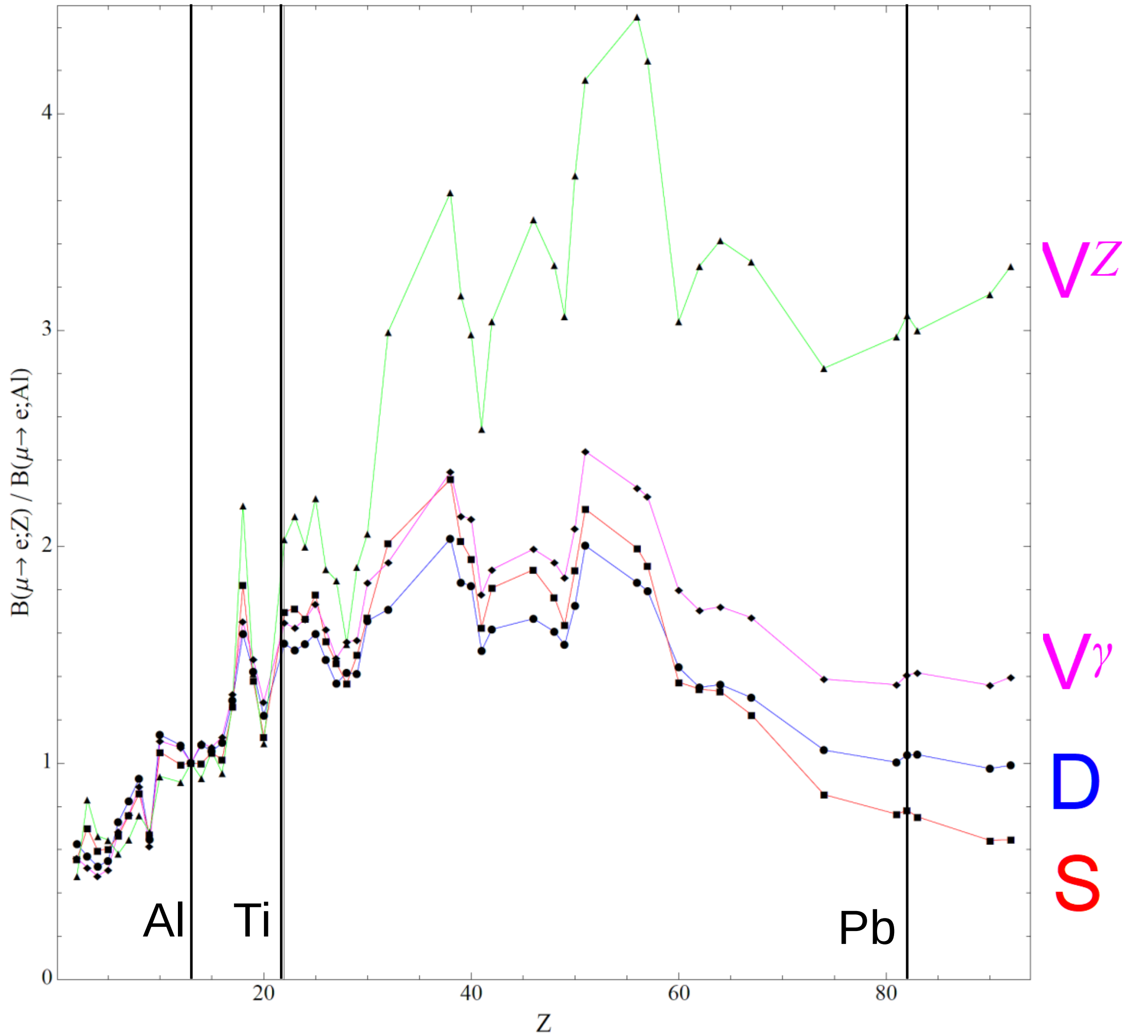

V. Cirigliano, R. Kitano, Y. Okada, P. Tuzon., arXiv:0904.0957 [hep-ph]; Phys.Rev. D80 (2009) 013002

DIO endpoint energy *vs.* Z

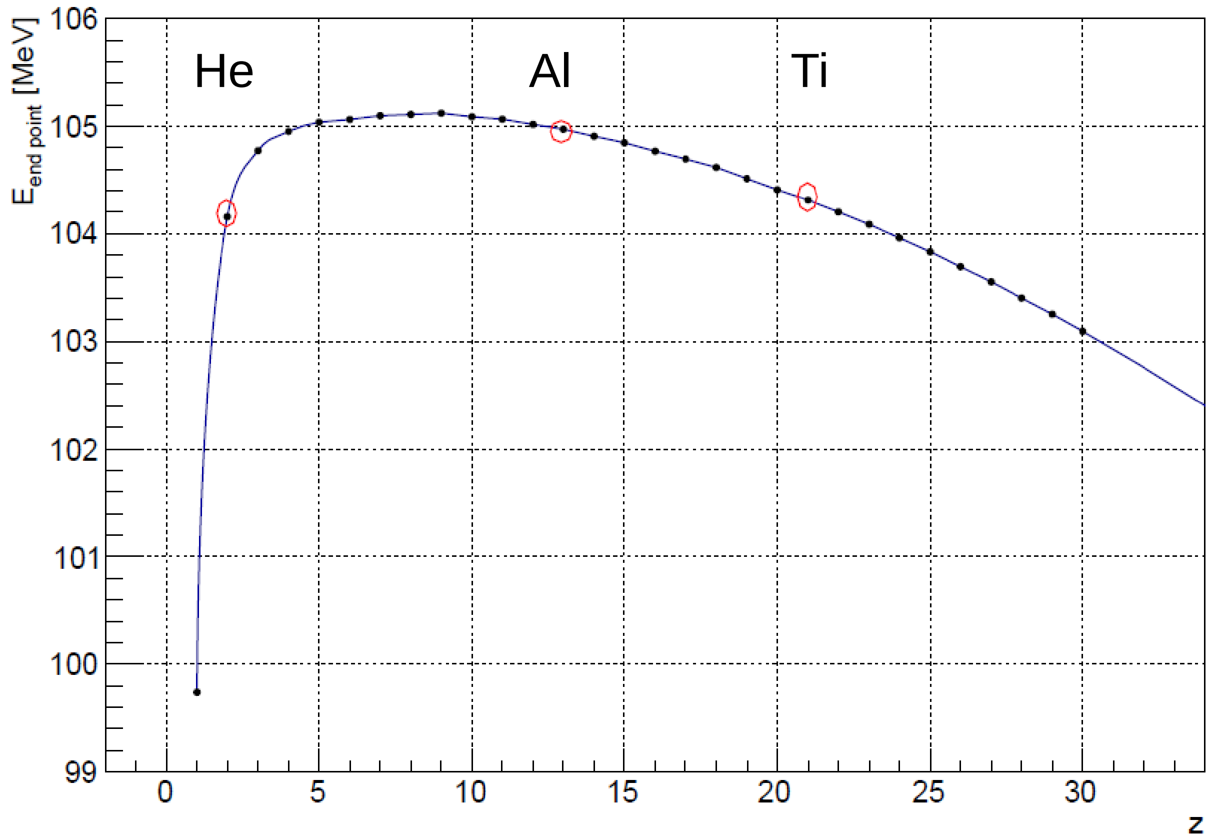

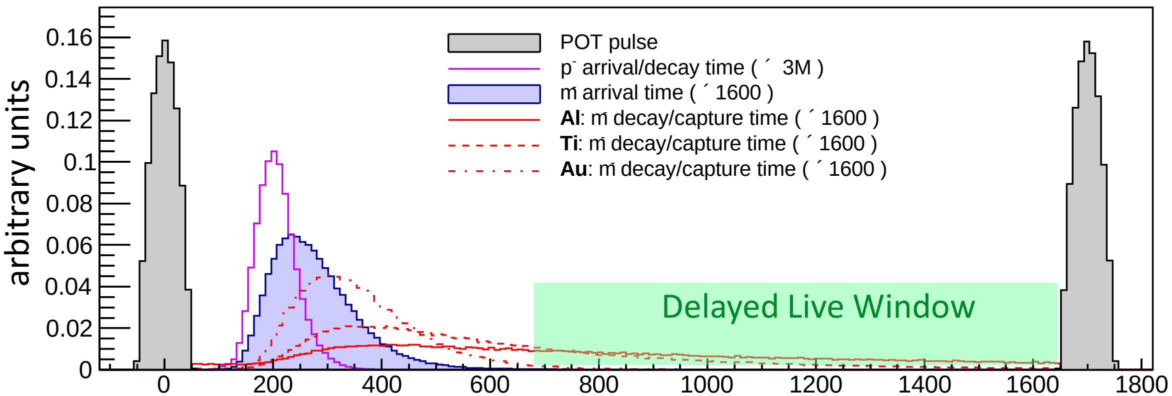

K. Knoepfel, *et al.*, arXiv:1307:1168 (2013).

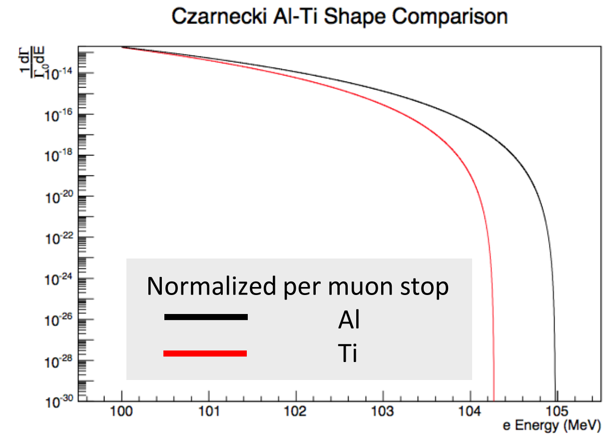

Element ($^A_Z N$)	Density (ρ_N)	Decay fraction (f_N)	Lifetime (τ_N)
$^{27}_{13}$Al	2.70 g/cm^3	0.39	864 ns
$^{46-50}_{22}$Ti	4.51 g/cm^3	0.15	329 ns

A. Czarnecki, X. Garcia I Tormo, & W.J. Marciano, PRD 84 (2011) 013006.

- Aluminum & Titanium stopping targets have been investigated
  - Accounted for differences in density, decay fraction, end-point energy, DIO spectrum
- **Total background can be kept ~1 event**
  - **Discovery sensitivity continues to scale linearly with single-event-sensitivity**

Mu2e-II Background estimates

Category	Source	Events (Al)	Events (Ti)
Intrinsic	μ decay in orbit	0.26	1.19
	Radiative μ capture	<0.01	<0.01
Late Arriving	Radiative π capture	0.04	0.05
	Beam electrons	<0.01	<0.01
	μ decay in flight	<0.01	<0.01
	π decay in flight	<0.01	<0.01
Miscellaneous	Anti-proton induced	--	--
	Cosmic ray induced	0.16	0.16
Total Background:		**0.46**	**1.40**

Table 1: Estimated background yields for the Mu2e-II experiment assuming an aluminum (Al) or a titanium (Ti) stopping target. These studies were performed for a proton beam energy of 1 GeV. The total uncertainty is about 20%. Reproduced from arXiv:1307.1168. Note that, unlike in the case of aluminum, the titanium analysis has not yet been rigorously optimized.

- From Feasibility study (arXiv:1307.1168)
  - Assumptions:
    - BaF_2 calorimeter
    - 8 μm thick straw walls for tracker
    - extinction 10^{-12}
    - CR veto efficiency of 99.99%
    - μ^- stops/POT same as Mu2e

We need even more muons

The Fermilab neutrino program (DUNE) also needs more neutrinos
This motivates a new accelerator, PIP-II, a linac that can run in both pulsed and CW modes
Is there an optimal proton beam energy to produce more ν, μ?
Examine from a Mu2e-centric perspective
(assume no change in geometry of Heat & Radiation Shield or production target)

Muon Yield Studies

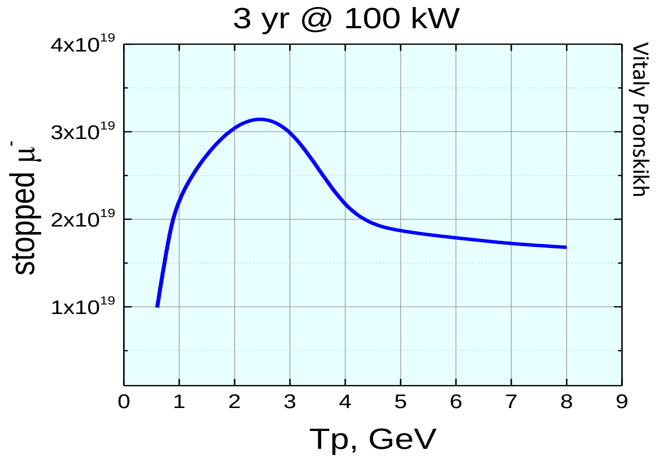

Coil Damage Studies

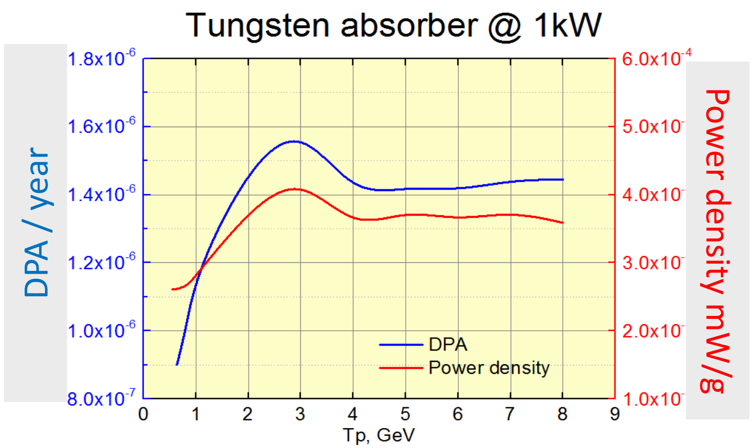

(nb. PS conductor can tolerate ~5x10^{-5} DPA/yr and ~3 x 10^{-2} mW/g Peak Power density)

- The muon yield at 0.8 GeV is ~same as at 8 GeV, while coil damage is ~30% smaller
- An energy below $\bar{p}$ production threshold (Tp < 4 GeV) is strongly preferred
- Upgrades to the Production Solenoid are required to enable it to tolerate 100 kW

(arXiv:1612.08931)

(DPA = displacements per atom)

PIP-II Capabilities

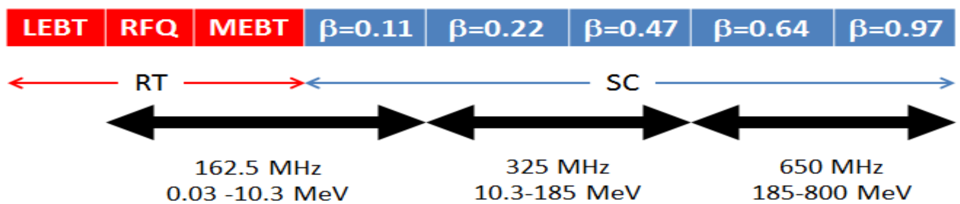

- PIP-II is capable of running in CW mode (with sufficient cooling)
  - 2 mA average current (H^-) at 800 MeV (1.6 MW)
  - LBNF/DUNE needs 1.2 MW at 60-120 GeV
  - **100 kW of 800 MeV beam for Mu2e-II is readily available with high spill fraction**

Chopper design optics

Figures from Paul Derwent

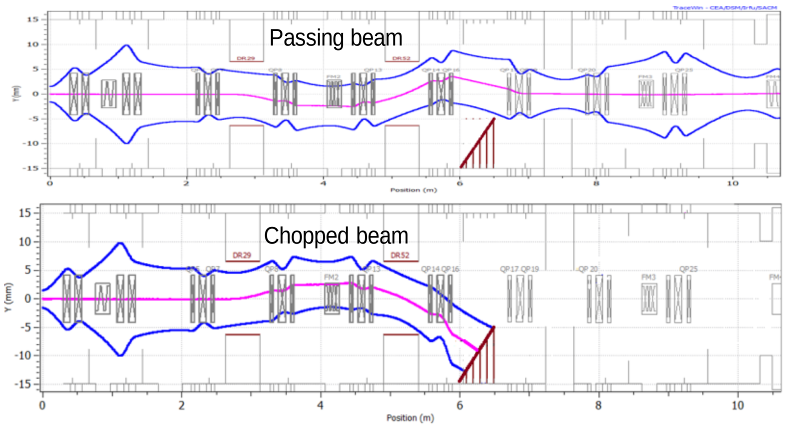

Measured performance at PIP2-IT

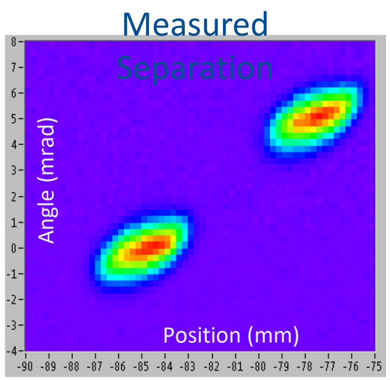

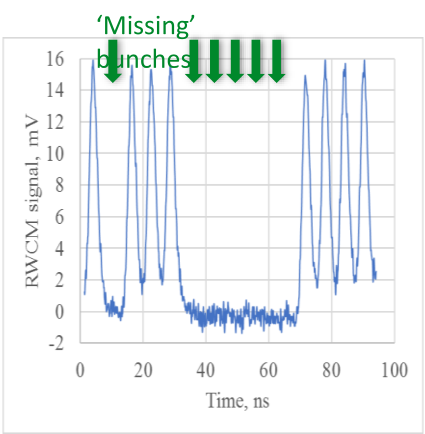

Possible Mu2e-II scenario: 6 full buckets+270 empty buckets = 40 ns wide pulses every 1.7 μs

- PIP-II is capable of delivering customized pulsed time structure
  - Utilizes a bunch-by-bunch "chopper" at end of MEBT section
  - **Prototype built & demonstrated to work at PIP2-IT facility**
  - **Required R&D: What's the level of extinction achieved by chopper alone?**

Beam Parameters for Mu2e-II

	Mu2e	Mu2e-II	Comments
source	Slow extracted from Delivery Ring	H- direct from PIP-II Linac	Mu2e-II will need to strip H- ions upstream of production target
beam energy (MeV)	8000	800	optimal beam energy 1-3 GeV
p pulse full width (ns)	250	<= 100	from PIP-II could range 40-100 ns for ~100 kW
p pulse spacing (ns)	1695	1699	assumes an Al. target; shorter spacing better for Ti or Au targets
p pulse full width (ns)	250	<= 100	from PIP-II could range 40-100 ns for ~100 kW
protons per pulse	4.00E+07	1.20E+09	
experimental duty factor	25%	>90%	important for keeping instantaneous rates under control
peak pulse rate	590 kHz	589 kHz	
avg. pulse rate	145 kHz	530 kHz	
protons per second	5.80E+12	6.36E+14	
stopped μ per second	1.16E+10	1.17E+11	
run time (sec/yr)	2.0E+07	2.0E+07	
run duration (yr)	3.0E+00	3.0E+00	
Total POT (3+1)y	4.7E+20	4.40E+22	approximate, depends on stopped-muon yield
Total stop-μ 3y	6.96E+17	7.00E+18	
extinction	1.0E-10	1.0E-11	ratio of (out-of-time / in-time) protons
average beam power (kW)	8	80	80kW is approximate; will depend on production target design and transport, which will affect mu-stop yield

- Total POT and beam power are approximate – will depend on details of production target design and transport, which affect the stopped-μ yield

- PIP-II is capable of meeting these requirements

Next generation capture solenoids

- Future capture solenoids must withstand higher power and more radiation
- May resemble muon collider concepts

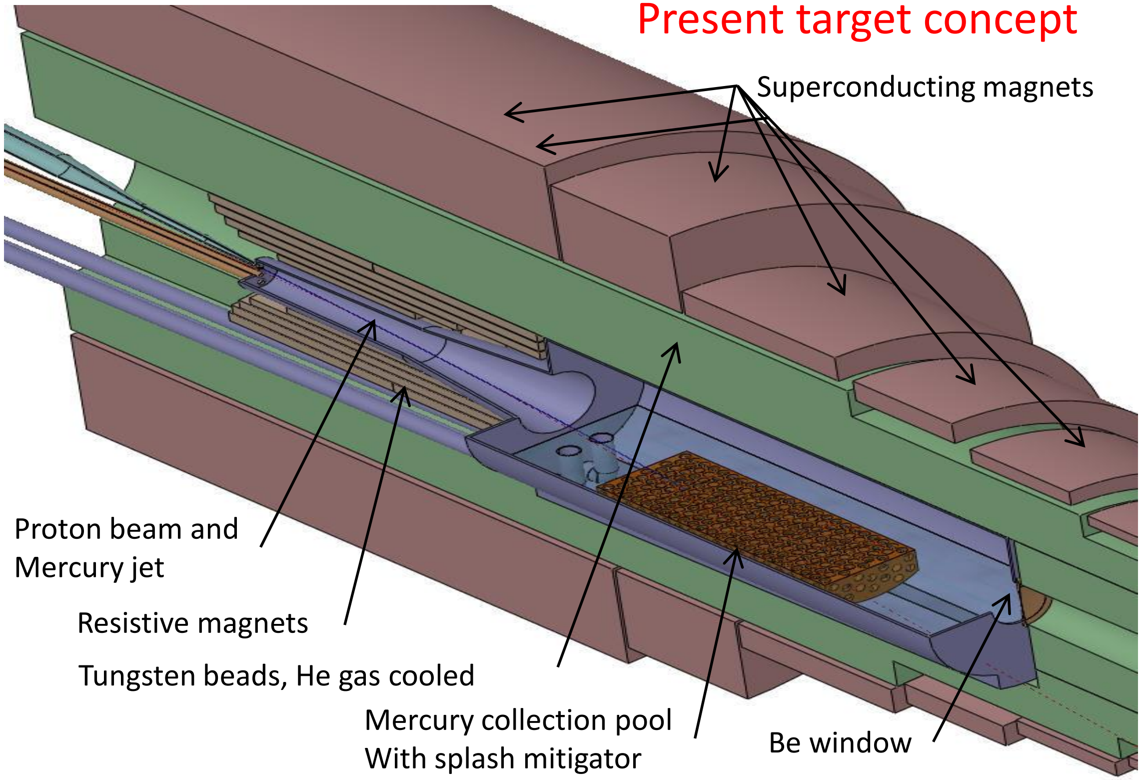

K. McDonald
RESMM'12

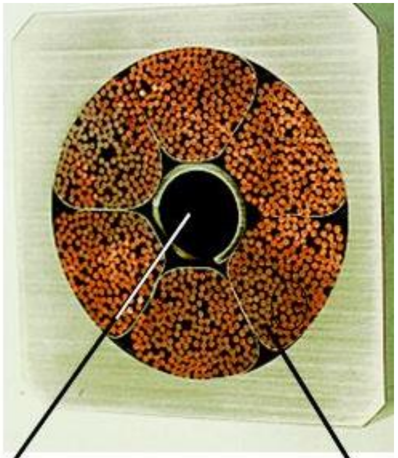

5-T copper magnet insert; 15-T Nb_3Sn coil + 5-T NbTi outsert

It would be desirable to replace the copper magnet by a 20-T HTC insert

PRISM

PRISM

Phase Rotated Intense Slow Muon source
A fixed field alternating gradient storage ring (FFAG)
To achieve a small energy spread, the storage ring lattice performs a phase rotation

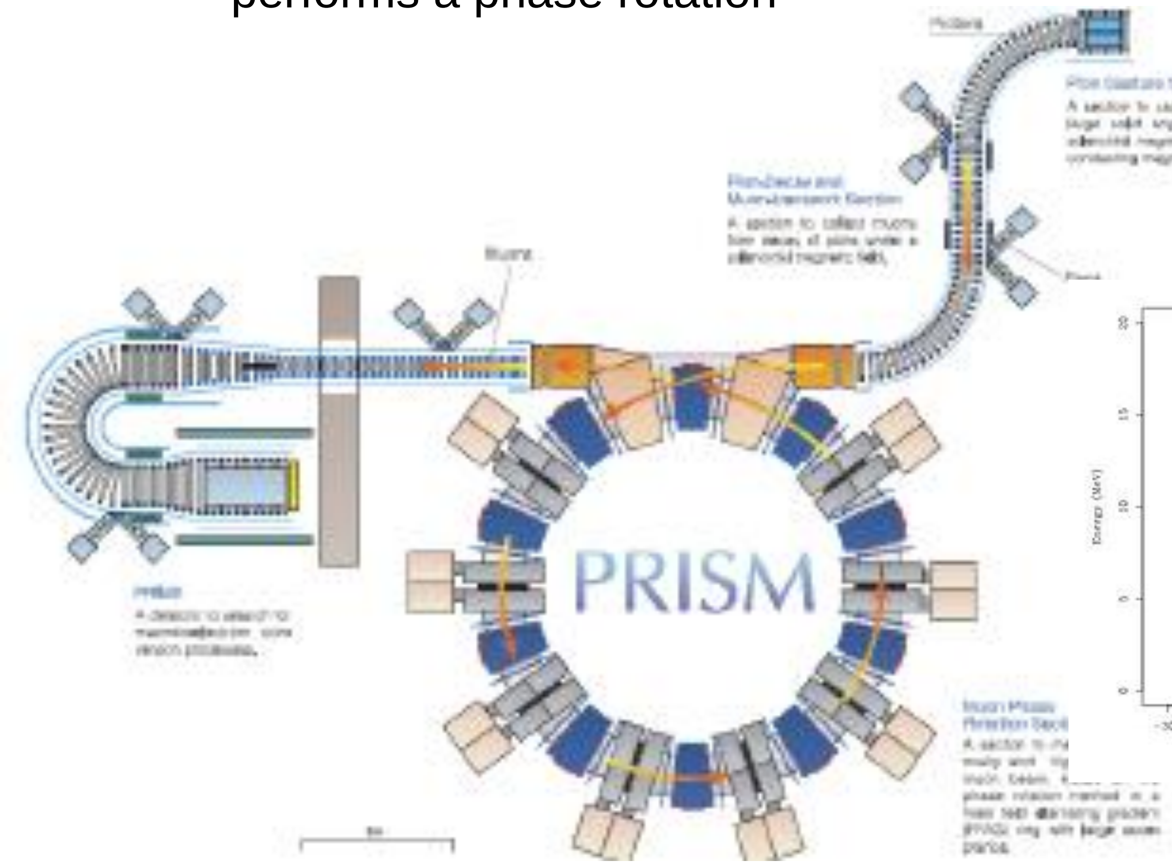

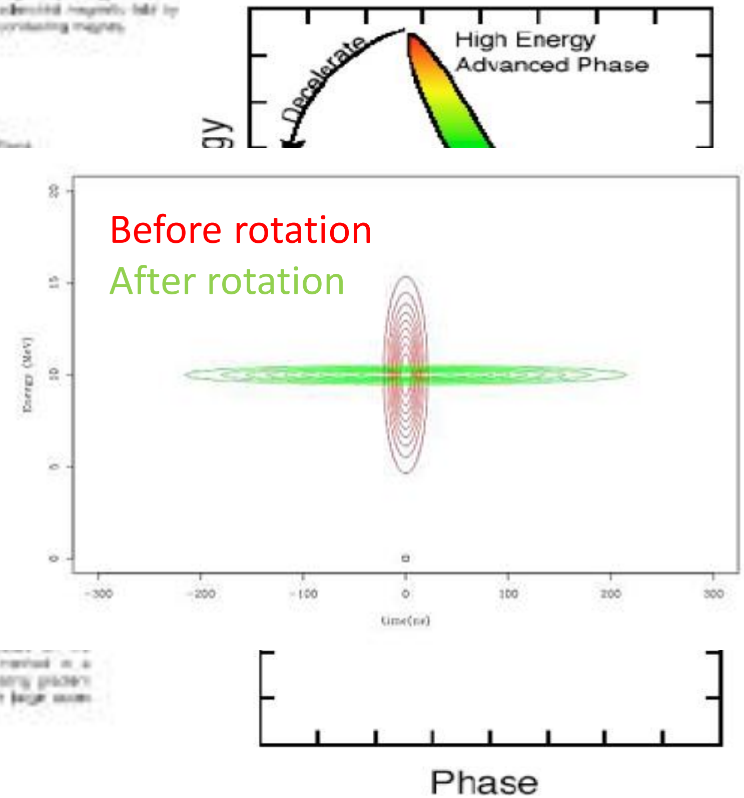

~10^{20} stopped muons/year ⇨ SES ~ 3×10^{-19}

PRISM/PRIME Challenges

- Proton source
  - Require MW beam, very short pulse (~10ns)
- Capture system
  - Active cooling of the target proton target
  - Active cooling an radiation hardness of production solenoid

Synergy with neutrino factory and muon collider R&D

- Transport system
  - Longer transport beamline:
  - FFAG(Fixed Field Alternating gradient) muon storage ring
    - Has been tested at Osaka

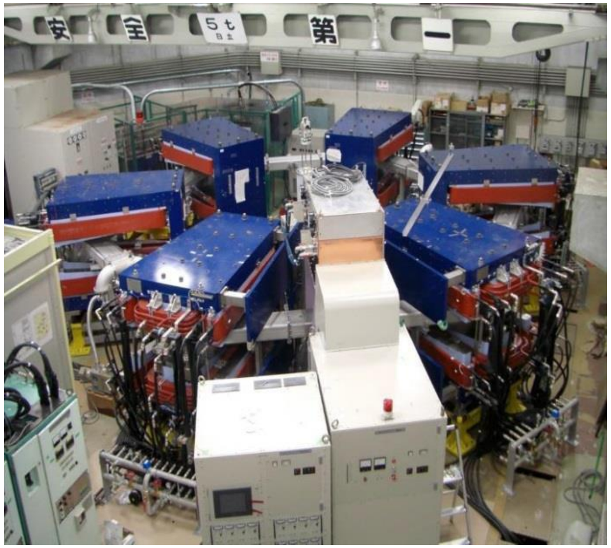

A bonus

$$\mu^- \longrightarrow e^+$$

Neutrinoless $\mu^- \to e^+$ Conversion

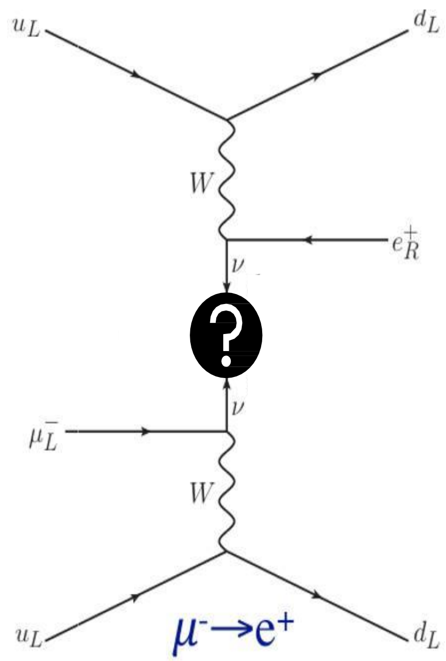

One of the Feynman diagrams contributing to $\mu^- + (A, Z) \to e^+ + (A, Z\text{-}2)$

- A secondary physics goal of the Mu2e is searching for neutrinoless muon-to-positron conversion

$$\mu^- + (A, Z) \to e^+ + (A, Z\text{-}2)$$

  - This process violates both charged lepton flavor and lepton number
  - Analogous to neutrinoless double beta decay
  - An incoherent process: capture to ground state and excited state via giant dipole resonance
  - A "free" measurement in Al (easier in Ti)
- Signal is a monoenergetic **92.3** MeV/c positron (gs), **84** MeV/c positron (GDR)
- Current experimental upper bound:
  - SINDRUM II: $1.7 \cdot 10^{-12}$ (90% CL) on Ti
    - Important backgrounds
      - Radiative Muon Capture (RMCγ)
      - Radiative Pion Capture (RPCγ)
      - Cosmic Rays

Hasung Song

NH ELSEVIER

12 March 1998

PHYSICS LETTERS B

Physics Letters B 422 (1998) 334–338

Table 1
Endpoint energies for $\mu^- \to e^+$ conversion and radiati
capture for the various titanium isotopes

A	abundance (%)	$E^{max}_{\mu^- e^+}$ (MeV)	E^{ma}_{RM} (Me
46	7.94	102.26	91.4 ±
47	7.44	100.66	93.2 ± 2.
48	73.78	98.99	89.7 ± 2.
49	5.51	95.98	91.8 ± 2.
50	5.34	91.39	86.9 ± 2.

$$B^{GS}_{\mu^- e^+} < 1.7 \cdot 10^{-12} \quad (90\%\,\mathrm{CL})$$

$$B^{GDR}_{\mu^- e^+} < 3.6 \cdot 10^{-11} \quad (90\%\,\mathrm{CL})$$

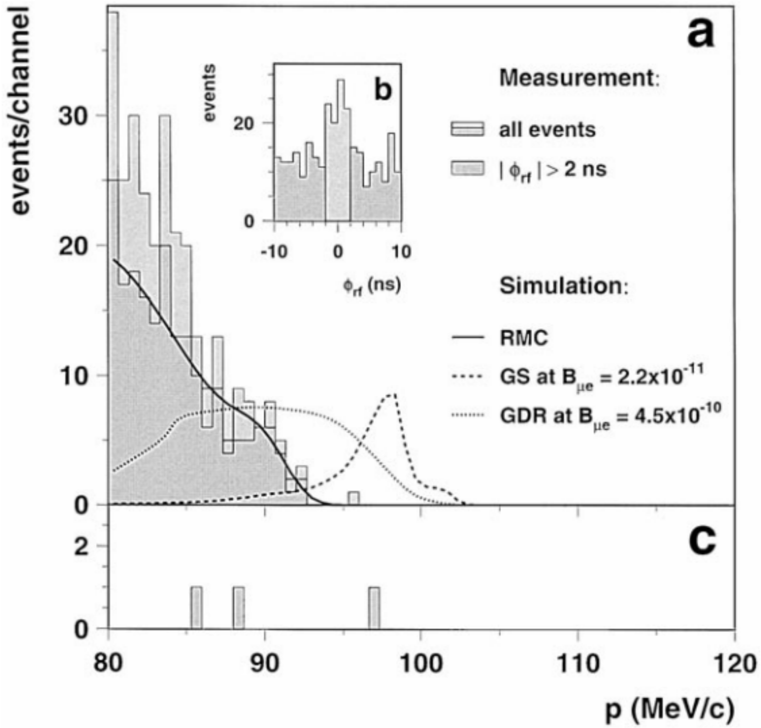

Fig. 2. Positron momentum distributions for measuring periods with (a,b) and without (c) muon beam. The measured distribution in part a is compared with the *GS* and *GDR* expectations for $\mu^- \to e^+$ conversion. The insert b shows the distribution of φ_{rf}, the decay time relative to the 50.63 MHz cyclotron frequency, exhibiting a peak caused by misidentified scattered beam electrons. The events from the grey region outside the peak have been interpreted as *RMC* events. Their momentum distribution is compared with the results from the *RMC* simulation discussed in the text.

Radiative muon capture

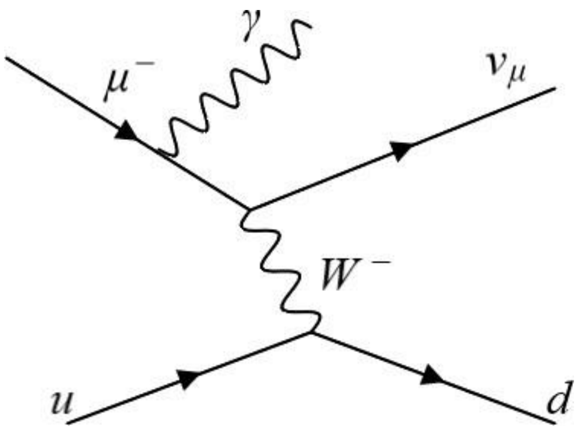

radiative muon capture

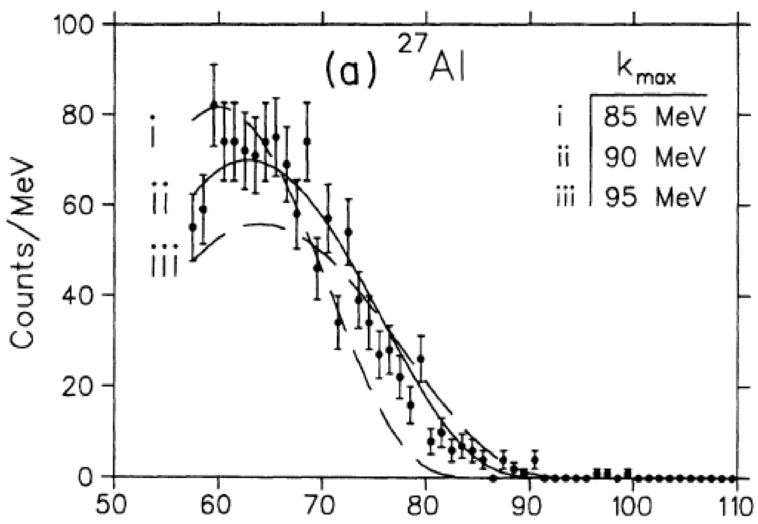

RMC gamma spectrum measured by TRIUMF with various closure approximation fits

- A muon stopped in the Al target is captured into an excited state and emits a photon that creates an electron-positron pair
- The photon energy spectrum is modeled in the closure approximation
  - $x = \frac{E_\gamma}{kma}$
  - $\frac{d}{dx}(x) = (1 + 2x + 2x^2)x(1-x)^2$

- The expected number of RMC positron background events is heavily dependent on the kinematic endpoint, k_{max} (How high RMCγ reaches)
- TRIUMF measured RMC k_{max} at 90.1±1.8[4] (MeV/c^2) but with low statistics
- Mu2e will independently measure the RMC k_{max}

Radiative Pion Capture (RPC)

The vast majority of pions decay before the stopping target, but a small number reach the target and undergo nuclear capture with the emission of a photon with sufficient energy to produce a signal-like positron

- Pion stops in the stopping target are suppressed by the pion decay time
- We will further suppress RPC backgrounds by cutting on time
- Most RPC events occur shortly after proton bunch arrival at production target

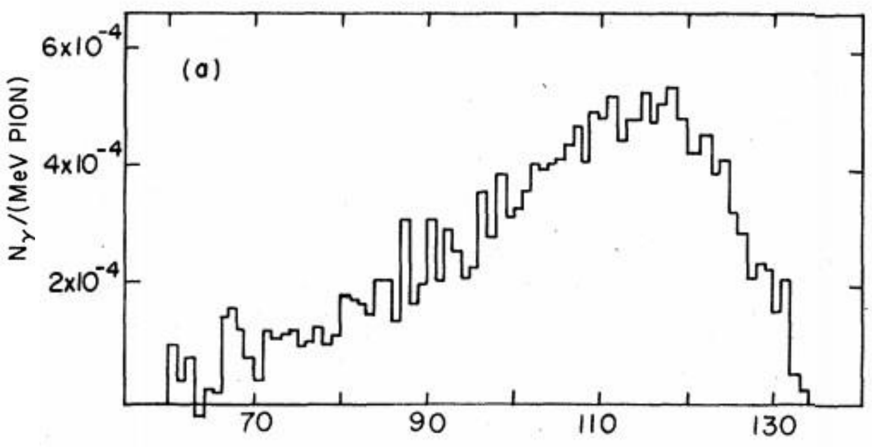

RPC Gamma Spectrum of Mg-24
J.A. Bistirlich *et al*., Phys Rev. C5, 1867 (1972)

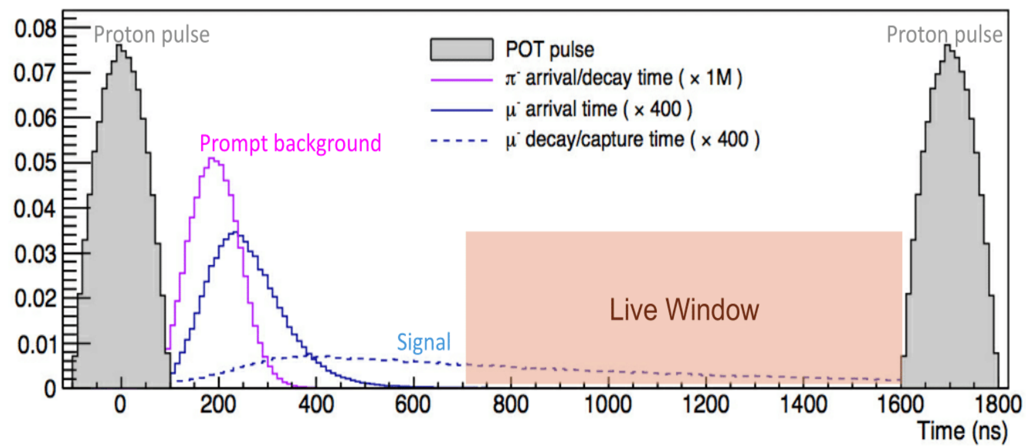

Positron Background Simulations

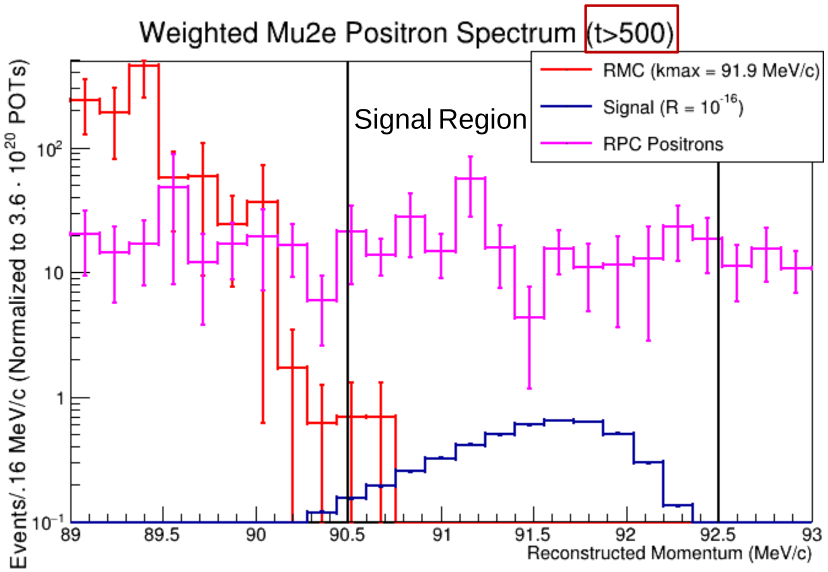

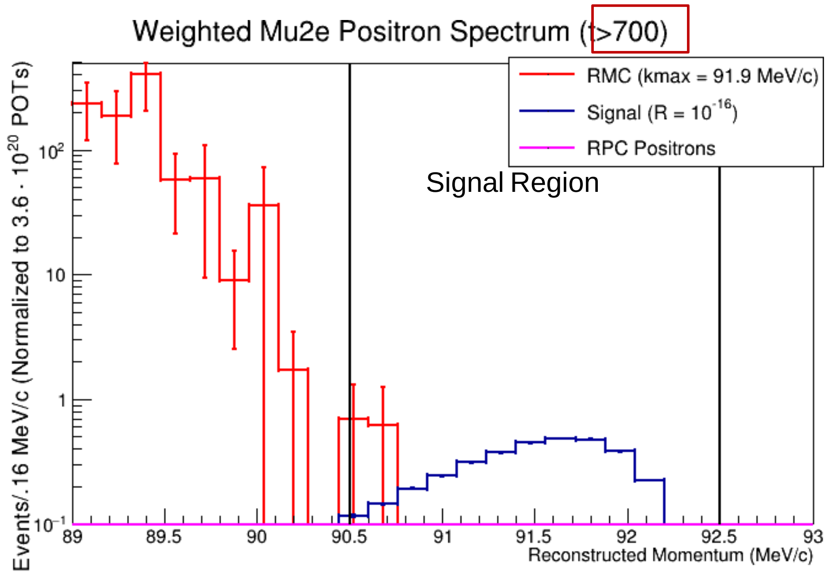

Mu2e Simulation (Preliminary)

- Total background estimates: (3 years)
  - RMC : 1.2 events
  - RPC : .004 events
- Preliminary Sensitivity Estimates:
  - SES = 2.7×10^{-17}
  - 90% CL = 1.0×10^{-16}
  - Four orders of magnitude better than SINDRUM II: 1.7×10^{-12} (90% CL) on titanium

Conclusions

- After more than seventy years, searches for charged lepton flavor violation are now approaching a sensitivity that, in a large variety of well-motivated theoretical models, may yield an observation, rather than an improved limit
- Searches for $\mu \rightarrow$e conversion, $\mu \rightarrow e\gamma$, $\mu \rightarrow 3e$, $\tau \rightarrow \mu\gamma$, …… with sensitivity improvements of from one to four orders of magnitude will be producing results on CLFV in the next few years
- It may be possible to search for lepton number violation as well
- I have attempted to provide some historical background to the efforts in $\mu \rightarrow e$ conversion, as well as to go into some depth about the current experimental landscape
- Whether the current suite of experiments sees a signal or improves the limits, it is possible to design experiments with even greater sensitivity, so the study of CLFV will continue into the foreseeable future

END